**Sentinel-5 Precursor
Mission Performance Centre**

Quarterly Validation Report of the Copernicus Sentinel-5 Precursor Operational Data Products #04: April 2018 – August 2019

S5P MPC

S5P MPC

Document Information and Approval

Document Identification	
Title	Quarterly Validation Report of the Copernicus Sentinel-5 Precursor Operational Data Products #04: April 2018 – August 2019
Type of document	S5P MPC Routine Operations Consolidated Validation Report (ROCVR)
Document ID	S5P-MPC-IASB-ROCVR-04.0.0-20190923
ROCVR update Issue number Date of issue Status	#04 version 04.0.0 2019-09-23 Final
Available at:	http://mpc-vdaf.tropomi.eu
Editors	J.-C. Lambert (BIRA-IASB), A. Keppens (BIRA-IASB), D. Hubert (BIRA-IASB), and B. Langerock (BIRA-IASB)
Contributors	K.-U. Eichmann (IUP-UB), Q. Kleipool (KNMI), M. Sneep (KNMI), T. Verhoelst (BIRA-IASB), T. Wagner (MPI-C), M. Weber (IUP-UB), C. Ahn (NASA/GSFC), A. Argyrouli (DLR), D. Balis (AUTH), K.L. Chan (DLR), S. Compernolle (BIRA-IASB), I. De Smedt (BIRA-IASB), H. Eskes (KNMI), A.M. Fjæraa (NILU), K. Garane (AUTH), J.F. Gleason (NASA/GSFC), F. Goutail (LATMOS), J. Granville (BIRA-IASB), P. Hedelt (DLR), K.-P. Heue (DLR), G. Jaross (NASA/GSFC), ML. Koukouli (AUTH), J. Landgraf (SRON), R. Lutz (DLR), S. Niemejer (s[&]t), A. Pazmiño (LATMOS), G. Pinardi (BIRA-IASB), J.-P. Pommereau (LATMOS), A. Richter (IUP-UB), N. Rozemeijer (KNMI), M.K. Sha (BIRA-IASB), D. Stein Zweers (KNMI), N. Theys (BIRA-IASB), G. Tilstra (KNMI), O. Torres (NASA/GSFC), P. Valks (DLR), C. Vigouroux (BIRA-IASB), P. Wang (KNMI)
Citation	Quarterly Validation Report of the Copernicus Sentinel-5 Precursor Operational Data Products – #04: April 2018 – August 2019. Lambert, J.-C., A. Keppens, D. Hubert, B. Langerock, K.-U. Eichmann, Q. Kleipool, M. Sneep, T. Verhoelst, T. Wagner, M. Weber, C. Ahn, A. Argyrouli, D. Balis, K.L. Chan, S. Compernolle, I. De Smedt, H. Eskes, A.M. Fjæraa, K. Garane, J.F. Gleason, F. Goutail, J. Granville, P. Hedelt, K.-P. Heue, G. Jaross, ML. Koukouli, J. Landgraf, R. Lutz, S. Niemejer, A. Pazmiño, G. Pinardi, J.-P. Pommereau, A. Richter, N. Rozemeijer, M.K. Sha, D. Stein Zweers, N. Theys, G. Tilstra, O. Torres, P. Valks, C. Vigouroux, and P. Wang. S5P MPC Routine Operations Consolidated Validation Report series, Issue #04, Version 04.0.0, 129 pp., September 2019.
Approval Record	
Checked by:	J.-C. Lambert (BIRA-IASB) MPC ESL-VAL Lead Q. L. Kleipool (KNMI) MPC ESL-L1 Lead D. Loyola (DLR) MPC ESL-L2 Lead J. P. Veefkind (KNMI) MPC Technical Manager A. Dehn (ESA) MPC Project Officer
Approved by:	A. Dehn (ESA) ESA Data Quality Manager

S5P MPC

Executive Summary

This document reports consolidated results of the routine operations validation service for the Sentinel-5 Precursor (S5P) Tropospheric Monitoring Instrument (TROPOMI) [ER_TROPOMI], a component of the European Earth Observation programme Copernicus [ER_CoperESA]. The S5P routine operations validation service is provided by the S5P Mission Performance Centre (MPC) for Level-1 and Level-2 data products generated by both the Near Real Time (NRTI) and Offline (OFFL) processors since the first public data release in July 2018. This Routine Operations Consolidated Validation Report (ROCVR) integrates results from the MPC Validation Data Analysis Facility (VDAF) consortium [ER_VDAF] with ad hoc support from S5P Validation Team (S5PVT) AO projects [ER_S5PVT]. The MPC routine operations validation service details and complements the conclusions and features described in the Product Readme Files (PRF) delivered with the S5P products, in which users can find practical recommendations on S5P data usage to be followed. This report covers the period of S5P routine operation data from April 2018 till August 2019. It includes preliminary checks of Level-2 data quality after the operations switch from the nominal ground pixel size of 7x3.5 km² to the smaller size of 3.5x3.5 km², activated on August 6, 2019.

Radiance and Irradiance

The validation of the wavelength assignment of the S5P L1B_UVN v01.00.00 products concludes to an agreement of 0.02 to 0.04 nm, which is within the pre-launch calibration accuracy. Initial validation of the L1B_RA reflectance with respect to OMI and OMPS independent satellite data indicates that TROPOMI is within 5% for the shorter wavelengths in band 3 and improving to 2% towards the longer wavelengths in band 4. For the short wave UV in band 1 TROPOMI L1B_RA is within 8% +/-2% of the expected modeled reflectance. In general radiometric errors in bands 1 and 3 are large but they vary slowly over wavelength and most L2 retrievals are insensitive to such errors. Additional validation indicates that for bands 3 to 7 the mission requirements for the reflectance are met. The largest source of error in the reflectance is due to the initial pre-launch irradiance calibration. This is a known issue that will be addressed in future updates of the L1B data products.

The validation of the TROPOMI L1B_IR irradiance product shows that it is within 3 to 10% depending on the used reference spectrum, and also that there is a radiometric mismatch between band 2 and 3. Additional validation with other solar irradiance spectra shows that the difference exhibits smooth wavelength dependence, most likely caused by optical setup effects during the on-ground calibration. This anomaly affects the UV and UVIS channels, and can be corrected for in the update of the Level-0-to-1b processor. After this correction the difference with respect to reference spectra reduces to 2% and is within the expected radiometric accuracy.

Ozone Column

The S5P L2_O3 NRTI and OFFL total ozone column data are in good overall agreement with correlative ground-based measurements from the Brewer, Dobson and NDACC ZSL-DOAS/SAOZ monitoring networks, and also with the MetOp-A/B GOME-2, Aura OMI, and Suomi-NPP OMPS-nadir satellite instruments. Across the networks the mean bias of about +0.8% (NRTI) and +0.4% (OFFL) and the standard deviation of the relative difference both comply with mission requirements, that is, a bias lower than 3.5% and an uncertainty due to random errors (dispersion) better than ±2.5%. The instrumental switch to smaller (along-track) ground pixels on the 6th of August 2019 does not show any effect on the agreement with the ground-based reference data.

The difference between S5P TROPOMI and other satellite data sets (GOME-2A, GOME-2B, OMI, OMPS) over cloudy scenes highlights differences in the cloud models used in the retrieval algorithms. Larger and/or systematic differences between satellite datasets also exist at high solar zenith angles (and hence at high latitudes), and in the case of uncertain ground albedo.

Tropospheric Ozone Column

The S5P L2_O3_TCL OFFL tropospheric ozone column data (CCD algorithm) are in good general agreement with correlative measurements from the ozonesonde monitoring network and the MetOp-B GOME-2 and Aura OMI satellite instruments. Across the ground-based network the mean bias (around +14% or +2.8 DU) and the mean dispersion of the relative difference (about 23% or 4.3 DU) both comply with mission requirements, that is, a bias lower than 25% and an uncertainty (dispersion) less than 25%.

However, during the first year of S5P operations and at several sites, the bias exhibits seasonal patterns exceeding mission requirements. During the 2018 biomass burning season the positive bias w.r.t. Atlantic and African ozonesonde data reaches peak values of up to 10-15 DU (or 40-60%). The onset of the positive bias period is seen again during the 2019 season at Paramaribo. Ozonesonde data from the other sites are expected to be available by the next issue of this document. In addition, unphysical biases of 1-2 DU between neighbouring latitude bands are found frequently in the S5P L2_O3_TCL data product. The progression of the orbital sampling by the S5P instrument imprints another, more elusive spatio-temporal bias pattern.

Nitrogen Dioxide

The S5P L2_NO2 (NRTI, OFFL, RPRO) data products up to version 01.03.02 are in good overall agreement with similar satellite data products (OMI) and correlative ground-based measurements from Pandonia Global Network (PGN), NDACC ZSL-DOAS/SAOZ and MAX-DOAS monitoring networks. Measurements were compared for the period from start of phase E2 until August 2019. In general, a low bias is detected.

The S5P L2_NO2 stratospheric NO_2 column data, taking diurnal variation into account, is generally lower by approximately 0.25 Pmolec/cm2 than the NDACC ZLS-DOAS ground-based measurements, deployed at 14 stations from pole to pole. The bias of roughly -11% is thus slightly above the S5P mission requirements of 10%, which is equivalent to 0.2-0.4 Pmolec/cm2, depending on latitude and season. The dispersion is within mission requirements (0.3 Pmolec/cm2), taking into account combined random errors and co-location mismatches.

The S5P L2_NO2 tropospheric NO_2 columns are compared to ground-based MAX-DOAS column data at 4 NDACC stations in Europe. The comparisons have shown a negative bias of roughly -30%, that is, within the mission requirements of 50%. On the other hand, comparisons of S5P with OMI tropospheric NO_2 data have shown good agreement, with difference of the order of 0.1 Pmolec/cm² (roughly 3%). The dispersion of less than 3 Pmolec/cm2 exceeds the mission precision requirements of 0.7 Pmolec/cm2.

The S5P L2_NO2 total NO_2 column data are compared to ground-based Pandora column data at 14 sites of the PGN network. The mean bias was -21% with a station-to-station scatter of 30%.

Ground-based validation show rather similar bias and uncertainty (dispersion) estimates for the L2_NO2 NRTI and L2_NO2 OFFL/RPRO datasets.

Formaldehyde

The S5P L2_HCHO (OFFL, RPRO) formaldehyde tropospheric column product is in good overall agreement, exhibiting a low bias in comparison to similar satellite data products (OMI, GOME-2) and correlative ground-based measurements from FTIR and MAX-DOAS monitoring networks.

The low bias with respect to the NDACC MAX-DOAS measurements from 2 European stations is roughly -40%, which is within the mission requirements (minimum bias of 40%). The dispersion of about 8 Pmolec/cm2 is within the uncertainty mission requirements of 12 Pmolec/cm2. Ground-based validation show similar bias and uncertainty (dispersion) estimates for the L2_HCHO NRTI and L2_HCHO OFFL/RPRO dataset.

The bias in comparison to OMI is less than -10% for most regions with some larger negative biases in Europe, US, and China (<30%). The dispersion is less than 2 Pmolec/cm^2.

Sulphur Dioxide

The S5P L2_SO2 (NRTI and OFFL) sulphur dioxide column data are found in general good agreement with ground-based measurements and with other satellite observations. The bias and dispersion with respect to validation data are typically below 0.2 DU. From these comparisons it can be concluded that over polluted regions the mission requirements are fulfilled. Over volcanic plumes the requirement on the bias is fulfilled, but the requirement on the random component of the uncertainty often is not fulfilled. Here it should be noted that the current random requirement is very strict (0.15 – 0.3 DU). For the often very high SO_2 column values in volcanic plumes it is unrealistic that the random requirement can strictly be fulfilled and it is recommended to reconsider this random requirement.

Carbon Monoxide

The S5P L2_CO (NRTI and OFFL) total carbon monoxide column data is in good overall agreement with correlative measurements from the NDACC and TCCON FTIR monitoring networks. It exhibits a positive bias of approximately +10% (NRTI) or +6% (OFFL) on an average, which falls well within the mission requirement (bias of maximum 15%). The standard deviation of the relative bias is on an average 4% against TCCON and 5% against NDACC, which is also with the mission requirement for precision (better than 10%). The averaged correlation coefficient reaches 0.9 for the TCCON network and 0.85 for the comparison against NDACC sites.

Methane

The S5P L2_CH4 (OFFL concatenated with RPRO) total methane column averaged data is in good overall agreement with correlative measurements from the NDACC and TCCON FTIR monitoring networks. The standard and bias-corrected S5P xCH4 column data exhibit a negative bias against TCCON of -0.8% and -0.3% respectively, which falls well within the mission requirement (bias of maximum 1.5%). The standard deviation of the relative bias is on an average 0.5% which is also with the mission requirement for precision (<1%). The averaged correlation coefficient 0.6 is rather low, probably because not all outlying pixels are filtered with the `qa_value` above 0.5 condition.

Clouds

The S5P L2_CLOUD (NRTI and OFFL) cloud height data and cloud top height data compare favourably with ground-based measurements from the CLOUDNET and ARM networks. For about half of the 13 stations the discrepancy agrees or narrowly exceeds the S5P data requirement on the bias (20%). However, the sensitivity of the TROPOMI NIR observations to clouds differs significantly from the sensitivity of CLOUDNET lidar/radar instruments used as a reference, and the error associated with the reference observations is also not yet included in those comparisons. Therefore, we consider present validation results as positive. The S5P L2_CLOUD cloud height data (for both the CAL and CRB retrieval approaches) shows a bias towards the *a-priori* for versions below 01.01.06. This known bug is fixed for versions 01.01.06 and onwards. The bias and spread between CLOUD CRB and CLOUDNET is broadly similar to that between S5P FRESCO and CLOUDNET, indicating that most of the discrepancy is not specific to a particular retrieval algorithm.

For S5P L2_CLOUD cloud fraction and cloud optical thickness, satellite-to-satellite intercomparisons offer better opportunities than comparisons with ground-based observations. For now the daily mean distribution of cloud fraction, cloud top height and optical thickness as a function of latitude is compared with MODIS on the EOS-Aqua satellite. Furthermore, a direct comparison for multiple days with co-located and re-gridded VIIRS cloud top height and cloud optical thickness has been performed.

The reduction in ground pixel size at orbit 9388 (on the 6th of August 2019) does not seem to have any effect on the retrieved L2_CLOUD data products.

Aerosol Index

The S5P L2_AER_AI (NRTI and OFFL) UV Aerosol Absorbing Index data is in good overall agreement with similar satellite data products from EOS-Aura OMI and Suomi-NPP OMPS. Although compliant with the mission requirement of 1 UVAI unit in 2018, the bias is currently slightly larger than 1 UVAI unit as compared to OMI and OMPS. The reasons for this increasing bias are related to wavelength-dependent degradation and will be addressed with the next update in S5P L1B data foreseen in 2020.

Processing Baseline Identification

This document reports consolidated validation results for the following S5P TROPOMI data products:

Product ID	Stream	Version	In operation from (orbit #, date)	In operation until (orbit, date)
L1B_RA1/2/…/8		01.00.00	2818, 2018-04-30	current version
L1B_IR_UVN/SIR		01.00.00	2818, 2018-04-30	current version
L2_O3	NRTI	01.00.00 01.01.02 01.01.05 01.01.06 01.01.07	2955, 2018-05-09 4245, 2018-08-08 5931, 2018-12-05 7631, 2019-04-04 7999, 2019-04-30	3943, 2018-07-18 5930, 2018-12-05 7631, 2019-04-04 7999, 2019-04-30 current version
	OFFL	01.01.07	7907, 2019-04-23	current version
	RPRO	01.01.07	2818, 2018-04-30	7906, 2019-04-23
L2_O3_TCL	OFFL (CCD)	01.01.05 01.01.06 01.01.07	2824, 2018-04-30 7435, 2019-03-21 7804, 2019-04-16	7421, 2019-03-20 7791, 2019-04-15 current version
L2_NO2	NRTI	01.00.01 01.00.02 01.01.00 01.02.00 01.02.02 01.03.00 01.03.01 01.03.02	2955, 2018-05-09 3745, 2018-07-04 3947, 2018-07-18 5336, 2018-10-24 5931, 2018-12-05 7519, 2019-03-27 7999, 2019-03-30 9159, 2019-07-20	3364, 2018-06-07 3946, 2018-07-18 5333, 2018-07-24 5929, 2018-12-05 7517, 2019-03-27 7999, 2019-03-30 9158, 2019-07-20 current version
	OFFL	01.02.00 01.02.02 01.03.00 01.03.01 01.03.02	5236, 2018-10-17 5840, 2018-11-29 7425, 2019-03-20 7907, 2019-04-23 8815, 2019-06-26	5832, 2018-11-28 7424, 2019-03-20 7906, 2019-04-23 8814, 2019-06-26 current version
	RPRO	01.02.02	2836, 2018-05-01	5235, 2018-10-17
L2_HCHO	NRTI	01.00.00 01.01.01 01.01.02 01.01.05 01.01.06 01.01.07	2955, 2018-05-09 3947, 2018-07-18 4245, 2018-08-08 5931, 2018-12-05 7636, 2019-04-04 7999, 2019-04-30	3943, 2018-07-18 4244, 2018-08-08 5929, 2018-12-05 7628, 2019-04-04 7999, 2019-04-30 current version
	OFFL	01.00.00 01.01.01 01.01.02 01.01.05 01.01.06 01.01.07	3202, 2018-05-27 3848, 2018-07-10 4147, 2018-07-31 5832, 2018-11-27 7546, 2019-03-29 7907, 2019-04-23	3847, 2018-07-10 4146, 2018-07-31 5831, 2018-11-27 7545, 2019-03-29 7906, 2019-04-23 current version
	RPRO	01.01.02 01.01.05	2818, 2018-04-30 3627, 2018-06-26	4147, 2018-08-01 5832, 2018-11-28
L2_SO2	NRTI	01.00.00 01.01.01 01.01.02 01.01.07	3202, 2018-05-27 3848, 2018-07-10 4147, 2018-07-31 5833, 2018-12-05	3847, 2018-07-10 4146, 2018-07-31 5832, 2018-12-04 current version

Product ID	Stream	Version	In operation from (orbit #, date)	In operation until (orbit, date)
L2_CO	OFFL	01.00.00	3202, 2018-05-27	3847, 2018-07-10
		01.01.01	3848, 2018-07-10	4146, 2018-07-31
		01.01.02	4147, 2018-07-31	5932, 2018-11-28
		01.01.07	5933, 2018-11-28	current version
	NRTI	01.02.00	5336, 2018-10-24	5929, 2018-12-05
		01.02.02	5931, 2018-12-05	7517, 2019-03-27
		01.03.00	7519, 2019-03-27	7999, 2019-04-30
		01.03.01	7999, 2019-04-30	8906, 2019-07-03
		01.03.02	8906, 2019-07-03	current version
	RPRO[2]	01.02.02	5236, 2018-10-17	5346, 2018-10-25
		01.03.01	2818, 2018-04-30	5832, 2018-11-28
		01.03.02	2463, 2018-04-04	2477, 2018-04-05
	OFFL	01.02.00	5346, 2018-10-25	5832, 2018-11-28
		01.02.02	5833, 2018-11-28	7424, 2019-03-20
		01.03.00	7425, 2019-03-20	7906, 2019-04-23
		01.03.01	7907, 2019-04-23	8814, 2019-06-26
		01.03.02	8815, 2019-06-26	current version
L2_CH4	RPRO[2]	01.02.02	0657, 2017-11-28	5346, 2018-10-25
		01.03.01	2818, 2018-04-30	5832, 2018-11-28
		01.03.02	2463, 2018-04-04	2477, 2018-04-05
	OFFL	01.02.02	5833, 2018-11-28	7424, 2019-03-20
		01.03.00	7425, 2019-03-20	7906, 2019-04-23
		01.03.01	7907, 2019-04-23	8814, 2019-06-26
		01.03.02	8812, 2019-06-26	current version
L2_CLOUD	NRTI	01.01.01	3947, 2018-07-18	4242, 2018-08-08
		01.01.02	4243, 2018-08-08	5929, 2018-12-05
		01.01.05	5931, 2018-12-05	7631, 2019-04-04
		01.01.06	7631, 2019-04-04	7999, 2019-04-30
		01.01.07	7999, 2019-04-30	current version
	OFFL	01.01.05	5833, 2018-11-28	7546, 2019-03-28
		01.01.06	7547, 2019-03-29	7906, 2019-04-23
		01.01.07	7907, 2019-04-23	current version
	RPRO	01.01.05	2818, 2018-04-30	5832, 2018-11-28
		01.01.07	2818, 2018-04-30	7906, 2019-04-23
L2_AER_AI	NRTI	01.02.00	5336, 2018-10-24	5929, 2018-12-04
		01.03.02	5932, 2018-12-05	current version
	OFFL	01.02.00	5336, 2018-10-24	5929, 2018-12-04
		01.03.02	5932, 2018-12-05	current version

Table 1 – S5P TROPOMI data products and processor versions (NRTI near-real-time and OFFL off-line). Note 1: the operational phase (E2) of the S5P TROPOMI mission starts with orbit #2818. Note 2: RPRO 01.03.01 and 01.03.02 have been used to fill gaps in the 01.02.02 RPRO and therefore processor start end dates are not sequential

Representative Quality Indicators

Based on the validation results reported in this document, representative values of key quality indicators (bias and spread) have been derived for the following S5P operational data products:

Product ID	Stream	Product	Bias	Dispersion	Special features
L2_O3	NRTI	O_3 column	0.8%	2.5%	
	OFFL	O_3 column	0.4%	2%	
L2_O3_TCL	OFFL (CCD)	O_3 tropospheric column	+14%	23%	Positive bias in biomass burning conditions. Geographical imprints of sampling-related biases.
L2_NO2	NRTI	NO_2 troposphere NO_2 stratosphere	-30% -11%	3 $Pmol/cm^2$ 0.3 $Pmol/cm^2$	Along track stripes (>2019-08-02) in both products.
	OFFL RPRO	NO_2 troposphere NO_2 stratosphere	-30% -11%	3 $Pmol/cm^2$ 0.3 $Pmol/cm^2$	
L2_HCHO	NRTI	HCHO column	-40%	8 $Pmol/cm^2$	Only two validation sites.
	OFFL RPRO	HCHO column	-40%	8 $Pmol/cm^2$	
L2_SO2	NRTI	SO_2 column	0.2 DU	0.2 DU	Lack of validation sites in high SO_2 areas.
	OFFL	SO_2 column	0.2 DU	0.2 DU	
L2_CO	NRTI	CO column	10%	5%	Along orbit stripes. High pollution underestimated.
	OFFL	CO column	6%	5%	
L2_CH4	OFFL	CH4 column	-0.3%	0.5%	Along orbit stripes. Underestimation at low albedo. Remaining outliers with `qa_value`>0.5
L2_CLOUD	NRTI	CAL CTH CRB CH CAL COT	-20% -30% +7.9 [-]	2 km 1 km	Bias towards the a priori cloud height up to and including 01.01.07. Snow/ice degrades retrievals. Occurrence of C(T)H equal to surface height at low cloud fraction. COT positive bias vs VIIRS.
	OFFL	CAL CTH CRB CH CAL COT	-20% -30% +7.9 [-]	2 km 1 km	
L2_AER_AI	NRTI	aerosol index	-1.1 AI unit	0.1 AI unit	Negative bias exceeding 1 AI unit after March 2019, attributed to irradiance data degradation.
	OFFL	aerosol index	-1.1 AI unit	0.1 AI unit	

Table 2 – Representative quality indicators (bias and dispersion) as estimated from the validation studies of the S5P TROPOMI operational data products identified in the **Table 1**. The processor version number is not mentioned as the estimates are representative for all versions available publicly. CTH: cloud-top-height; CH: cloud height; COT: cloud optical thickness.

Table of Contents

1   Introduction

1.1   Background information on Sentinel-5 Precursor TROPOMI

TROPOspheric Monitoring Instrument (TROPOMI) [ER_TROPOMI] is the unique payload of the ESA/Copernicus Sentinel-5 Precursor mission (S5P) launched on October 13, 2017. The prime function of TROPOMI is to monitor the global distribution of atmospheric trace gases and aerosols for a better understanding of air quality, the ozone layer, atmospheric chemistry, transport, ultraviolet radiation, and climate change. The instrument is a nadir-viewing hyperspectral spectrometer measuring, in the ultraviolet and visible (270-495 nm), near-infrared (675-775 nm) and shortwave infrared (2305-2385 nm), the solar radiation scattered by the Earth's atmosphere and reflected by the Earth's surface and by clouds, as well as solar spectral irradiance. Daily coverage at the high horizontal resolution of 7 x 3.5 km^2 before and 3.5 x 3.5 km² after the operations switch to smaller ground pixel size activated on the 6th of August 2019, is accomplished thanks to a Sun-synchronous polar orbit (equator crossing time of 13:30 local solar time) and a wide swath width of 2600 km across track. From the TROPOMI radiometric measurements of Earth's radiance and solar irradiance, on-ground data processors retrieve the atmospheric abundance of ozone (O_3), nitrogen dioxide (NO_2), formaldehyde (HCHO), sulphur dioxide (SO_2), carbon monoxide (CO), methane (CH_4), as well as cloud and aerosol properties.

With a 7-year operation lifetime, the S5P mission aims at filling in the anticipated observational gap of key atmospheric composition data between, from one part, Envisat SCIAMACHY (operational in 2002-2012), EOS-Aura OMI (operational since 2004) and the EUMETSAT EPS MetOp GOME-2 series (initiated in 2006, with the latest MetOp-C launched in November 2018), and from the other part, the upcoming series of Copernicus Sentinel-4 and Sentinel-5 missions scheduled after 2022. The S5P mission is also a key component of the space segment of the European Earth Observation programme Copernicus [ER_CoperESA]. As such, it has also an operational and service-oriented vocation.

1.2   Mission Performance Centre – Routine Operations Validation Service

Procured by an international consortium contracted by the European Space Agency (ESA), the S5P Mission Performance Centre (MPC) provides an operational service-based response to the S5P mission requirements for quality control, calibration, validation and end-to-end system performance monitoring during the Routine Operations phase of the S5P mission.

In-flight calibration and characterisation of the TROPOMI instrument, long-term monitoring of the instrument sensor performance and ageing, and routine Quality Control (QC) of the operational Level-1 (radiometric) and Level-2 (geophysical) data products are coordinated by the Royal Dutch Meteorological Institute (KNMI), and documented on the *TROPOMI Portal for Instrument and Calibration* [ER_MPS] and the *TROPOMI Portal for Level-2 Quality Control* [ER_L2QC].

Geophysical validation of the operational Level-1 and Level-2 data products is coordinated by the Royal Belgian Institute for Space Aeronomy (BIRA-IASB), and documented on the Portal of the *TROPOMI Validation Data Analysis Facility* (VDAF) [ER_VDAF]. The TROPOMI routine operations validation service makes use of Fiducial Reference Measurements (FRM) and other correlative data of documented quality (ground-based and satellite measurements, dedicated field campaigns), to assess the overall quality, the compliance with mission requirements and the validity of uncertainty estimates of the TROPOMI data products. This service monitors validation results on a cyclic basis and produces every three months the present *Routine Operations Consolidated Validation Report* (ROCVR). It also contributes quality assessment support to the evolution of data processors.

1.3   Purpose, scope and outline of this document

The present document (DI-MPC-ROCVR) reports consolidated validation results for the S5P TROPOMI Level-1 and Level-2 operational data products. This report has been produced by the S5P MPC Routine Operations Validation Service. It integrates validation results from the MPC Validation Data Analysis Facility (VDAF) consortium (**Table 11**) with support from other activities and dedicated field campaigns documented on the TROPOMI website [ER_TROPOMI], as well as ad hoc contributions from S5P Validation Team (S5PVT) AO projects [ER_S5PVT].

Updated with a trimestral frequency, S5P data quality information provided in this document supersedes that provided in previous versions. It complements S5P data quality information provided in the *Product Readme Files* (PRFs) attached to S5P data products released publicly. For details and for recommendations for data usage, data users are encouraged to read the PRF, *Product User Manual* (PUM) and *Algorithm Theoretical Basis Document* (ATBD) associated with the data products, all available on the Copernicus Sentinel Portal for S5P products and algorithms [ER_CoperATBD] and also on the TROPOMI Portal [ER_TROPOMI].

This ROCVR update #04 presents quality information for the S5P operational data products generated since the first public data release in July 2018 until August 2019. It is structured as follows:

2   S5P Data Quality Requirements

Validation results can be interpreted to evaluate whether or not S5P Level 2 data products meet user requirements. Targets for key quality indicators of the S5P Level 2 data products have been formulated in the *S5P Geophysical Validation Requirements* document ([S5PVT-Req], Page 19) and the *S5P Cal/Val Plan for the Operational Phase* ([S5P-CSCOP], Page 14). Maintenance of these requirements is supported by the Sentinel-5p Quality Working Group (QWG). Expressed in terms of measurement bias (estimate of the systematic measurement error) and dispersion (measurement uncertainty, that is, dispersion of the quantity values being attributed to the measurand), these targets are reproduced hereafter in **Table 3**. Quality targets are typical of several known applications; nevertheless, it always remains the uttermost responsibility of any users to check the fitness of the S5P data for their own purpose, with respect to their own particular requirements.

ID	S5P TROPOMI Level-2 Data Product	Requirement: Vertical Resolution	Requirement: Bias	Requirement: Dispersion
L2_O3	Total O_3	total column	3.5-5%	1.6%-2.5%
L2_O3_PR	O_3 profile (incl. troposphere)	6 km	10-30%	10%
L2_O3_TCL	O_3 tropospheric column	tropospheric column	25%	25%
L2_NO2	NO_2 tropospheric column	tropospheric column	25-50%	0.7 Pmolec.cm^{-2}
	NO_2 stratospheric column	stratospheric column	10%	0.5 Pmolec.cm^{-2}
L2_SO2	Enhanced total SO_2	total column	30%	0.3 (0.12) DU
	Total SO_2	total column	50%	1-3 (1.2) DU
L2_HCHO	Total HCHO	total column	40-80%	12 Pmolec.cm^{-2}
L2_CO	Total CO	total column	15%	10%
L2_CH4	Total CH_4	total column	1.5%	1%
L2_CLOUD	Cloud Fraction	total column	20%	0.05
	Cloud Height (pressure)	total column	20%	0.5km (P<30hPa)
	Cloud Optical Thickness	total column	20%	0.05 (10)
L2_AER_AI	Aerosol Absorbing Index	total column	1 AAI	0.1 AAI
L2_AER_ALH	Aerosol Layer Height	total column	100 hPa	50 hPa

Table 3 – Data quality targets for the operational Sentinel-5 Precursor TROPOMI Level 2 data products: measurement bias and (random) measurement uncertainty (adapted by Sentinel-5p QWG from [S5PVT-Req] and [S5P-CSCOP]).

3   Validation Results: L1B_RA and L1B_IR

3.1   L1B products

This Section reports on the validation of the S5P TROPOMI L1B product identified in **Table 4**.

Table 4 – Identification of the S5P TROPOMI L1B products evaluated in this Section.

Product	Stream	Version	In operation from	In operation until
L1B_RA1/…/8		01.00.00	orbit 2818, 2018-04-30	current version
L1B_IR_UVN/SIR		01.00.00	orbit 2818, 2018-04-30	current version

Note: The operational phase (E2) of the S5P TROPOMI mission starts with orbit #02818.

3.2   Recommendations for data usage followed

The product is stored as NetCDF4 file. The NetCDF4 file contains both the data and the metadata for the product.

For OFFL and RPRO data the product is stored as a single file per satellite orbit, for NRTI data the product is stored as multiple files per orbit.

An overview of the Sentinel-5p mission, the TROPOMI instrument and the algorithms for producing the L1b data products can be found in the Algorithm Theoretical Basis Document. Details of the data format are provided in the Input/Output Data Specification. The metadata contained in the L1b data products are described in the Metadata Specification. All these documents are available on https://sentinels.copernicus.eu/web/sentinel/technical-guides/sentinel-5p/products-algorithms.

For Level 2 processing and related validation, the following additional notices have been applied:

- The L0-1b data processor annotates the data with quality assessment data in the fields `spectral_channel_quality`, `measurement_quality` and `ground_pixel_quality`. Level 2 developers are strongly encouraged to observe these quality fields in their retrievals and exclude flagged data as needed.

- All 8 bands are processed individually in the L0-1b data processor. In case of missing data, for example in case of data drop-outs during downlinks, this does not necessarily impact all bands (to the same extent). This means that a scanline can be missing for some bands, where it is not missing for other bands. When combining data from multiple bands, Level 2 algorithms should therefore always check and match the `delta_time` for these data and, in case of non-co-registered bands, the geolocation as well.

- For calculating reflectance from the radiance products, it is recommended to use the irradiance product with the sensing time close to the sensing time of the radiance product.

3.3   Validation approach

In-flight calibration and characterisation of the TROPOMI instrument, long-term monitoring of the instrument sensor performance and ageing, and routine Quality Control (QC) of the operational L1B data products are reported continuously on the *TROPOMI Portal for Instrument and Calibration* [ER_MPS].

The S5P TROPOMI Level-1b data products have also been compared to modelling output and to other satellite measurements, specifically from EOS-Aura OMI and from Suomi-NPP OMPS.

3.4   Validation of L1B NRTI

The near-real time L1b products are not distributed to users, and they are not validated separately. NRTI products use the same L01b data processor algorithms, and can only differ when the Calibration Key Data (CKD) used differs from OFFL. Currently no CKD is dynamically updated in OFFL, and hence no difference exists between NRTI and OFFL.

3.5   Validation of L1B OFFL

The validation of the wavelength assignment of the L1B_UVN products shows agreement of 0.02 to 0.04 nm, which is within the pre-launch calibration accuracy.

Initial validation of the L1B_RA reflectance with respect to OMI and OMPS data indicates that TROPOMI is within 5% for the shorter wavelengths in band 3 and improving to 2% towards the longer wavelengths in band 4. For the short wave UV in band 1 TROPOMI is within 8% +/-2% of the expected modeled reflectance.

In general radiometric errors in bands 1 and 3 are large but they vary slowly over wavelength and most L2 retrievals are insensitive to such errors. Additional validation indicates that for bands 3 to 7 the mission requirements for the reflectance are met if the uncertainty of the method of 3 to 5% is taken into account.

The largest source of error in the reflectance is due to the initial pre-launch irradiance calibration. This is a known issue and will be addressed in future updates.

The validation of the TROPOMI L1B_IR irradiance product shows that it is within 3 to 10% depending on the used reference spectrum and that there is a radiometric mismatch between band 2 and 3.

Additional validation with other solar irradiance spectra concludes that the difference shows a smooth wavelength dependence, most likely caused by optical setup effects during the on-ground calibration. This anomaly affects the UV and UVIS channels, and can be corrected for in the update of the L01b processor. After this correction the differences with reference spectra reduces to 2% and is within the expected radiometric accuracy. For the NIR and SWIR channels the difference shows no wavelength dependence but an offset that is within the radiometric accuracy budget. For these channels no correction is foreseen.

4   Validation Results: L2_O3

4.1   L2_O3 products and requirements

This Section reports on the validation of the S5P TROPOMI L2_O3 product identified in **Table 1**. Validation results are discussed with respect to the product quality targets outlined in **Table 3**. The NRTI and OFFL processors using different approaches, their respective validation is reported in separate subsections.

4.2   Validation approach

4.2.1   Ground-based networks

S5P TROPOMI L2_O3 total ozone column data are routinely compared to reference measurements acquired by instruments contributing to WMO's Global Atmosphere Watch (GAW): (1) Brewer (Kerr et al., 1981,1988) and (2) Dobson (Basher, 1982) UV spectrophotometers, and (3) NDACC Zenith Scattered Light (ZSL) DOAS UV-Visible spectrometers (Pommereau and Goutail, 1988, Hendrick et al., 2011). Co-locations between S5P TROPOMI and direct-sun (DS) measurements are defined as "pixel contains station", with a maximum time difference of 3 hours. Note that direct-sun measurements obtained through the WOUDC archive are usually daily means of the individual measurements. To reduce co-location mismatch errors due to the significant difference in horizontal smoothing between S5P and ZSL-DOAS measurements, S5P O3 column values (from afternoon ground pixels at high resolution) are averaged over the footprint of the larger air mass to which the ground-based twilight zenith-sky measurement is sensitive. For more details about the validation methodology, see Lambert et al. (1997, 1999), Balis et al. (2007), Koukouli et al. (2015), Verhoelst et al. (2015), and Garane et al. (2019).

4.2.2   Satellites

S5P TROPOMI L2_O3 total ozone column data have also been compared to MetOp-A and MetOp-B GOME-2 ozone column data (version GDP 4.8), to Suomi-NPP OMPS-nadir ozone column data, and to S5P ozone column data retrieved with the other S5P operational processor (NRT vs. OFFL).

4.2.3   Field campaigns and modelling support

None for this report.

4.3   Validation of L2_O3 NRTI

4.3.1   Recommendations for data usage followed

Data users are encouraged to read the Product Readme File (PRF), Product User Manual (PUM) and Algorithm Theoretical Basis Document (ATBD) associated with this data product, all available on https://sentinels.copernicus.eu/web/sentinel/technical-guides/sentinel-5p/products-algorithms.

In order to avoid misinterpretation of the data quality, it is recommended to use only those TROPOMI pixels associated with a qa_value above 0.5. According to validation results this criterion might be relaxed, but nevertheless, caution remains required for qa_value below 0.5. An alternative set of filter criteria for L2_O3 NRTI are the following:

- ozone_total_vertical_columnn should be within [0 to 0.45];

- ozone_effective_temperature should be within [180 to 280];

- fitted_root_mean_square should not be larger than 0.01.

4.3.2   Status of validation

This section presents a summary of the key validation results obtained by the MPC VDAF and by S5P Validation Team (S5PVT) AO projects. It is based on updates of the preliminary results reported at the S5P First Public Release Validation Workshop (ESA/ESRIN, June 25-26, 2018). Individual contributions to the workshop are archived in https://nikal.eventsair.com/QuickEventWebsitePortal/sentinel-5p-first-product-release-workshop/sentinel-5p, while up-to-date validation results and consolidated validation reports are available through the MPC VDAF Portal at http://mpc-vdaf.tropomi.eu.

Current conclusions are based on the S5P data obtained in the operational phase E2, from May 2018 until August 2019, and on the reference data available at the time of this report (typically until end of June 2019 for the Dobson and Brewer data, and up to the middle of August 2019 for the ZSL-DOAS SAOZ data). For the current report, Brewer and Dobson measurements were obtained through the World Ozone and UV Radiation Data Centre (WOUDC) in Toronto, the NDACC Data Host Facility, and WMO's Ozone Mapping Centre in Thessaloniki. If a station archives data both into WOUDC and NDACC HDF, the source with the most recent data is adopted. ZSL-DOAS measurements were collected through the SAOZ network Real-Time processing facility operated by LATMOS (LATMOS_RT). The validation is carried out using the Automated Validation Server of the S5P MPC VDAF, the Multi-TASTE versatile validation system operated at BIRA-IASB, and the ozone validation system operated at AUTH.

Over the period, with respect to the reference data available at the time of this analysis, of the order of 40 to 350 unique co-locations have been identified at about 40 Brewer and Dobson sites and at 12 ZSL-DOAS SAOZ sites, sampling many latitudes from the Arctic to the Antarctic (**Figure 1**).
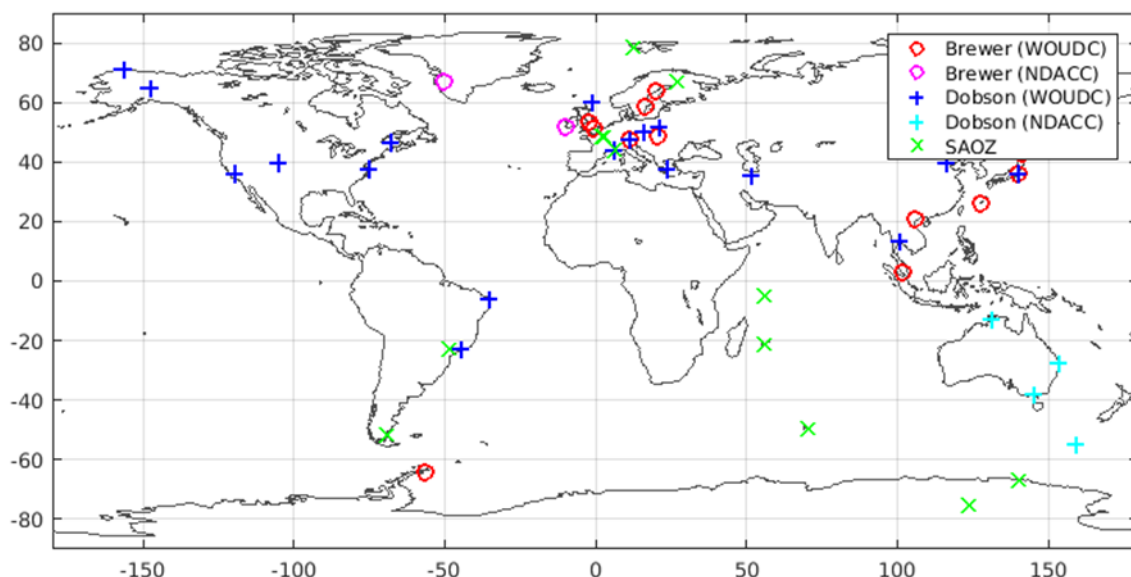
Figure 1: Geographical distribution of Brewer, Dobson and ZSL-DOAS ground-based stations for which suitable co-locations with S5P L2_O3 NRTI ozone data have been identified (May 2018 until August 2019).

4.3.3   Bias

The systematic difference between S5p L2_O3 NRTI and reference ground-based data at individual stations rarely exceeds 2%, as depicted in **Figure 2**. The median bias calculated over the entire ground-based networks is of the order of +0.5-1%, S5P reporting higher values than the networks. Between 50˚S and 50˚N, the mean agreement with other satellite data is mostly within 1% as well (**Figure 3**). This median bias value falls well within the mission requirements (max. bias 3.5-5%).
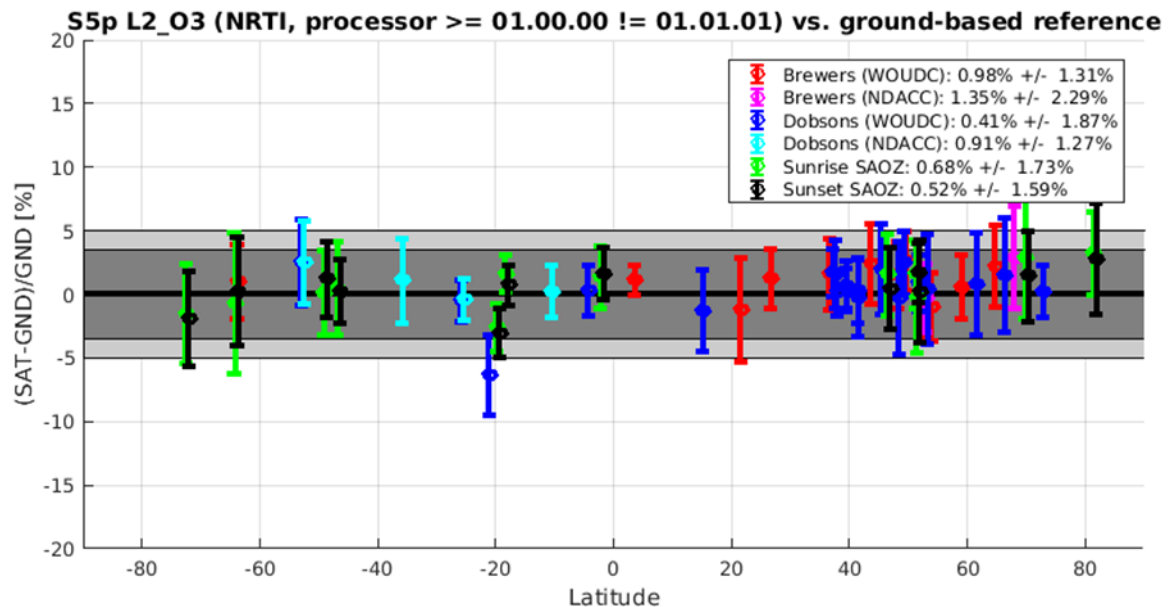
Figure 2: Meridian dependence of the median (the circular markers) and spread (±1 sigma, the error bars) of the percent relative difference between S5P TROPOMI L2_O3 (PDGS NRTI processor v1.0.0 up to v1.1.7, 25 August 2019) and ground-based (GND) ozone column data, represented at individual stations from the Antarctic to the Arctic and per measurement type (Brewer, Dobson, and ZSL-DOAS). The values in the legend correspond to the median and spread of all median (per station) differences. For clarity, sunrise and sunset ZSL-DOAS results are represented separately (offset by -0.5˚ and +0.5˚ in latitude).
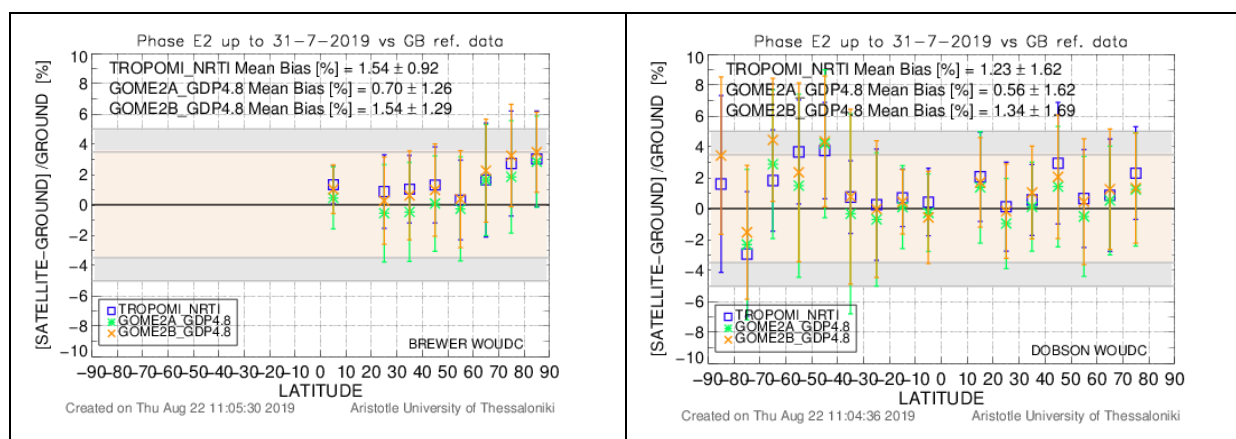
Figure 3: Comparison of the bias between three satellite products (S5P TROPOMI L2_O3 NRTI, GOME-2 A GDP 4.8 and GOME-2B GDP 4.8) and Brewer (left-hand panel) and Dobson (right-hand panel) network total ozone data (datasets from WOUDC only). The time period of data used for these plots is May 2018 – July 2019 (not later due according to ground-based data availability).

4.3.4   Dispersion

The ±1σ dispersion of the difference (between S5P and reference ground-based network data) around their median value rarely exceeds 3-4% for the comparisons with direct-sun instruments (cf. the error bars depicted in **Figure 2**). Combining random errors in both satellite and reference measurements with irreducible co-location mismatch effects, it is concluded that the random uncertainty on the S5P measurements falls within the mission requirements of max.±2.5%.

4.3.5   Dependence on influence quantities

The evaluation of potential dependence of the S5P bias and dispersion on the Solar Zenith Angle (SZA), Air Mass Factor (AMF) and cloud fraction (CF) of the TROPOMI measurement does not reveal any variation of the bias larger than 2% over the range of those influence quantities.

The scatter of the data comparisons of about 2-4% increases up to 7% at large SZAs and at latitudes beyond 50° (**Figure 4**), which is expected knowing that random errors in both satellite and reference measurements as well as irreducible co-location mismatch effects increase at high latitudes and low sun elevation.
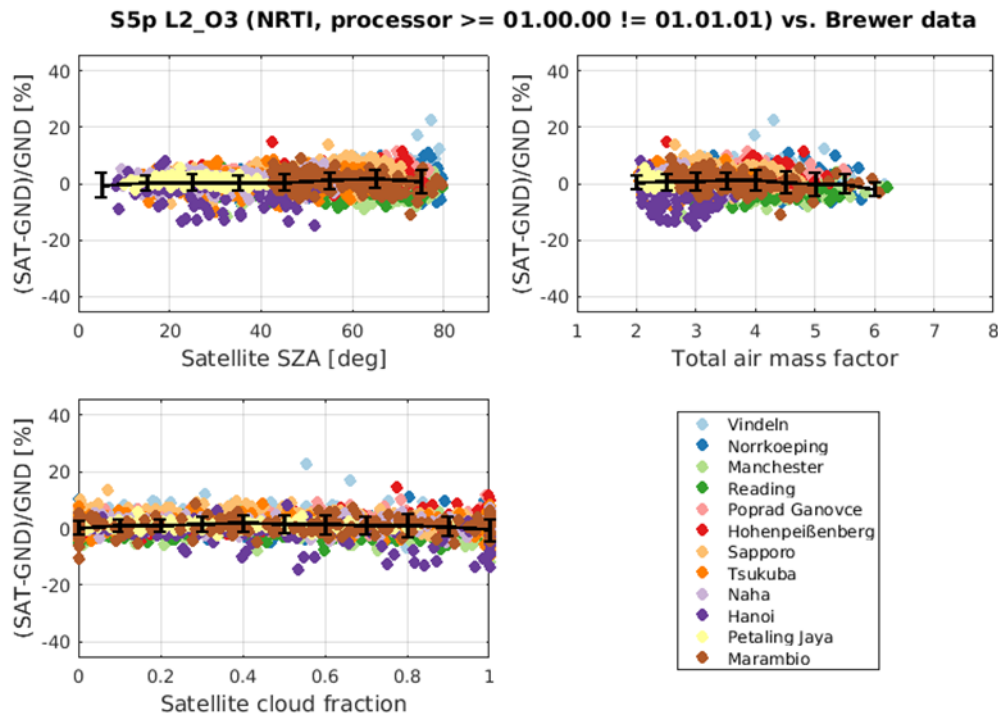
Figure 4: Dependence of the difference between S5P and ground-based Brewer ozone data on the satellite solar zenith angle (SZA), the satellite fractional cloud cover, and the satellite air mass factor, including a mean and standard deviation per 10-degree, 0.1 CF-increment or 1 AMF-increment bin.

4.3.6   Short term variability

Qualitatively, at all of the 50 ground-based reference stations, short scale temporal variations in the ozone column as captured by ground-based instruments are reproduced very similarly by S5P, as illustrated in **Figure 5**. The overall good agreement is corroborated by Pearson correlation coefficients always above 0.95.
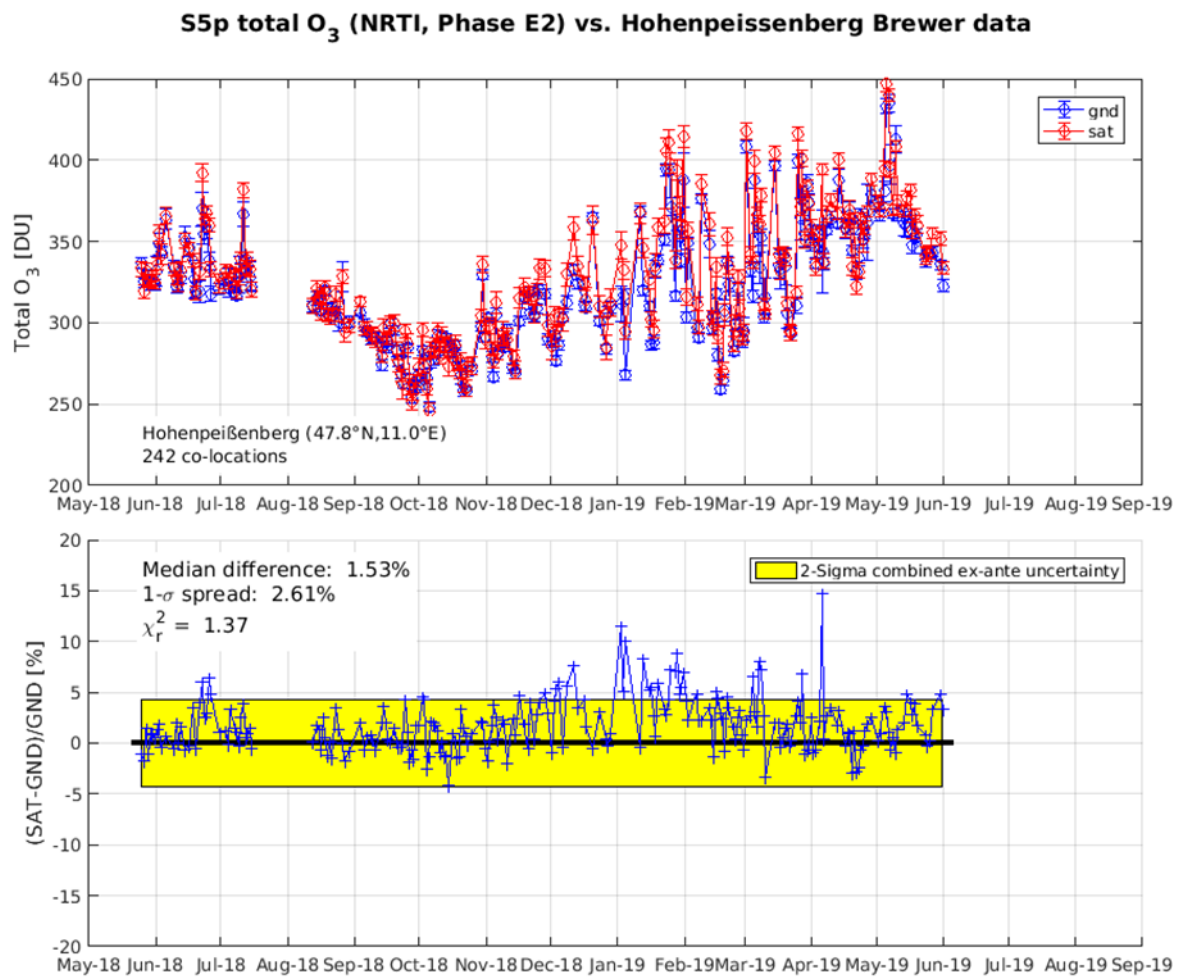
Figure 5: Time series of S5P and Brewer total ozone data at the NDACC station of Hohenpeißenberg (Germany). Original time series of co-located data are presented in the upper panel, the differences in the lower panel. The slight positive bias in local winter is not a network-wide feature but may be related to the course resolution of the assumed surface albedo not representing perfectly the complexity of the actual albedo (patchy snow) in this mountainous region. It is not present in the OFFL product for which an effective albedo is retrieved.

4.3.7   Geographical patterns

The bias between S5P L2_O3 and other satellite data sets exhibits patterns correlating with weather patterns, atmospheric circulation features, and ground albedo types. When looking at satellite datasets obtained from different satellites (e.g., TROPOMI on S5P in the early afternoon and GOME-2 on MetOp-A in the mid-morning), patterns correlating with weather structures and atmospheric circulation might simply reflect – at least partly – real ozone changes between the different satellite overpass times. But patterns correlating with ground albedo types cannot. Furthermore, looking at S5P ozone datasets retrieved from the same Level-1 data processed with different Level-1-to-2 retrieval algorithms, those patterns subsist, as illustrated in **Figure 6** where NRTI and OFFL data are compared.

Geographical patterns in the L2_O3 ozone data products – revealed by comparisons with other satellite datasets – are likely to be associated with differences in the processing of the cloud properties, in the use of either a surface albedo climatology or a fitted effective albedo, and, in the case of a comparison of data from two different satellites, to differences in overpass times (3.5 hours difference between S5p and GOME-2).
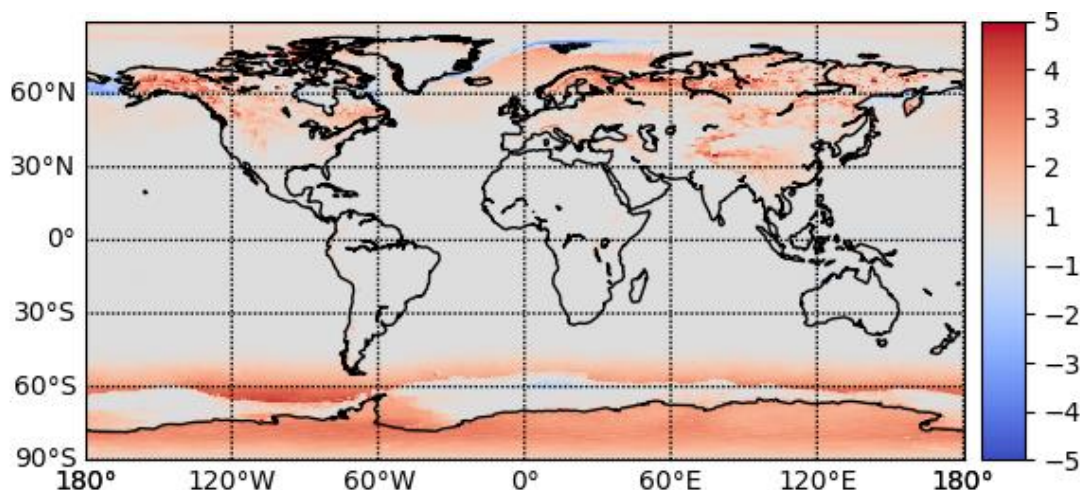
Figure 6: Percent relative difference between S5PL2_O3 total ozone data retrieved with the NRTI and OFFL processors (period November 2017 through September 2018). Geographical patterns in this case cannot be associated with real ozone features but reveal rather the effect of using either a surface albedo climatology (NRTI product) or fitting an effective albedo (OFFL product).

4.3.8   Other features

None to report.

4.3.9   Switch to smaller ground pixel size

On 6 August 2019, the nominal ground pixel resolution of the TROPOMI measurement was reduced to $3.5 \times 5.5 km^2$, i.e. shorter in the along-track direction, by reducing the integration time. **Figure 7** shows no evidence of a negative effect on the agreement between satellite and reference data since this switch in resolution, with the caveat that this judgement is based on a very small set of co-locations (related to the availability of reference data at the time of this comparison). This early conclusion needs to be confirmed by longer time series in the next report.
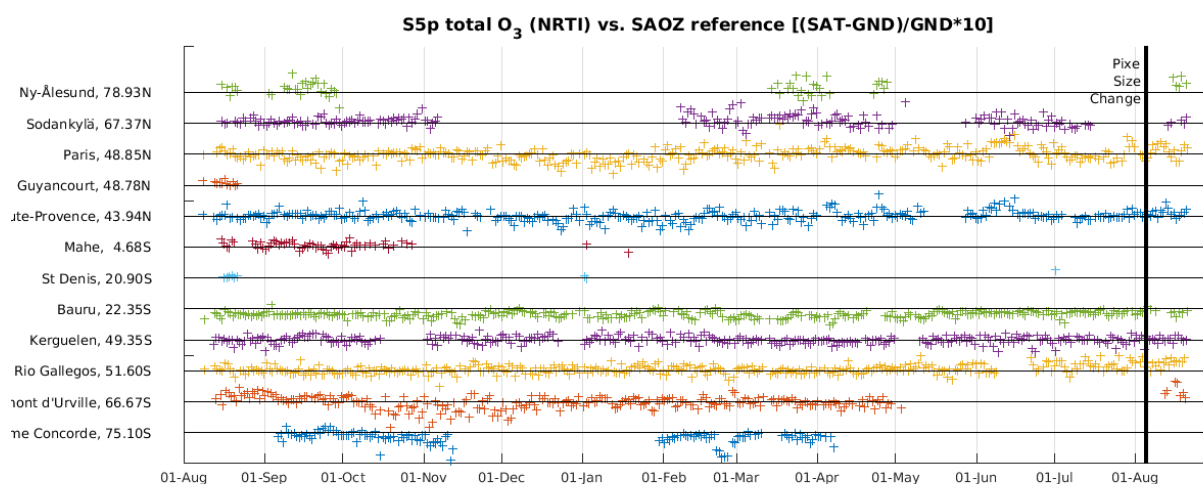
Figure 7: Time series of the difference between the S5P NRTI L2_O3 ozone column data and the SAOZ reference data at 12 stations from pole to pole, from August 2018 until the end of August 2019. The moment of the switch in TROPOMI pixel size (reduction to $3.5 \times 5.5 km^2$) is indicated by the solid vertical line.

S5P MPC

4.4 Validation of L2_O3 OFFL

4.4.1 Recommendations for data usage followed

Data users are encouraged to read the Product Readme File (PRF), Product User Manual (PUM) and Algorithm Theoretical Basis Document (ATBD) associated with this data product, all available on https://sentinels.copernicus.eu/web/sentinel/technical-guides/sentinel-5p/products-algorithms.

In order to avoid misinterpretation of the data quality, it is recommended to use only those TROPOMI pixels associated with a $\mathrm{qa\_value}$ above 0.5. Nevertheless, it must be noted that at this threshold all data with solar zenith angles larger than 80° are removed, leading to a significant rejection of measurements at high latitudes. Validation results suggest that also measurements at larger solar zenith angles are reliable and hence that this cut-off at 80° is not necessary.

According to validation results this criterion might be relaxed, but nevertheless, caution remains required for $\mathrm{qa\_value}$ below 0.5. Additional filter criteria for L2_O3 OFFL are the following:

- ozone_total_vertical_columnn should range within [0 to 0.45];

- ozone_effective_temperature should range within [180 to 280];

- fitted_root_mean_square should not be larger than 0.01.

4.4.2 Status of validation

This section presents a summary of the key validation results obtained by the MPC VDAF and by S5P Validation Team (S5PVT) AO projects. It is based on updates of the preliminary results reported at the S5P First Public Release Validation Workshop (ESA/ESRIN, June 25-26, 2018). Individual contributions to the workshop are archived in https://nikal.eventsair.com/QuickEventWebsitePortal/sentinel-5p-first-product-release-workshop/sentinel-5p, while up-to-date validation results and consolidated validation reports are available through the MPC VDAF Portal at http://mpc-vdaf.tropomi.eu.

Current conclusions are based on the S5P data obtained in the operational phase E2, from May 2018 until August 2019, and on the reference data available at the time of this report (typically until end of June 2019 for the Dobson and Brewer data, and until the middle of August 2019 for the ZSL-DOAS SAOZ data). For the current report, Brewer and Dobson measurements were obtained through both the World Ozone and UV Radiation Data Centre (WOUDC) in Toronto, the NDACC Data Host Facility, and WMO's Ozone Mapping Centre in Thessaloniki. If a station archives data into both WOUDC and NDACC HDF, the source with the most recent data is adopted. ZSL-DOAS measurements were collected through the SAOZ network Real-Time processing facility operated by LATMOS (LATMOS_RT). The validation is done using the Automated Validation Server of the MPC VDAF, the Multi-TASTE versatile validation system operated at BIRA-IASB, and the ozone validation system operated at AUTH.

Over the period, with respect to the reference data available at the time of this analysis, of the order of 40 to 250 unique co-locations have been identified at about 40 Brewer and Dobson sites and at 12 SAOZ sites, sampling many latitudes from the Arctic to the Antarctic (**Figure 8**).
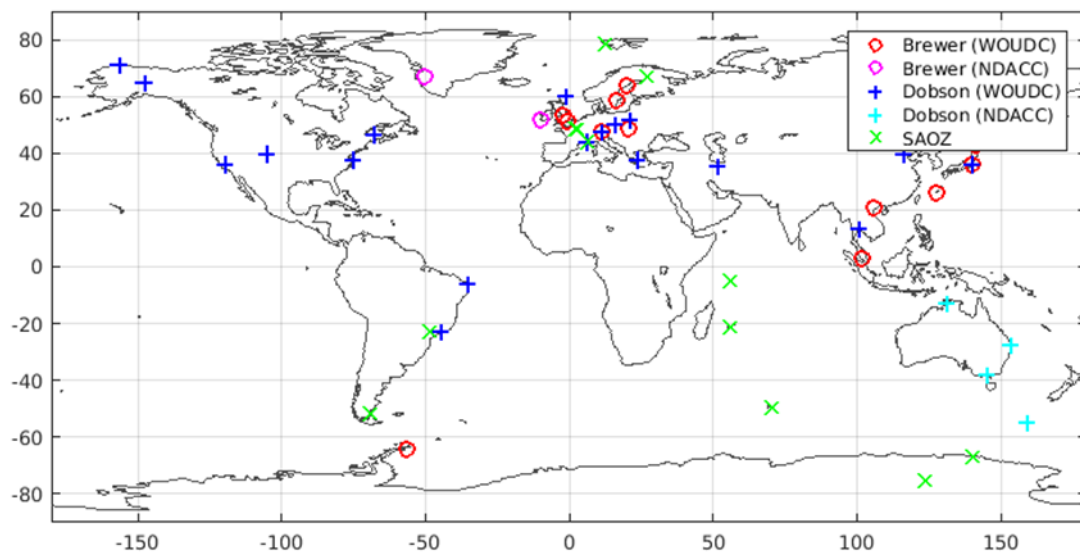
Figure 8: Geographical distribution of Brewer, Dobson and ZSL-DOAS ground-based stations for which suitable co-locations with S5P L2_O3 OFFL ozone data have been identified (period up to August 2019).

4.4.3   Bias

The systematic difference between S5p L2_O3 OFFL and reference ground-based data at individual stations rarely exceeds 2%, as depicted in **Figure 9**. The median bias calculated over the entire ground-based networks is of the order of +0.4%. Between 50˚S and 50˚N, the mean agreement with other satellite data derived with the same processor (GODFIT v4) is mostly within 1% as well (**Figure 10**). This median bias value falls well within the mission requirements (max. bias 3.5-5%).
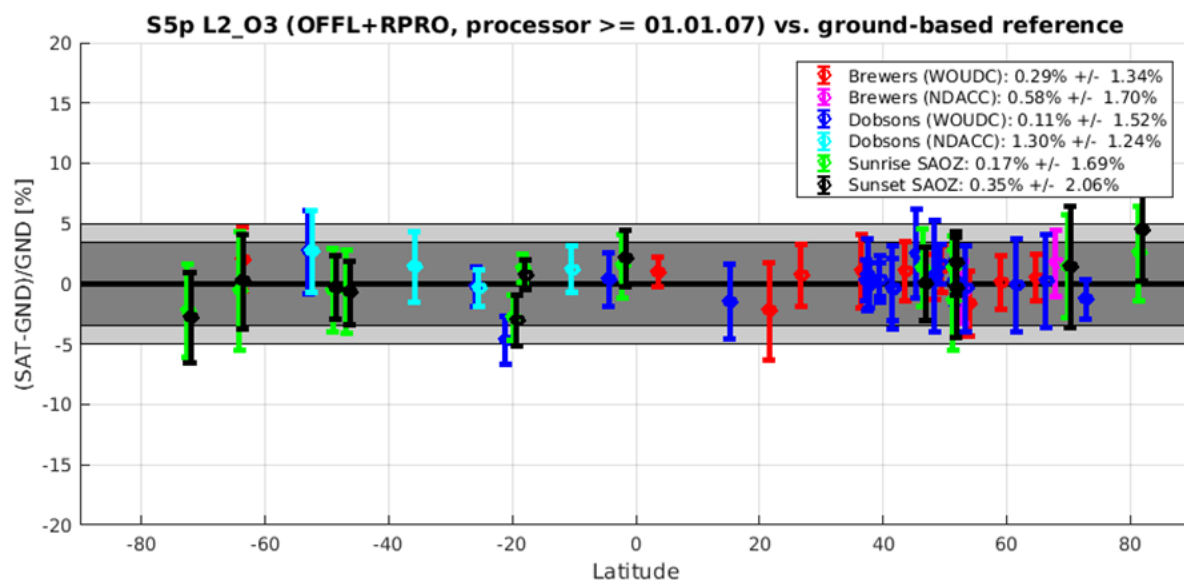
Figure 9: Meridian dependence of the median (the circular markers) and spread (±1 sigma, the error bars) of the percent relative difference between S5P TROPOMI L2_O3 (PDGS OFFL processor v1.1.7) and ground-based (GND) ozone column data, represented at individual stations from the Antarctic to the Arctic and per measurement type (Brewer, Dobson, and ZSL-DOAS). The values in the legend correspond to the median and spread of all median (per station) differences. For clarity, sunrise and sunset ZSL-DOAS results are represented separately (offset by -0.5˚ and +0.5˚ in latitude).
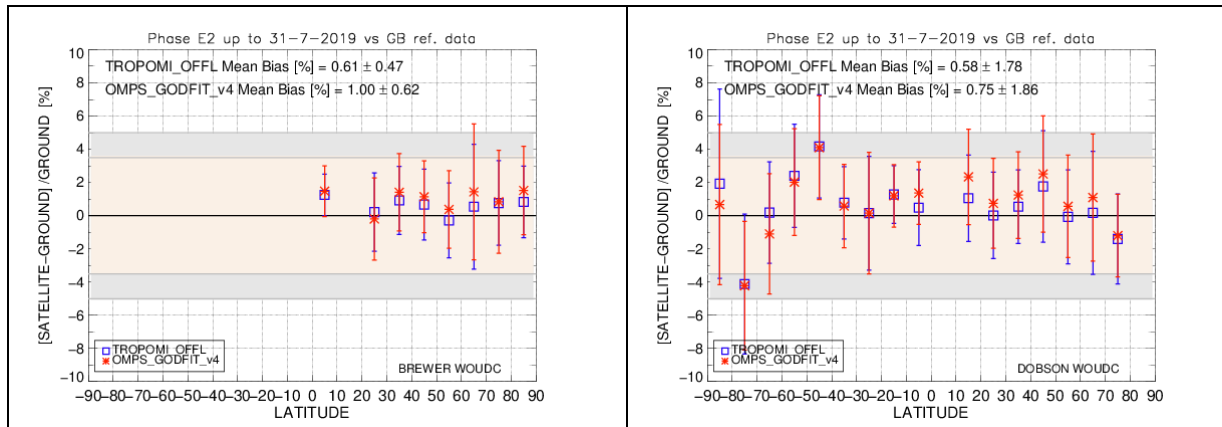
Figure 10: Comparison of the bias between two satellite products (S5P L2_O3 OFFL and OMPS GODFIT v4), and the Brewer (left-hand panel) and Dobson (right-hand panel) network total ozone data (datasets from WOUDC only). The time period of data used for these plots is May 2018 – July 2019 (not later due to ground-based data availability).

4.4.4 Dispersion

The ±1σ dispersion of the difference (between S5P and reference ground-based network data) around their median value rarely exceeds 3-4% for the comparisons with direct-sun instruments (cf. the error bars depicted in **Figure 9**). Combining random errors in both satellite and reference measurements with irreducible co-location mismatch effects, it is concluded that the random uncertainty on the S5P measurements falls within the mission requirements of max. 2.5%.

4.4.5   Dependence on influence quantities

The evaluation of potential dependence of the S5P bias and dispersion on the Solar Zenith Angle (SZA), Air Mass Factor (AMF) and cloud fraction (CF) of the TROPOMI measurement ….

The scatter of the data comparisons of about 2-3% increases up to 5% at large SZAs and at latitudes beyond 50° (**Figure 11**), which is expected knowing that random errors in both satellite and reference measurements as well as irreducible co-location mismatch errors increase at high latitude and low sun elevation. Similarly, there is a modest increase in scatter for measurements at largest cloud fraction.
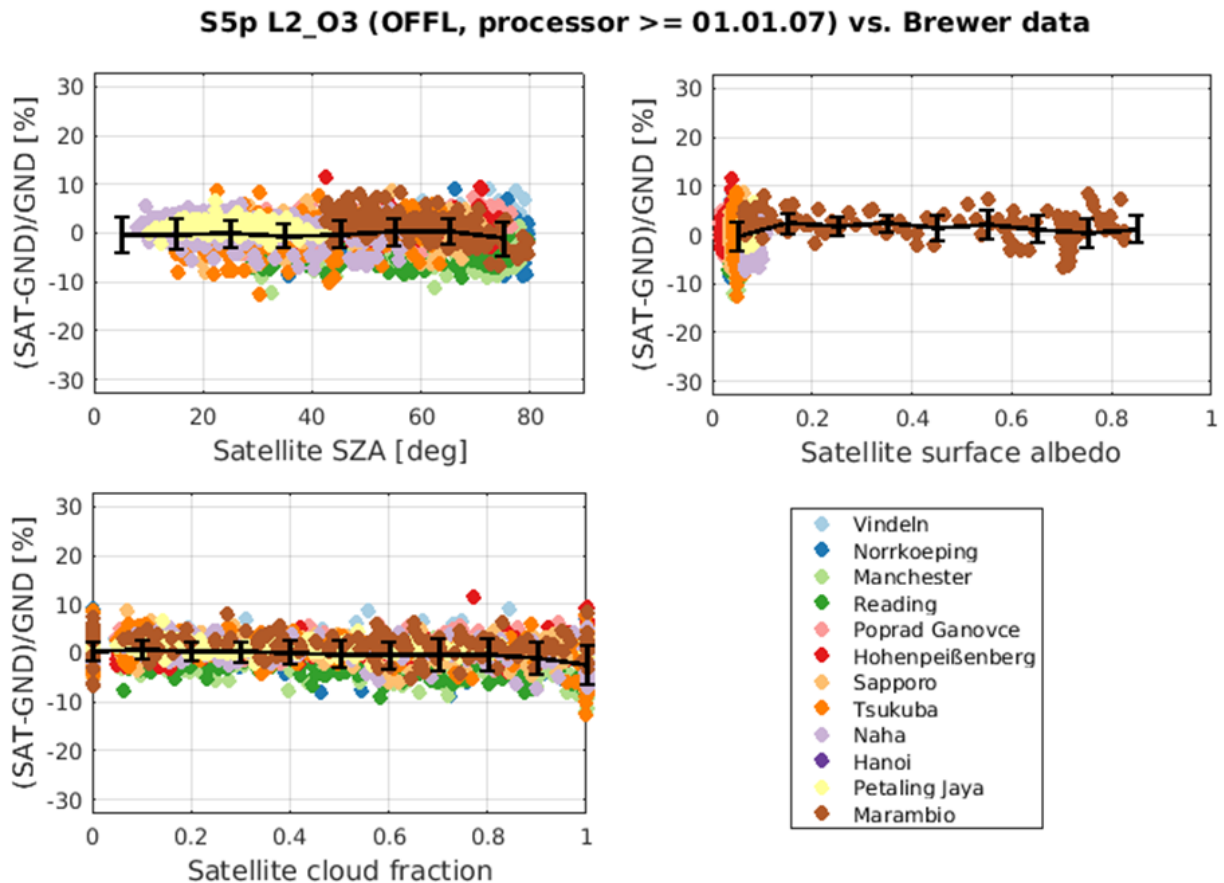
Figure 11: Dependence of the difference between S5P and ground-based Brewer ozone data on the satellite solar zenith angle (SZA), on the satellite fractional cloud cover (CF), and on the surface albedo, including a mean and standard deviation per 10-degree, 0.1 CF-increment and 0.1 albedo increment bin.

4.4.6   Short term variability

Qualitatively, at all of the 50 ground-based reference stations, short scale temporal variations in the ozone column as captured by ground-based instruments are reproduced very similarly by S5P, as illustrated in **Figure 12**. The overall good agreement is corroborated by Pearson correlation coefficients always above 0.95.
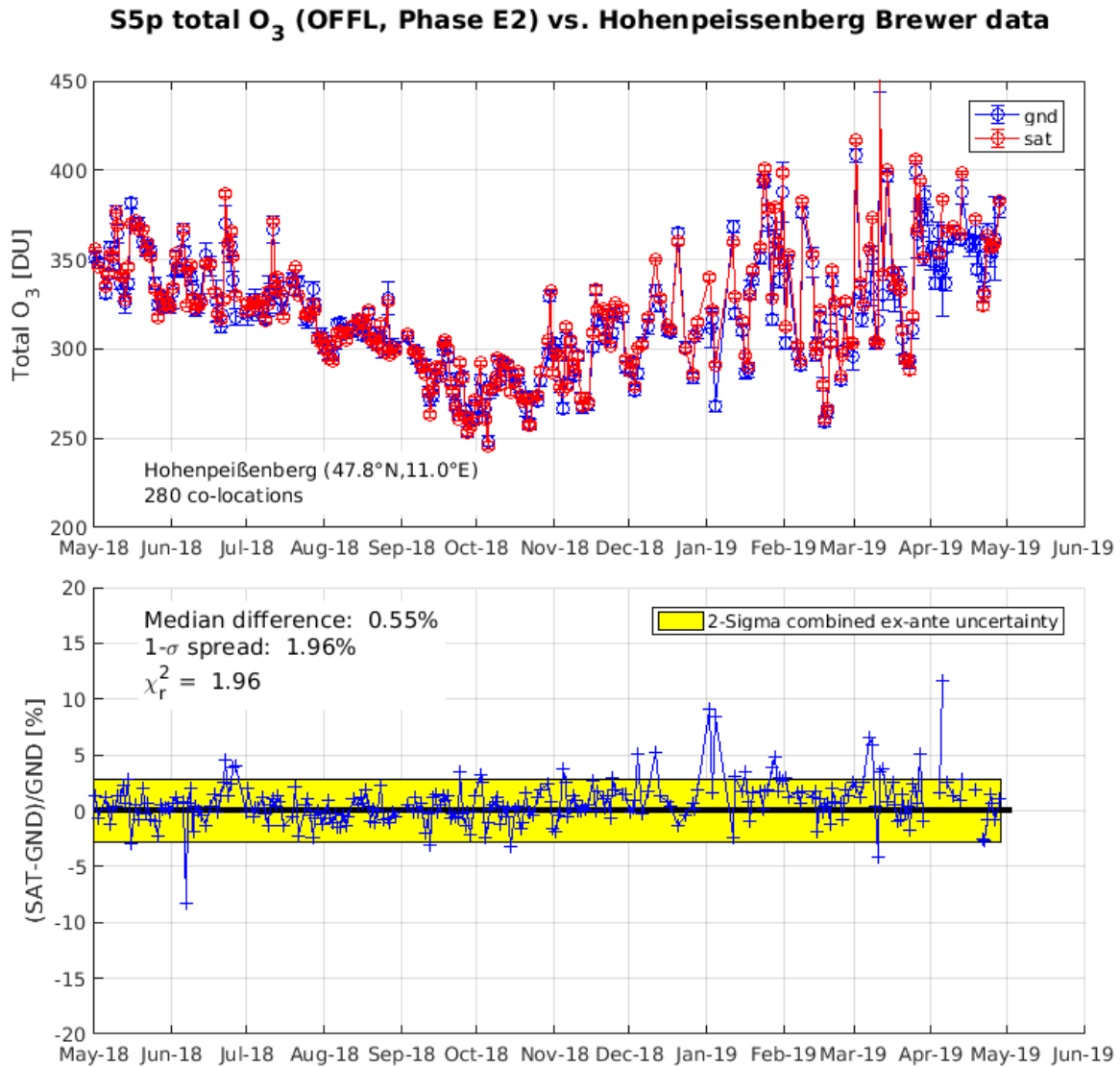
Figure 12: Time series of S5P and Brewer total ozone data at the NDACC station of Hohenpeißenberg (Germany). Original time series of co-located data are presented in the upper panel, the differences in the lower panel.

4.4.7   Geographical patterns

The bias between S5P L2_O3 and other satellite data sets exhibits patterns correlating with weather patterns, atmospheric circulation features, and ground albedo types. When looking at satellite datasets obtained from different satellites (e.g., TROPOMI on S5P in the early afternoon and GOME-2 on MetOp-A in the mid-morning), patterns correlating with weather structures and atmospheric circulation might simply reflect – at least partly – real ozone changes between the different satellite overpass times. However, patterns correlating with ground albedo types cannot. Furthermore, looking at S5P ozone datasets retrieved from the same Level-1 data processed with different Level-1-to-2 retrieval algorithms, those patterns subsist, as illustrated in **Figure 6** where NRTI and OFFL data are compared.

Geographical patterns in the L2_O3 ozone column data products – revealed by comparisons with other satellite datasets – are likely to be associated with differences in the processing of the cloud properties, in the use of either a surface albedo climatology or a fitted effective albedo, and, in the case of a comparison of data from two different satellites, to differences in overpass times (3.5 hours difference between S5P and GOME-2).

4.4.8   Other features

None to report.

5   Validation Results: L2_O3_TCL

5.1   L2_O3_TCL products and requirements

This Section reports on the validation of the S5P TROPOMI L2_O3_TCL product identified in **Table 1**. Validation results are discussed with respect to the product quality targets outlined in **Table 3**.

The S5P O3_TCL data files contain tropospheric ozone columns obtained by the Convective Cloud Differential algorithm (CCD). The CCD data are sampled daily. They represent the three-day average of the ozone partial column between surface and 270 hPa (~10.5 km) under cloud-free conditions on a 0.5° latitude by 1° longitude grid between 20°S and 20°N. Hence, in contrast to most other S5P products in this document, it concerns a gridded data set, and, it covers about 2/3 of the full vertical range of the tropical troposphere.

Variables related to a second tropospheric ozone algorithm, the Cloud Slicing Algorithm (CSA), are present in the data files but all corresponding entries are set to a fill value for the time being, until further maturation of the algorithm and public release of the CSA product. The CSA data are not discussed in the following.

5.2   Validation approach

Routine validation of the S5P TROPOMI L2_O3_TCL tropospheric ozone data products entails both qualitative, visual inspections of daily maps of product variables, and quantitative comparisons of these to independent reference measurements by ground-based and satellite instruments.

5.2.1   Ground-based networks

Reference measurements by ozonesondes launched at nine sites of the ground-based SHADOZ network (ER_SHADOZ) are compared routinely to S5P data. The SHADOZ data version used here is V06. The ozonesonde profile data are first quality controlled (Hubert et al., 2016) and then integrated over the vertical range of the S5P CCD product (surface to 270 hPa) to obtain a comparable tropospheric column value. A reference measurement is assumed to be in co-location with a TROPOMI measurement provided that: (a) the SHADOZ station is located in the S5P CCD grid cell, and, (b) the ozonesonde was launched in the satellite time window. Data that do not match these criteria are not used in the calculation of the quality indicators (**Figure 15** and **Figure 17**). If more than one reference tropospheric ozone column falls in a co-location window, then these are averaged prior to comparison. Such a double coincidence occurs very rarely in the considered data sample. Finally, it is important to note that the spatial and temporal sampling properties of satellite and reference data records are quite different, which adds mismatch uncertainties in the comparison results on top of the combined data uncertainties.

5.2.2   Satellites

S5P TROPOMI L2_O3_TCL tropospheric ozone column data are also compared to Aura OMI and MetOp-B GOME-2 tropospheric ozone column data using the GODFIT_v4 CCI algorithm developed within ESA's Climate Change Initiative (CCI). It is based on the GODFIT total column data but the sampling was adapted to allow a more direct comparison to TROPOMI, i.e. 5 days averaging windows instead of monthly data and the tropospheric top pressure set to 270 hPa instead of 200 hPa. The horizontal resolution of the OMI and GOME-2B data products was increased from 1.25°x2.5° to 1°x2°.

5.2.3   Field campaigns and modelling support

None for this report.

5.3   Validation of L2_O3_TCL OFFL (CCD)

5.3.1   Recommendations for data usage followed

Data users are encouraged to read the Product Readme File (PRF), Product User Manual (PUM) and Algorithm Theoretical Basis Document (ATBD) associated with this data product, all available on https://sentinels.copernicus.eu/web/sentinel/technical-guides/sentinel-5p/products-algorithms.

In order to avoid misinterpretation of the data quality, we followed the recommendation to use only TROPOMI grid cells associated with a $\mathrm{qa\_value}$ strictly above 0.7.

5.3.2   Status of validation

This section presents a summary of the key validation results obtained by the MPC VDAF and by S5P Validation Team (S5PVT) AO projects. It is based on updates of the first results reported at the S5P L2_O3_TCL and L2_CH4 Data Release Workshop (teleconference, February 20, 2019). Individual contributions to the workshop are archived in https://earth.esa.int/web/sentinel/technical-guides/sentinel-5p/calibration-validation-activities/sentinel-5p-third-products-release-workshop, while up-to-date validation results and consolidated validation reports are available through the MPC VDAF Portal at http://mpc-vdaf.tropomi.eu.

Over the period 30 April 2018 – 31 August 2019, the ground-based validation analysis considers 490 S5P OFFL CCD data products and 479 ozonesonde flights at nine sites across the tropics (**Figure 13** and **Figure 14**). S5P data averaged over the entire tropical region are also intercompared (**Figure 16**) to GOME-2B data (May 2018 – November 2018) and to OMI data (May 2018 – April 2019).
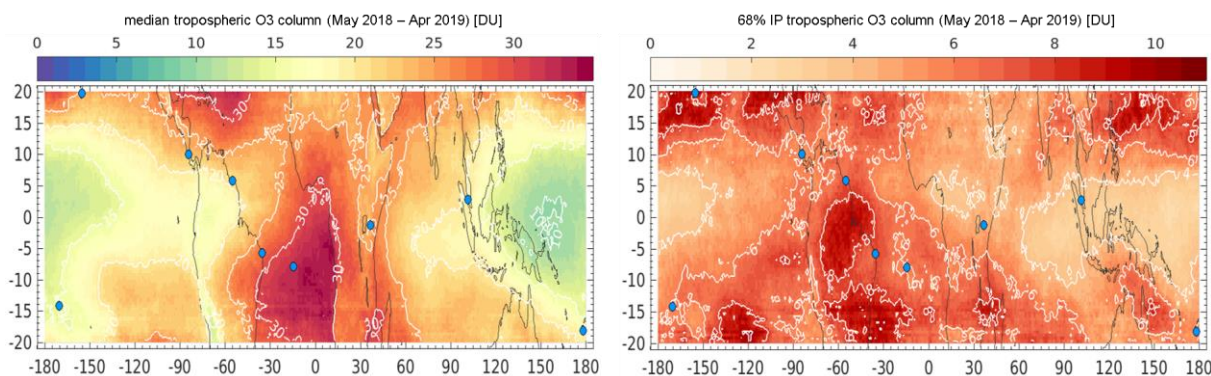
Figure 13: Median value (left) and 68% interpercentile (right) of S5P OFFL tropospheric O_3 column data (CCD) over a full year of operations (September 2018 – August 2019). Blue markers locate the nine ground-based ozonesonde stations used in the validation analysis. These maps provide context to **Figure 14** and **Figure 15**.

5.3.3   Bias

S5P tropospheric O_3 column values are on average larger than the ozonesonde values at 8 out of the 9 sites (**Figure 15** and **Figure 17**). The mean bias over the network is +14% or +2.8 DU (**Figure 17**, centre and bottom left). This is compliant with the mission requirement for a systematic uncertainty of maximum 25%.

Difference time series between S5P and comparable satellite data (OMI and GOME-2B) averaged over the 20°N – 20°S tropical belt are shown in **Figure 16**. The agreement with OMI is good, with a mean difference of -0.6 DU or -3%. The larger mean difference of +1.6 DU or +7% compared to GOME-2B might indicate a slight general overestimation of TROPOMI and may also -at least partly- be attributed to the different overpass times of MetOp-B (9:30 desc) and S5P (13:30 asc) in combination with the diurnal cycle of tropospheric ozone.

5.3.4   Dispersion

The half 68% interpercentile of the difference (between S5P and ozonesonde data) ranges within 12-34% or 2.8-7.2 DU (**Figure 15** and **Figure 17**), and the network average is 23% or 4.3 DU (**Figure 17**, centre and bottom right). Dispersion values at five sites are not compliant with the mission requirement for the random component of the uncertainty (<25%). However, all five are located in an area with large natural percentage variability in the tropospheric O_3 field and there is a considerable difference in spatio-temporal sampling between S5P and ozonesonde. In addition, the random component of the uncertainty of the ozonesonde measurement contributes about 5-10% to the observed spread in the differences. Hence, the uncertainty of the S5P data is better than the 23% observed spread in the comparisons to ozonesonde and therefore overall compliant with the mission requirement.

Satellite intercomparisons exhibit a dispersion of 4.1-4.2 DU or ~19% when averaged over the entire tropical belt (**Figure 16**), which is in line with the average dispersion found in comparisons to the ground-based network.

5.3.5   Dependence on influence quantities

Nothing to report.

5.3.6   Short term variability

S5P time series in **Figure 14** show the anticipated impact of biomass burning (high tropospheric O_3 values) at Atlantic and African sites (Heredia, Paramaribo, Natal, Ascension Island, Nairobi) and signs of intense convective activity (low tropospheric O_3 values) at Pacific stations (Samoa, Suva, Sepang Airport). During the 2018 biomass burning season the positive S5P bias w.r.t. Paramaribo, Heredia and Nairobi is clearly larger than during the rest of the year. The temporary, additional bias amounts to about 25% or 5 DU. This finding is possibly related to a S5P data quality issue and is being monitored during the 2019 biomass burning season. Comparisons to Paramaribo data during July-August 2019 show the onset of another period of elevated positive bias. Ozonesonde data at the other Atlantic and African sites are not yet available but should be by next update of this document. Co-located S5P and reference measurements correlate fairly well for sites with well-sampled comparison time series. Pearson's skipped correlation coefficients range between 54% and 78% at individual stations, while the network average is 63% (**Figure 17**, top left).

5.3.7   Geographical patterns

Annual median TROPOMI data (September 2018 – August 2019, **Figure 13**) capture the well-known South Atlantic ozone maximum associated with biomass burning, lightning and ozone precursors, as well as the well-known equatorial Pacific lows. Higher mean levels in the 15°-20° tropical belts are a result of intrusion of ozone-rich air from higher latitudes. It shows the ability of S5P to observe the expected large-scale geographical patterns. At smaller scales, however, two artificial sampling-related patterns are noted.

The CCD algorithm requires an ample sampling of input total O_3 column data to allow a robust estimate of a reference stratospheric O_3 column. This requirement is not always fulfilled. As a result, biases of 1-2 DU between neighbouring latitude bands are found in many S5P data products. The orbital sampling by the S5P instrument progression imprints another, somewhat more elusive spatio-temporal bias pattern that will be quantified in the near-term future.

5.3.8   Other features

CCD data availability is much reduced poleward of ~15° latitude in the winter hemisphere (see e.g. time series at Hilo, Suva or Samoa in **Figure 14**) since the algorithm requires a sufficient number of highly convective opaque clouds. Most of these are formed in or close to the Intertropical Convergence Zone located mainly in the summer hemisphere. Suitable cloud conditions therefore occur less frequently in the winter hemisphere.

Filtering on $qa\_value > 0.7$ does not remove all data considered bad. In some S5P products the screening procedure omits 0.5° latitude bands poleward of 15° latitude in the winter hemisphere which should have been removed. This issue will be tackled in future version of the processor. For the time being, a stricter threshold may solve the issue in some cases.
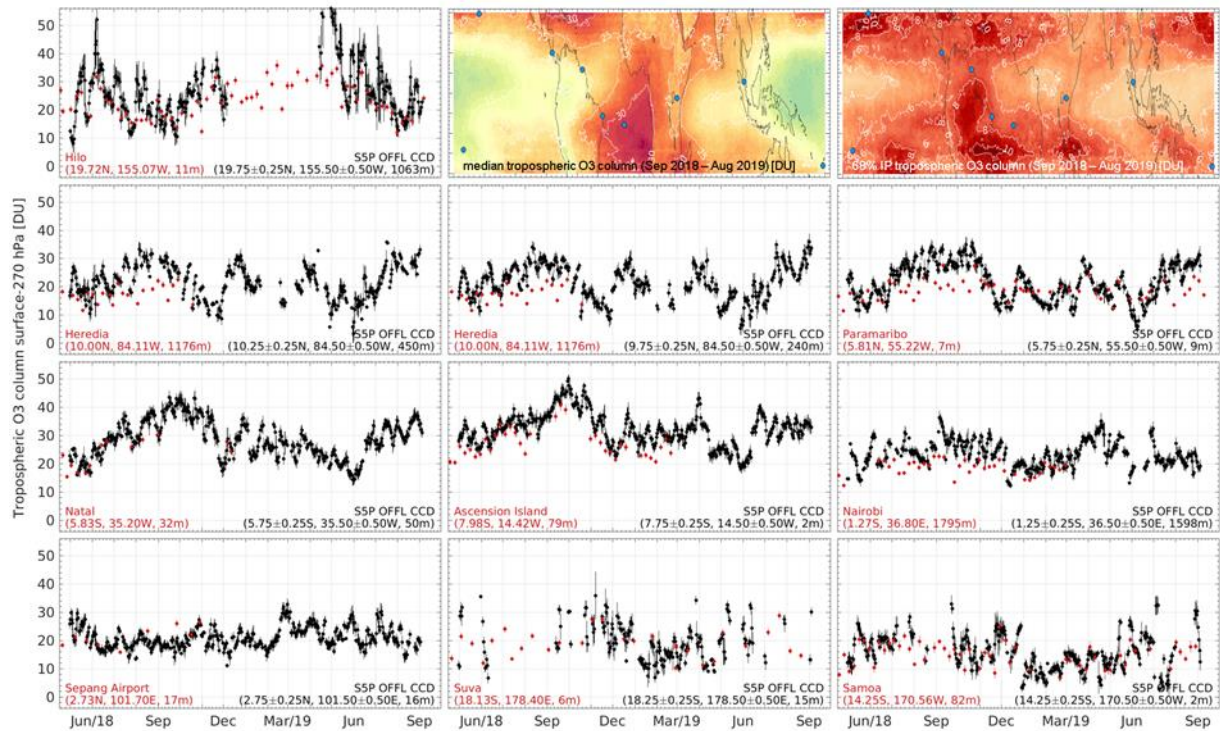
Figure 14: Time series of spatially co-located tropospheric O_3 column data by ozonesonde (red) and by S5P OFFL v01.01.05+v01.01.06+v01.01.07 (black). All data have been screened following recommendations by the data providers. The first row also maps the location of the ozonesonde sites and the characteristics of the tropospheric O_3 field (median and 68% interpercentile over one year of S5P data, see **Figure 13**).
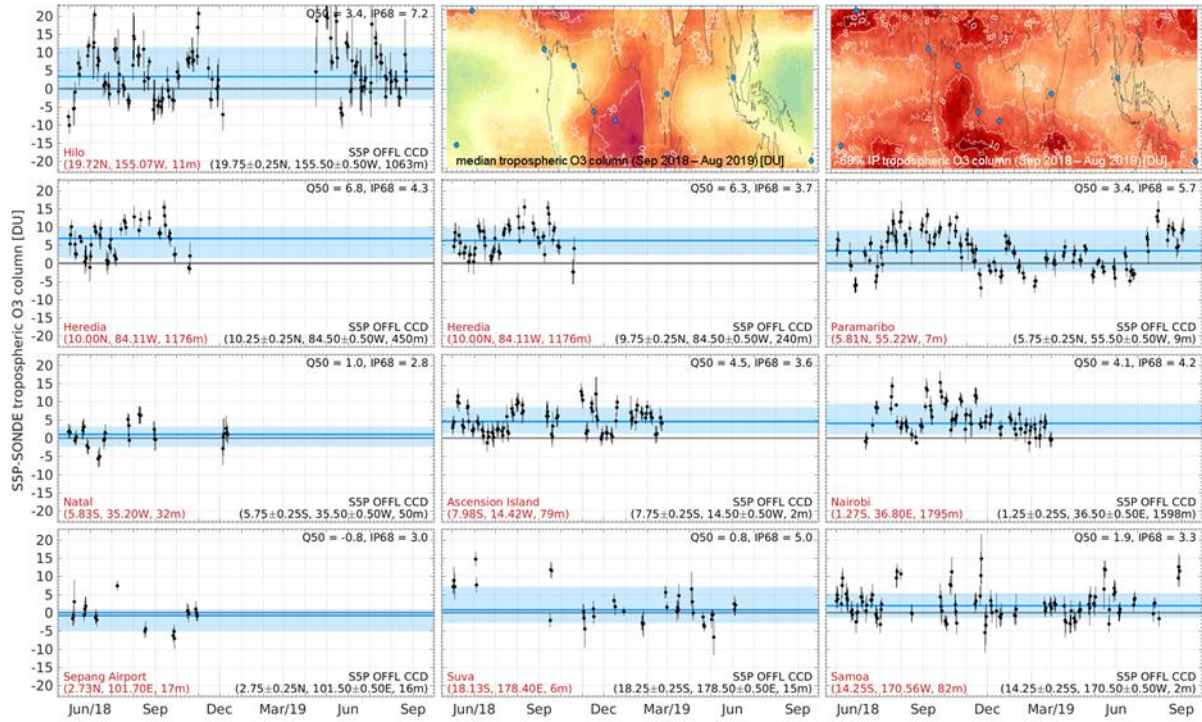
Figure 15: Time series of the absolute difference between spatially and temporally co-located S5P and ozonesonde tropospheric O_3 column data. The blue line and shaded area shows the median value and the range between the 16% and 84% percentiles. Positive values indicate a high bias of S5P w.r.t. the reference. The first row also maps the location of the ozonesonde sites and the characteristics of the tropospheric O_3 field (median and 68% interpercentile over one year of S5P data, see **Figure 13**).
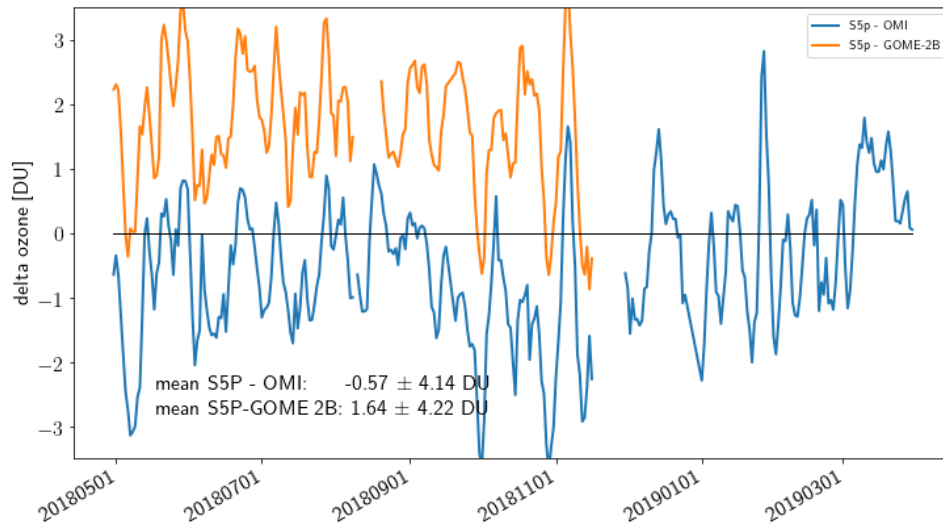
Figure 16: Difference time series of daily tropospheric O_3 column data averaged over the 20°S – 20°N tropical belt. S5P OFFL CCD data are compared to satellite data by OMI and GOME-2B, positive values indicate a high bias of S5P w.r.t. the reference.
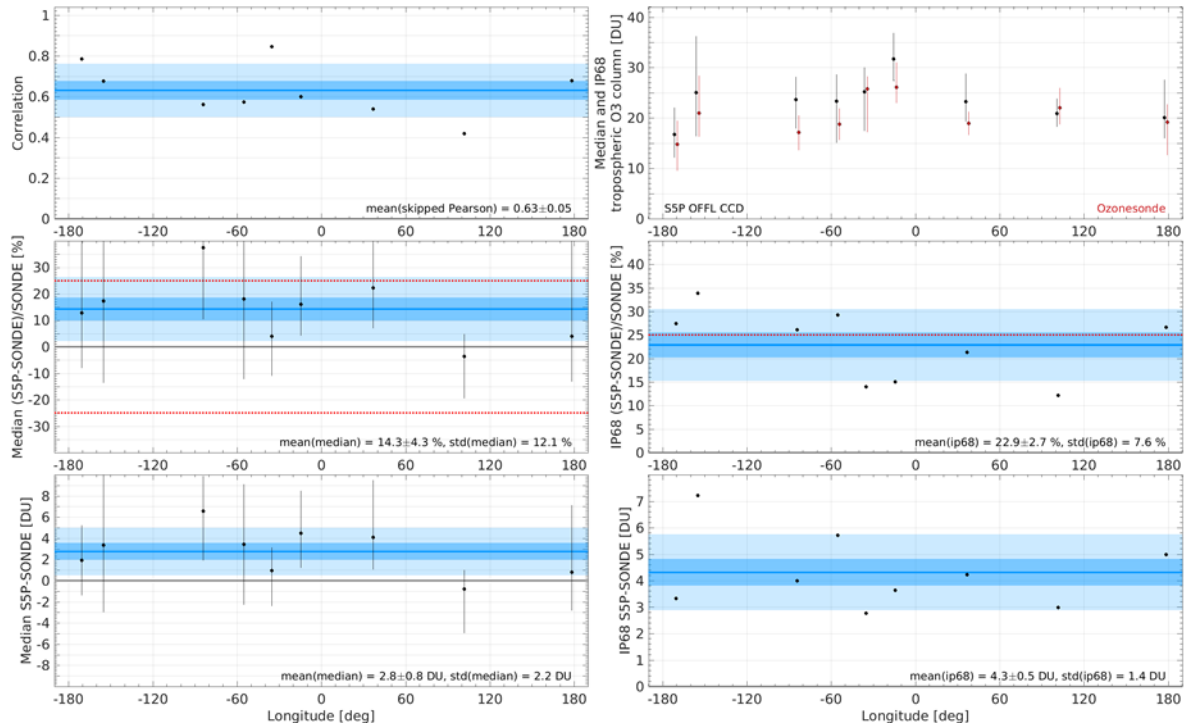
Figure 17: Overview of correlation (top left), median bias (middle & bottom left) and intercomparison spread (middle & bottom right) of S5P tropospheric O_3 column data for each SHADOZ site (black markers). Black vertical bars represent the 68% interpercentile of the comparison time series. The mean, standard error of the mean (1σ) and standard deviation (1σ) of the quality indicator across the network are shown as a horizontal blue line and shaded areas.

5.3.9   Other features

None to report.

6 Validation Results: L2_NO2

6.1 L2_NO2 products and requirements

This Section reports on the validation of the following geophysical variables of the S5P TROPOMI L2_NO2 data products identified in **Table 1**: the NO_2 stratospheric column, the NO_2 tropospheric column, and the NO_2 total column. Validation results are discussed with respect to the product quality targets outlined in **Table 3**.

The NRTI and OFFL processors are producing very similar results. Thus, mainly the validation of the L2_NO2 OFFL product is reported hereafter. This product is more advanced due to the reprocessing of S5P data. Subsection 0 demonstrates evidence that NRTI and OFFL data do not differ significantly and that their respective validations yield similar conclusions.

6.2 Validation approach

6.2.1 Ground-based monitoring networks

Stratospheric NO_2 – ZSL-DOAS UV-Visible Spectrometers

S5P TROPOMI L2_NO2 stratospheric nitrogen dioxide column data are compared routinely to reference measurements acquired by ZSL-DOAS (Zenith-Scattered Light Differential Optical Absorption Spectroscopy) UV-Visible spectrometers (Pommereau and Goutail, 1988; Hendrick et al., 2011). Those instruments perform network operation in the context of the Network for the Detection of Atmospheric Composition Change (NDACC). ZSL-DOAS data have a bias of less than 10% and a random uncertainty better than 1%.

To account for effects of the photochemical diurnal cycle of stratospheric NO_2, the ZSL-DOAS measurements, obtained twice daily at twilight at each station, are adjusted to the S5P overpass time using a model-based factor. The latter is calculated with the PSCBOX 1D stacked-box photochemical model (Errera and Fonteyn, 2001; Hendrick et al., 2004), initiated with daily fields from the SLIMCAT chemistry-transport model (CTM). The amplitude of the adjustment depends strongly on the effective SZA assigned to the ZSL-DOAS measurements. It is taken here to be 89°. The uncertainty related to this adjustment is on the order of 10%. To reduce mismatch errors due to the significant difference in horizontal smoothing between S5P and ZSL-DOAS measurements, S5P NO_2 values (from ground pixels at high resolution) are averaged over the footprint of the air mass to which the ground-based zenith-sky measurements are sensitive.

At this stage of the S5P routine operations, most of the ZSL-DOAS validation data have been obtained through the SAOZ near-real-time processing facility operated by the CNRS LATMOS, from the 14 stations located between 79°N and 75°S. Most of them are highlighted in **Figure 18**.

Tropospheric NO_2 – MAX-DOAS UV-Visible Spectrometers

S5P TROPOMI L2_NO2 tropospheric nitrogen dioxide column data are routinely compared to reference measurements acquired by MAXDOAS (Multi-AXis Differential Optical Absorption Spectroscopy) UV-Visible spectrometers. Several of those instruments perform network operation in the context of the Network for the Detection of Atmospheric Composition Change (NDACC).

At the present stage of S5P routine operation, four MAX-DOAS stations have contributed data (Athens and Bremen from IUP-B and Cabauw and De Bilt from KNMI) and are included in the operational validation. MAXDOAS tropospheric NO_2 column data have a bias of maximum 20% and a precision better than 30% at this set of stations.
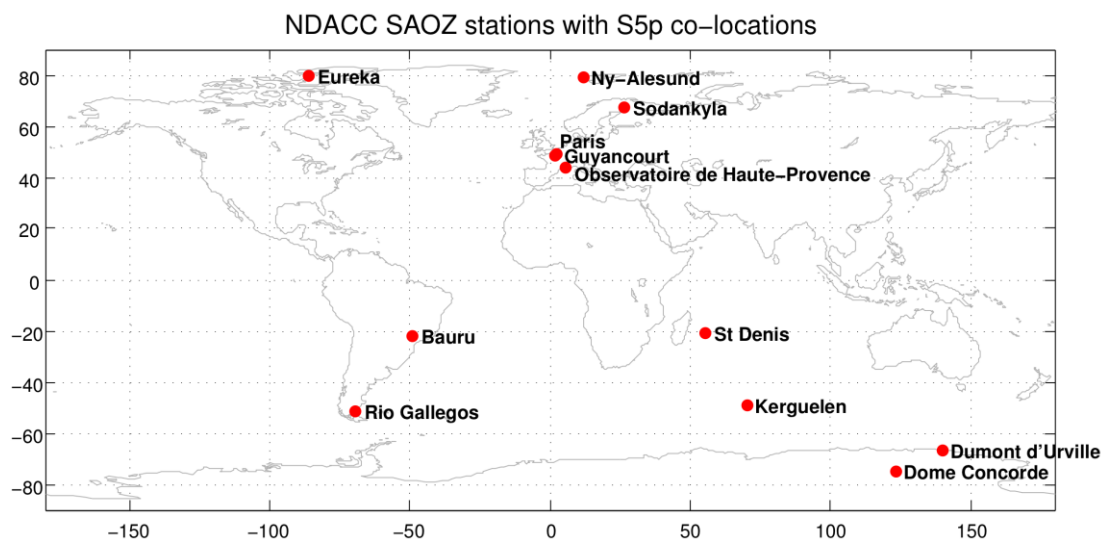
Figure 18: Geographical distribution of the ZSL-DOAS/SAOZ instruments measuring routinely stratospheric NO_2 and yielding, thanks to the LATMOS_RT facility, co-locations with the current S5P L2_NO2 data set.

Total NO_2 – Pandora Direct-Sun UV-Visible Spectrometers

S5P TROPOMI L2_NO2 nitrogen dioxide summed column data (troposphere + stratosphere) are routinely compared to reference measurements acquired by the Pandora system. Those instruments perform network operation in the context of the Pandonia Global Network (PGN). Pandora total NO2 data have a bias of maximum 10-15% and a precision of roughly 0.28 Pmolec/cm² (about 10%). Comparisons at 14 sites are operational on the VDAF Automated Validation Server. The comparison criteria on the VDAF-AVS are: qa_value > 50; pixel covers site; Pandonia measurement with flag not 0, 1, 10 or 11 is excluded; |Δt|<30 min; closest Pandonia measurement in time, In this work, comparison data from the VDAF-AVS are further filtered: only Pandonia measurements with flag value of 0 or 10 are kept.

If the Pandora instrument is situated at an elevated site above low-lying tropospheric pollution, the Pandora measurement can be more closely related to stratospheric NO_2, but one must keep in mind a potential free troposphere component as well.

6.2.2   Satellites

S5P TROPOMI L2_NO2 nitrogen dioxide column data are also compared to similar data from the Ozone Monitoring Instrument (OMI) retrieved with both the QA4ECV and the IUP-UB algorithm. OMI is onboard the EOS-Aura satellite, launched in July 2004.

6.2.3   Field campaigns and modelling support

None for this report.

6.3 Validation of L2_NO2

6.3.1 Recommendations for data usage

In order to avoid misinterpretation of the data quality, it is recommended at the current stage to only use those TROPOMI pixels associated with a qa_value above 0.75. This removes cloudy scenes (cloud radiance fraction > 0.5), scenes covered by snow/ice, several other errors, and problematic retrievals. As clouds are less of a problem for S5P stratospheric NO2 retrievals and for stratospheric data comparisons, data with qa_value above 0.5 are nevertheless used hereafter. For further details, data users are encouraged to read the Product Readme File (PRF), Product User Manual (PUM) and Algorithm Theoretical Basis Document (ATBD) associated with this data product, all available on https://sentinels.copernicus.eu/web/sentinel/technical-guides/sentinel-5p/products-algorithms

6.3.2 Status of validation

This section presents a summary of the key validation results obtained by the MPC VDAF and by S5PVT AO projects. The validation is done using the Automated Validation Server of the MPC VDAF, the Multi-TASTE versatile validation system operated at BIRA-IASB, the validation tools of IUP-UB, and the HARP toolset (version 1.6).

The NRTI data covers the full range of versions from 01.00.01 to 01.03.02 as there is no reprocessing necessary. The OFFL data has been reprocessed now to version 01.02.02 from 2018-05-01 until 2018-10-17. After that, we now have 5 different processor versions from 01.02.00 up to 01.03.02, which is the current version started in 2019-06-26.

6.3.3   Bias

Stratospheric NO$_2$ Column

The VDAF site supplies validation results from 14 NDACC SAOZ stations, sampling the latitude range from 80°N (Eureka) to -75°S (DOME-C). Overall, 2375 measurement pairs over the first year (May 2018 – August 2019) have been identified. The SAOZ stratospheric NO$_2$ column values measured at twilight are converted to the measurement time of TROPOMI using the aforementioned PSCBOX 1D stacked-box photochemical model initiated by SLIMCAT fields.
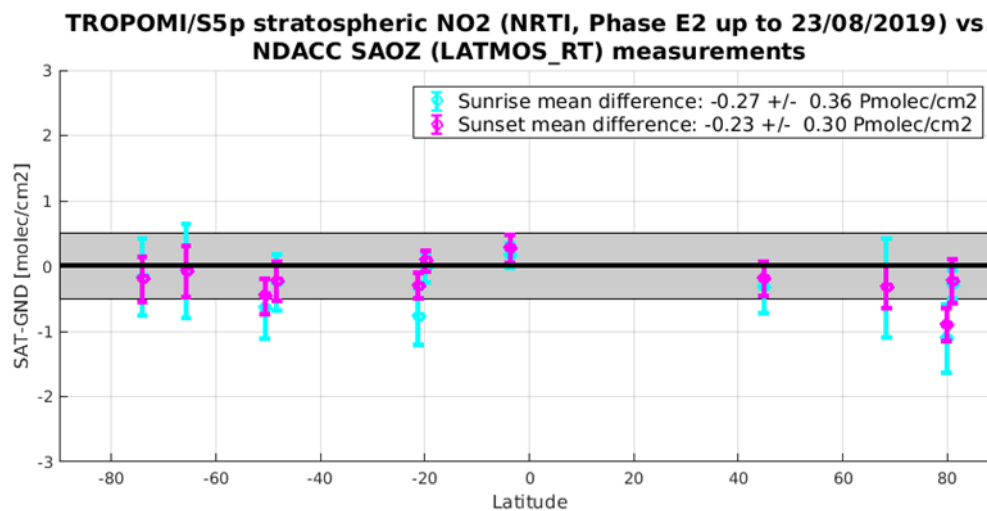
Figure 19: Meridian dependence of the mean (the circular markers) and spread (±1σ error bars) of the differences between S5P TROPOMI L2_NO2 (NRTI) stratospheric column data and SAOZ reference data, represented at individual NDACC stations from the Antarctic to the Arctic. The values in the legend correspond to the mean and spread of all mean (per station) differences. This graph includes results for processor versions greater or equal to 1.1.0.

S5P L2_NO2 NRTI stratospheric column data are generally lower than the ground-based values by approximately 0.25 Pmolec/cm^2, with a station-to-station scatter of this bias of similar magnitude (**Figure 19**). This is within the mission requirement of a maximum bias of 10% (equivalent to 0.2-0.4 Pmolec/cm^2, depending on latitude and season). The measurement number weighted bias for the OFFL data (2743 measurement pairs) is -11.4% with a station-to-station scatter of 9%, which is slightly higher than the bias requirement of 10%.

The Pandora instrument at Izaña is at an elevated site (2360 m) and the measured signal corresponds more closely to the S5P L2_NO2 stratospheric column rather than the total column. At the date of inspection of the VDAF-AVS (2019-08-26), 183 co-located points were available for comparison (after excluding Pandora measurements with flag=11, and one additional negative Pandora outlier), between 2018-11-26 and 2019-08-10. The mean difference of S5P L2_NO2 OFFL stratospheric column vs Pandora at Izaña is -0.02±0.04 Pmolec cm^{-2} and the median difference -0.05 Pmolec cm^{-2}. Mean and median relative differences are 0.7% and -2%, respectively. It should be noted that, although the Pandora instrument at Izaña usually is above low-lying tropospheric pollution, it is still sensitive to NO$_2$ in the free troposphere. This suggests therefore a small positive bias for S5P. Note that restricting to cloud fraction > 0.2 (which improves the correlation, but leaves only 41 co-located points) to filter out tropospheric NO$_2$ pollution, the bias slightly increases to -0.04 Pmolec cm^{-2}.

Tropospheric NO$_2$ Column

S5P L2_NO2 RPRO+OFFL tropospheric columns are compared to the ground-based MAX-DOAS column data at 4 sites in Europe (between 174 to 270 colocations per site, 843 measurement pairs) using the VDAF Automated Validation Server (inspection at 2019-08-27). The mean difference at each site varies between -1.2 Pmolec cm^{-2} and -2.3 Pmolec cm^{-2} and the median difference between -0.2 Pmolec cm^{-2} and -1.9 Pmolec cm^{-2}. The median relative difference varies between -5% (Athens) and -30% (Cabauw, Bremen).

The measurement number weighted bias (823 measurement pairs) is -29.5% with a scatter of 7%. These results are within the accuracy requirements of 50%.

Total NO$_2$ Column

Based on measurements from 14 Pandora stations (**Figure 20**) between 64.9°N and -35.3°S, the overall bias weighted by the number of measurements (2915 measurement pairs) is -21.1% with a high station-to-station scatter of 30%. These results are within the accuracy requirements of 30%, which is the average of the tropospheric and stratospheric bias maxima.

We highlight here 3 different comparison cases. At Alice Springs (Australia), where NO$_2$ column values are small (mostly between 2-4 Pmolec/cm^2), a small bias of 0.3 Pmolec cm^{-2} is seen (+10% median relative difference). At New York Bronx (United States), there is a wider distribution of NO$_2$ values (2-30 Pmolec/cm^2), but still the bias is quite small (mean difference = -0.6 Pmolec cm^{-2}, median relative difference = -5%). Finally, at Sapienza (Rome, Italy), Pandonia column values can reach almost 40 Pmolec cm^{-2}. S5P displays a bias (mean difference) of -8 Pmolec cm^{-2} (-45% median relative difference) here. Locally enhanced NO$_2$ probably contributes to this bias.

6.3.4   Dispersion

Stratospheric NO$_2$ Column

The ±1σ dispersion of the difference between S5P stratospheric column and reference data around their mean value rarely exceeds 0.3 Pmolec/cm² at sites without tropospheric pollution (cf. the error bars in **Figure 19**). When combining random errors in the satellite and reference measurements with irreducible co-location mismatch effects, it can be concluded that the random uncertainty on the S5p stratospheric column measurements falls within mission requirements of max. 0.5 Pmolec/cm².

The ±1σ dispersion of the difference between S5P stratospheric column and Pandonia data at Izaña is 0.4 Pmolec/cm^2 when expressed as standard deviation, and 0.3 Pmolec/cm^2 when expressed as the ½ of the 68 interpercentile (½ IP68)), i.e., below the 0.5 Pmolec/cm^2 requirement. Taking only cloudy pixels into account, also the standard deviation becomes 0.3 Pmolec/cm^2. Differences in dispersion arises from errors in satellite and reference measurements, and comparison errors, therefore the 0.3 Pmolec/cm^2 is an upper limit. The Pearson correlation coefficient is 0.73, and this increases to 0.81 when taking only clouded pixels (cloud fraction>0.2) into account, to limit the impact of tropospheric NO$_2$. Using this cloud filter, and in the limit of assigning all difference dispersion to errors from reference measurement and from comparison error, an ordinary least square regression of Pandonia versus S5P NO2 stratospheric column results in a slope near unity and small negative intercept (see **Figure 21**).
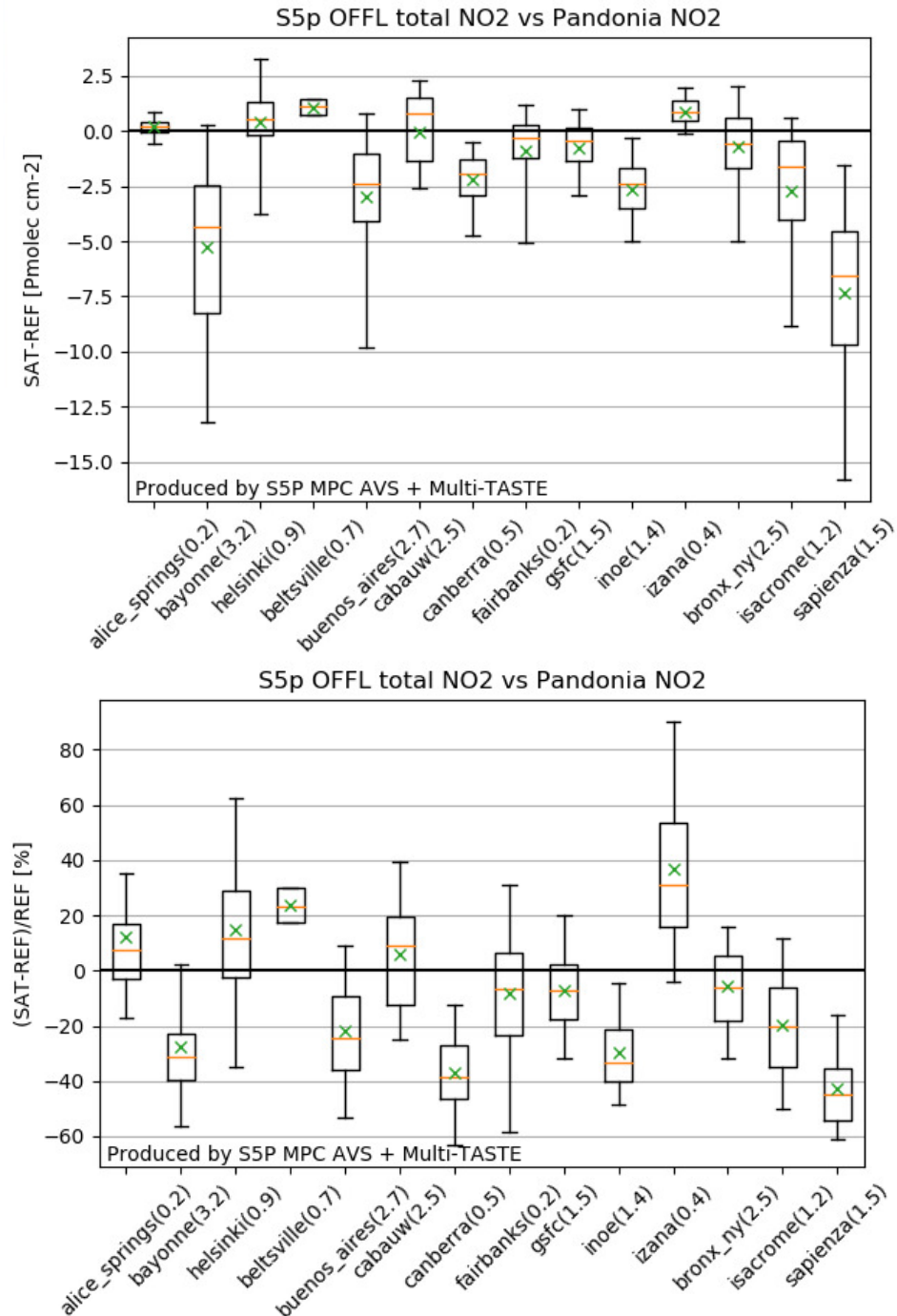
Figure 20: Boxplots of S5P OFFL total NO_2 column vs. Pandonia total NO_2 column. Difference (top) and relative difference (bottom). Per site, the tropospheric NO_2 /stratospheric NO_2 ratio is provided between brackets. Data was obtained from the VDAF Automated Validation Server on 29/05/2019. Note that regarding Pandonia data, only data with flags 0 and 10 are kept. Regarding S5P data, filter qa_value>0.5 was applied if tropospheric NO_2 /stratospheric NO_2 ratio < 1; qa_value>0.75 was applied otherwise. Boxplot conventions: box bounds are at first and third quartile. Orange line is median. Whiskers are at 5 and 95 percentiles. Green cross is mean.
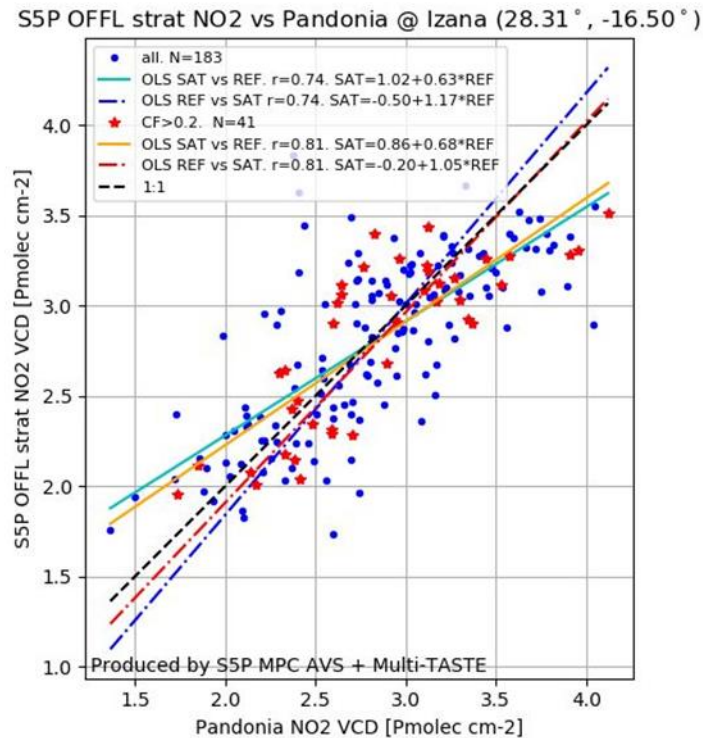
Figure 21: Comparison of the S5P stratospheric NO_2 (RPRO 01.02.02+OFFL 01.02.0x) with Pandonia measurements at Izaña. Data obtained from the automatic validation server on 2019-08-26.

Tropospheric NO₂ Column

The standard deviation of S5P tropospheric column vs MAX-DOAS varies between 3 and 4 Pmolec/cm^2. This exceeds by far the mission precision target of 0.7 Pmolec/cm^2, but it must be noted that also reference error sources and comparison errors contribute to the dispersion. Moreover, systematic error (e.g., a seasonal cycle) can contribute to the dispersion. One can attempt to remove (a part of) the systematic error component. Instead of calculating the standard deviation of S5P-MAX-DOAS, one estimates the spread around the OLS regression line (Schneider et al., 2006). The residual spread is then somewhat lower, between 2 and 3 Pmolec/cm^2.

There is a reasonably good correlation between S5P tropospheric column and MAX-DOAS data, with the Pearson R varying between 0.63 (Bremen) and 0.78 (Athens).

Total NO₂ Column

The dispersion of differences with respect to Pandora measurement depends strongly on the site. Small standard deviations are obtained at Alice Springs and Izaña (0.5-0.6 Pmolec/cm^2 i.e., comparable to the mission precision target), and higher values elsewhere (e.g., 3 Pmolec/ cm^2 at New York Bronx and 5 Pmolec/ cm^2 at Sapienza Rome).

The Pearson-R varies from relatively low (e.g., 0.41 at Helsinki) to high (0.94 at New York Bronx). An exceptional case is at Fairbanks (Alaska) where the Pearson-R is close to zero; this case deserves further investigation.

6.3.5 Dependence on influence quantities

Potential dependence of the S5P stratospheric column bias and dispersion on the Solar Zenith Angle (SZA), Air Mass Factor (AMF) and fractional cloud cover (CF) of the S5P measurement is evaluated. At this stage their evaluation does not reveal any variation of the bias much larger than 0.4 Pmolec/cm^2 over the range of those influence quantities (**Figure 22**).
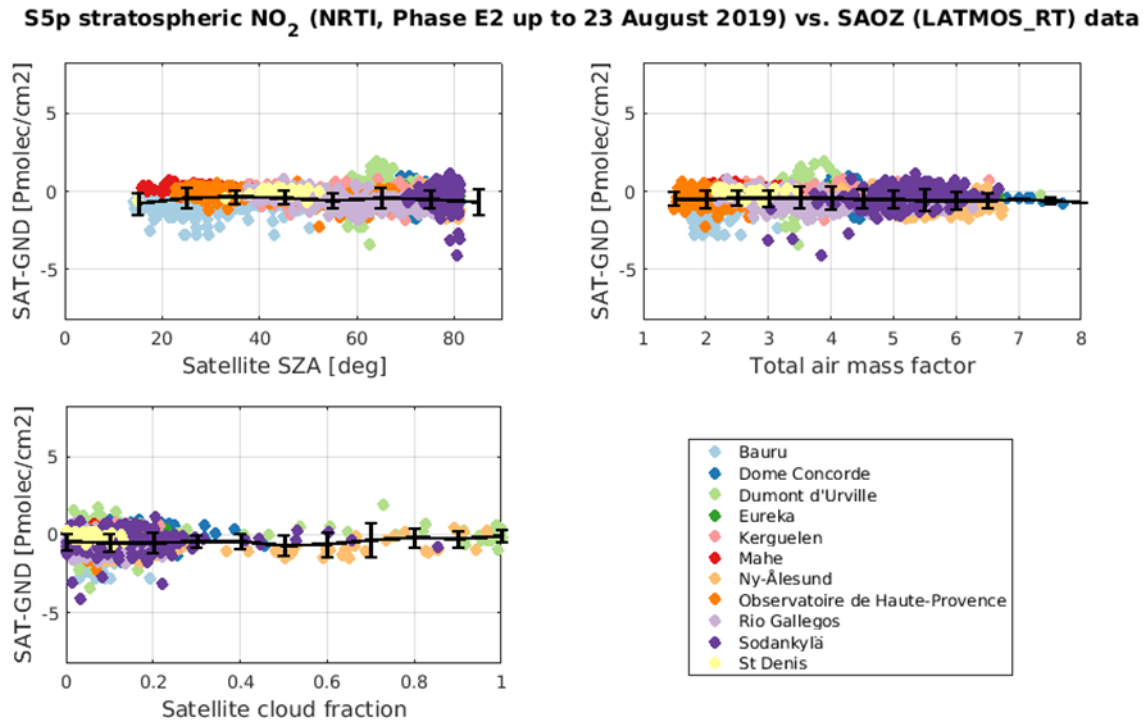
Figure 22: Dependence of the difference between S5P L2_NO2 NRTI and ground-based SAOZ stratospheric NO$_2$ column data on the satellite solar zenith angle (SZA), satellite cloud fraction, and satellite total air mass factor, including a mean and standard deviation bin (bin widths of 10 degrees in SZA, 0.1 in CF, and 0.5 in AMF).

6.3.6   Short term variability

Stratospheric NO$_2$ Column

S5P and ground-based ZSL-DOAS instruments capture similarly the short-term variability (at the monthly scale) of the NO$_2$ stratospheric columns, as illustrated at the NDACC station of Kerguelen Island in **Figure 23**. The ground-based SAOZ data acquired at twilight were adjusted to account for the photochemical diurnal variation between twilight and the S5P overpass time.
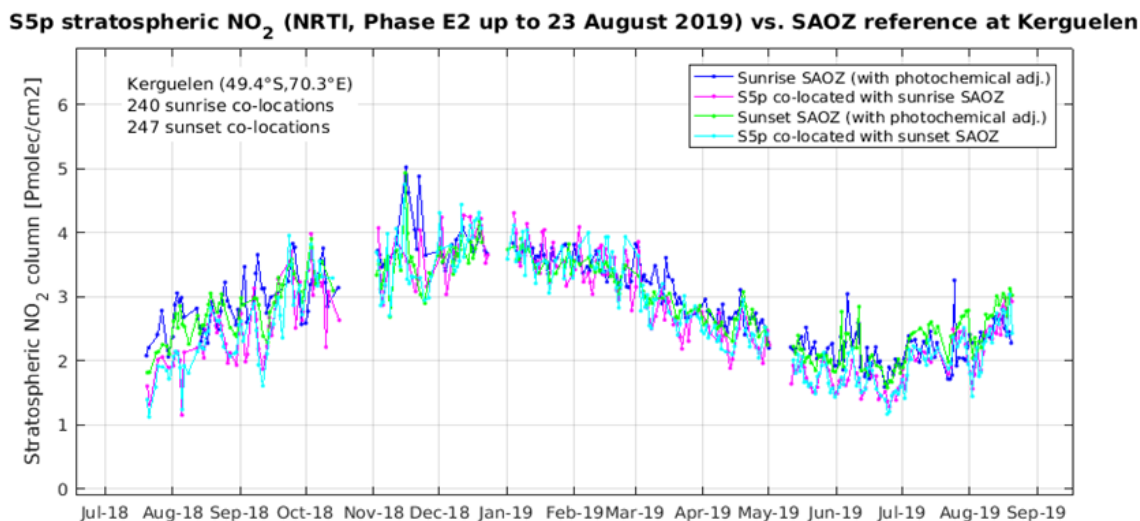
Figure 23: Time series of S5P L2_NO2 stratospheric NO$_2$ column data co-located with ground-based SAOZ twilight measurements performed by LATMOS at the NDACC southern mid-latitude station of Kerguelen Island.

Tropospheric NO$_2$ Column

At the sites Cabauw (**Figure 24**) and De Bilt (**Figure 25**), a higher underestimation is seen end of March 2019 and early April 2019, when MAX-DOAS measures tropospheric NO$_2$ peak values.
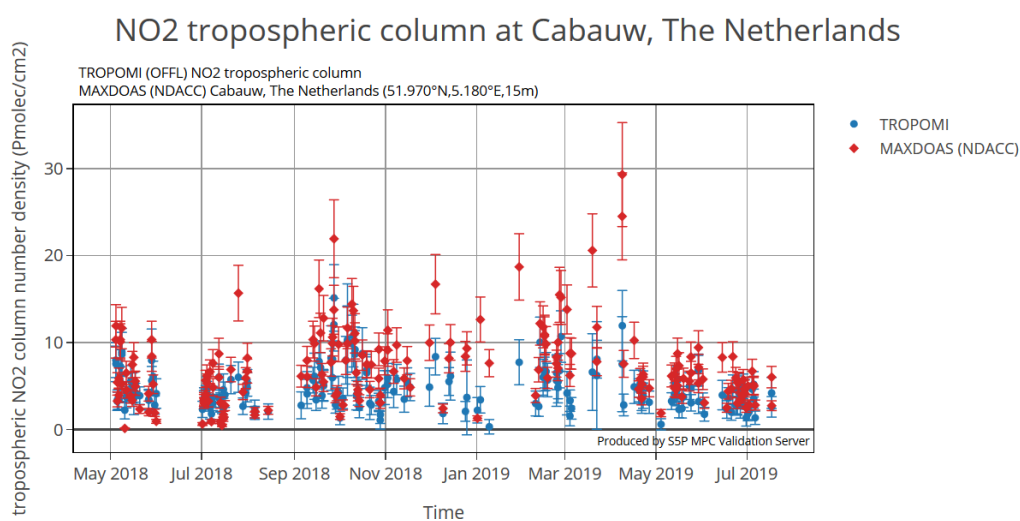
Figure 24: Comparison of the S5P tropospheric NO$_2$ with MAXDOAS measurements at Cabauw.
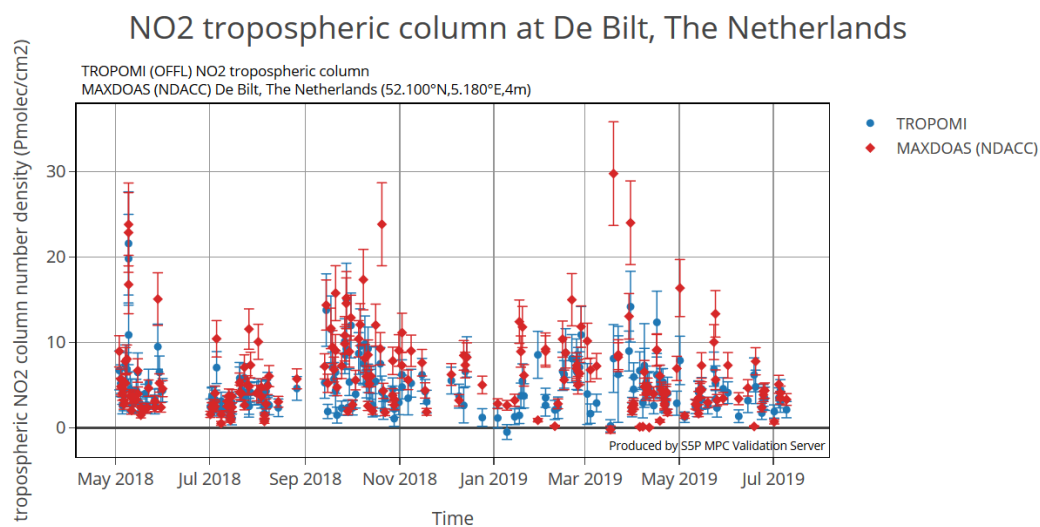
Figure 25: Comparison of the S5P tropospheric NO$_2$ with MAXDOAS measurements at De Bilt.

6.3.7   Geographical patterns

Tropospheric NO₂ Column

In general, no geographical patterns or artefacts can detected in the latest OFFL versions, as shown in the 3 monthly mean over central Europe (**Figure 26**).
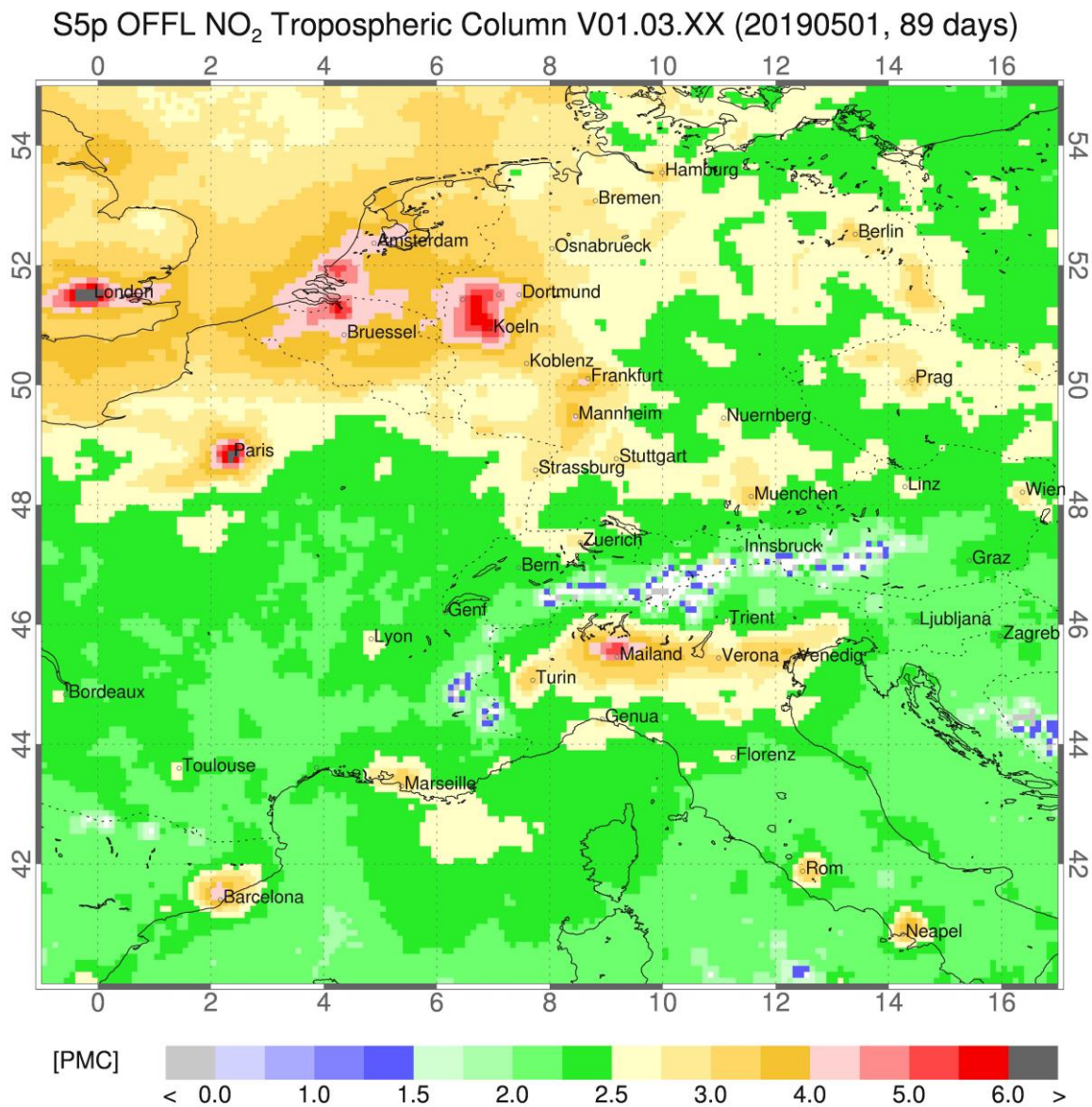
Figure 26: Tropospheric NO$_2$ over central Europe. Processor versions OFFL 01.03.00-02 were used to bin the data on a 0.1°x0.1° grid for a 3-month period starting May 2019. The quality value larger than 0.5 and a CF<0.6 were chosen to reduce the amount of data and exclude cloudy scenes.

6.3.8   Switch to smaller ground pixel resolution

Stratospheric NO_2 Column

The effect of the change in TROPOMI ground pixel size on 6 August 2019 on the S5P stratospheric NO_2 column data was investigated by perusal of the time series of satellite-ground differences at the ZSL-DOAS hosting stations with sufficiently rapid data delivery. **Figure 27** shows that the satellite-ground agreement seems unaffected by the pixel size change.
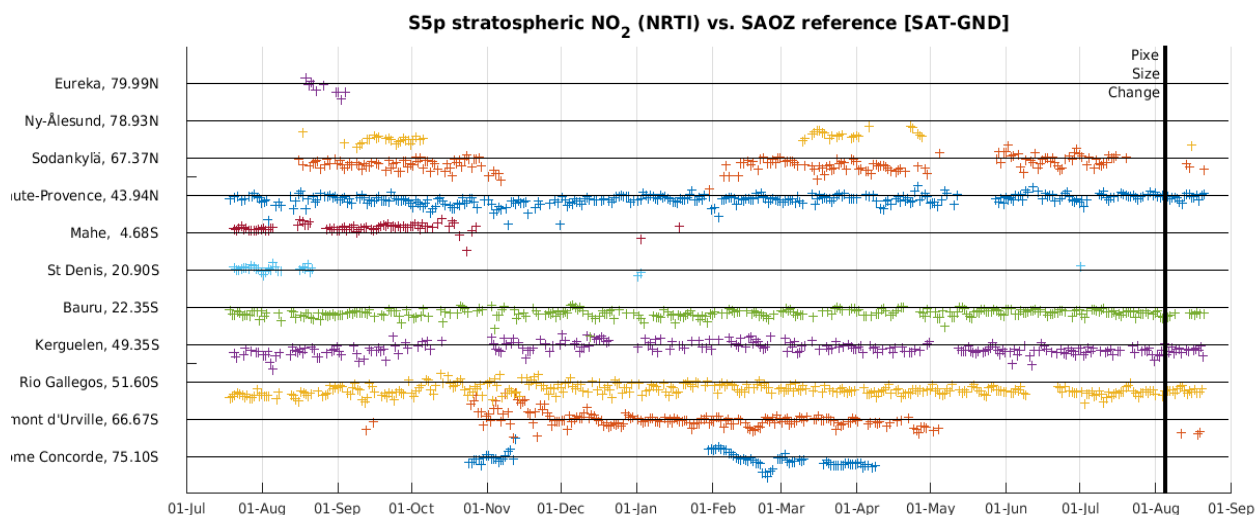
Figure 27: Time series of absolute differences between S5P and ground-based NDACC SAOZ reference data. Solid horizontal lines are spaced by 1×10^{15} molec/cm^2.

6.3.9   Other features

In the L2_NO2 NRTI data, a visible spike appeared after 2019-08-02 that is not detectable in the OFFL data.

Tropospheric NO_2 Column

Ordinary linear regression (OLS) of S5P (y) vs MAX-DOAS (x) yields fairly good correlation coefficients (0.63-0.78, see before) but low slopes. In S5P=a*MXD+b, a varies between 0.3 (Bremen) to 0.5 (Athens). It is known however that this approach is correct only in the limit that all random error is in y. OLS of MAX-DOAS vs S5P (i.e., assuming the opposite limit that all random error is in x), one obtains slopes closer to unity: in S5P=a*MXD+b, where a varies now between 0.73 (Bremen, Cabauw) and 0.94 (De Bilt).

Total NO_2 Column

OLS of S5P vs Pandora yields moderate to high correlation coefficients (0.4 to 0.9, see above, but excluding the Fairbanks case) but most often slopes lower than unity. Performing instead OLS of Pandora vs S5P, the slopes are closer to unity in most cases. An example is provided in **Figure 28**.
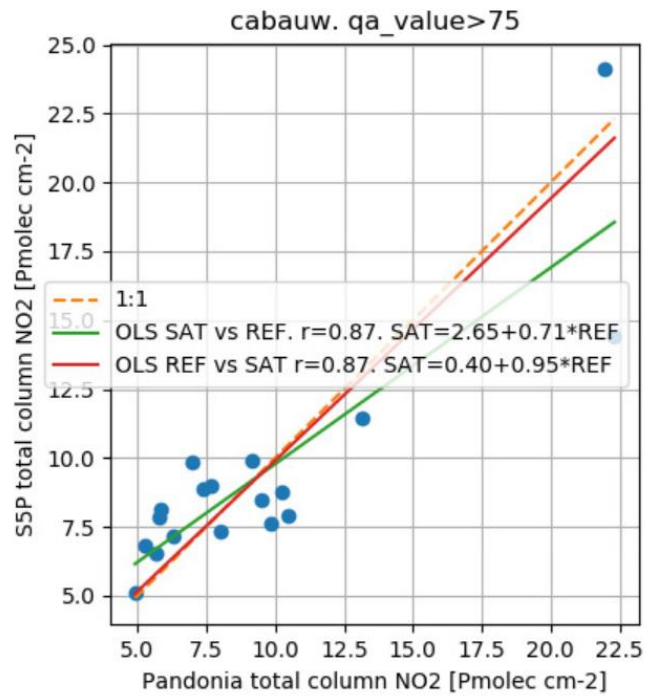
Figure 28: Correlation plot of S5P total NO_2 column (RPRO 01.02.02+OFFL >=01.02.00) vs Pandonia. Regression lines of S5P vs Pandonia and Pandonia vs S5P are also indicated.

6.4   Equivalence of L2_NO2 NRTI and OFFL products

This section shows evidence that the L2_NO2 NRTI and OFFL products do not differ significantly and that their respective validations yield similar conclusions. We show the differences between the two datasets for the three different products (stratospheric, tropospheric, and total column).

6.4.1   Total NO$_2$ Column

The comparison of total NRTI vs. OFFL data show that both the overall values and the standard deviations are very close to each other (**Figure 29**). The relative difference is in the range of -1%, where NRTI values are slightly higher.
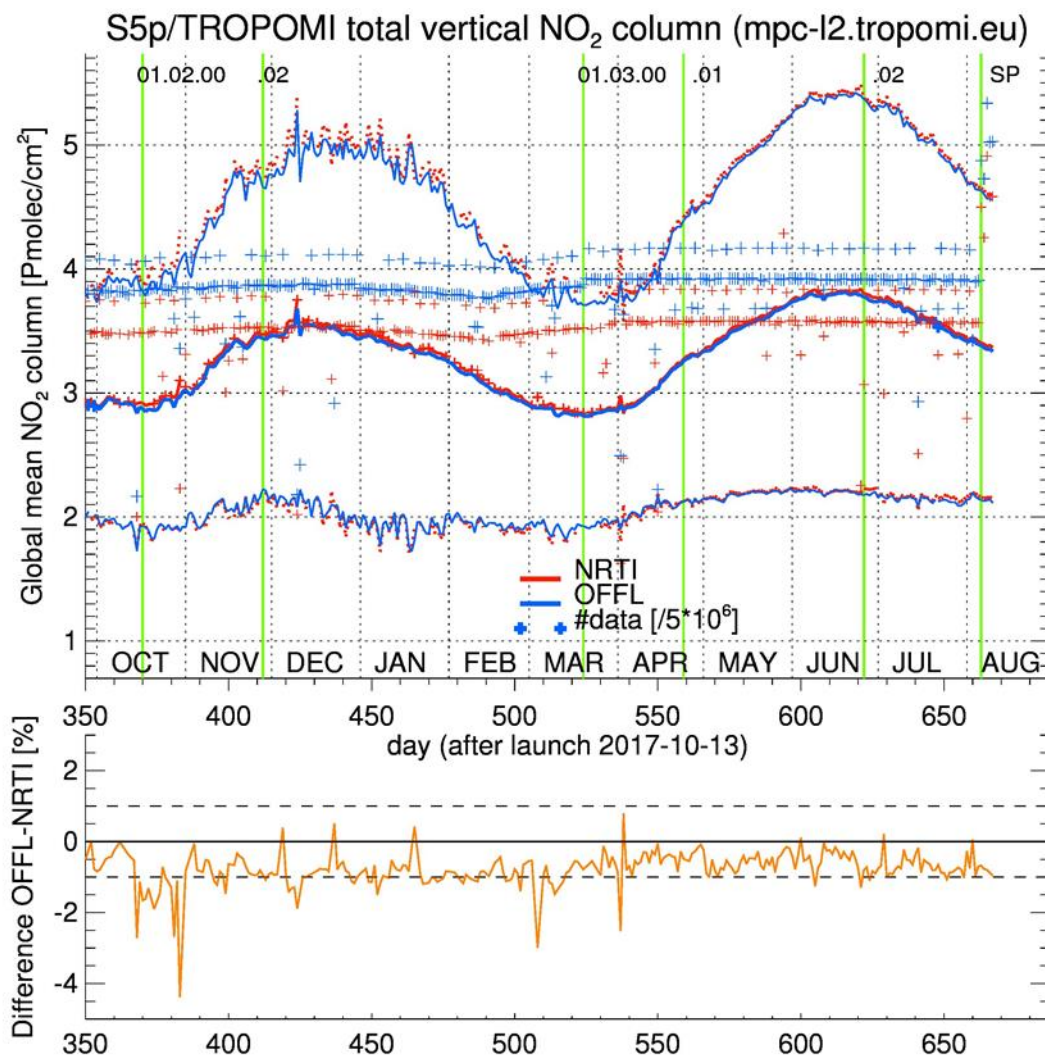
Figure 29: Time series (October 2018 – August 2019) of the global mean of NRTI (red) and OFFL (blue) NO2 total column data [Pmolec/cm²]. Data is taken from the TROPOMI QC portal. The ±1σ standard deviations are shown as solid and dotted lines. The number of data points for the NRTI/OFFL data are shown by crosses. The value were divided by a factor of 5*10^6. Superimposed are the points of processor changes as green vertical lines. The lower plot shows the difference [%] between OFFL vs. NRTI daily means. Data is taken from the TROPOMI QC portal.

6.4.2   Stratospheric NO$_2$ Column

The similarity of the two products can be investigated by comparing the processing of a randomly chosen orbit. **Figure 30** shows this approach for orbit 7407 on March 19, 2019. It reveals differences mostly below the mission requirement on the precision (0.5 Pmolec/cm^2). Since these differences, representing up to 20% of the stratospheric column, do exceed the mission requirement on the bias (10%), and because a much more comprehensive orbit-by-orbit analysis is needed to ensure differences remain reasonable under all conditions, the full validation analysis as performed for the NRTI product was repeated on the OFFL product. The resulting pole-to-pole graph is shown in **Figure 31**, illustrating that in the end, OFFL performs very similarly to NRTI.
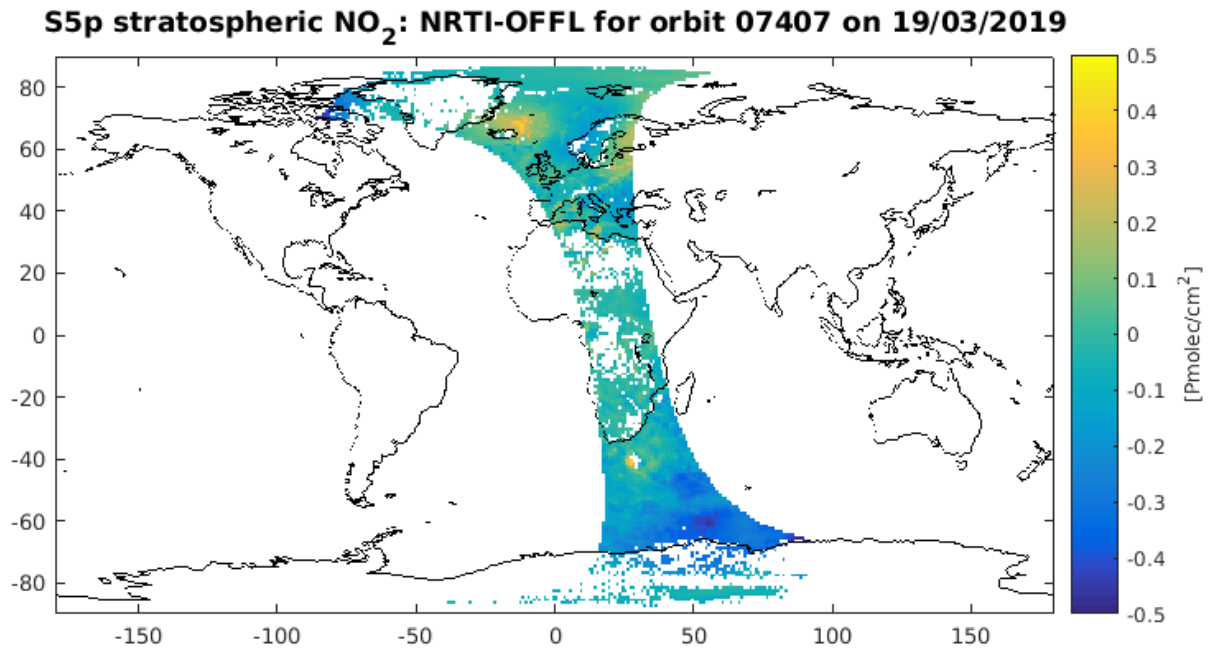
Figure 30: Comparisons of NRTI to OFFL stratospheric NO$_2$ columns for a single orbit (gridded to 1°x1° resolution).
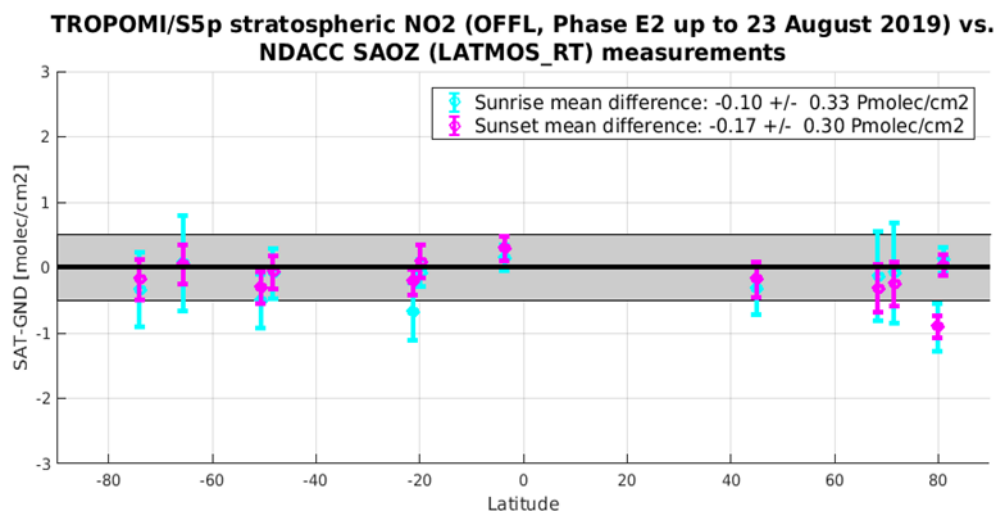
Figure 31: Meridian dependence of the mean (the circular markers) and spread (±1σ error bars) of the differences between S5p TROPOMI L2_NO2 (OFFL) stratospheric column data and SAOZ reference data, represented at individual stations from the Antarctic to the Arctic. The values in the legend correspond to the mean and spread of all mean (per station) differences.

6.4.3   Tropospheric NO2 Column

To demonstrate the closeness of L2_NO2 NRTI and OFFL products at the MAX-DOAS sites Athens, Bremen, De Bilt and Cabauw, L2_NO2 NRTI (processor version 01.00.02 to01.03.02) and L2_NO2 OFFL (RPRO processor version 01.02.02 + OFFL processor version 01.02.00 to01.03.02), each co-located with MAX-DOAS, were obtained from the validation server, and the subset of pixels, common to both NRTI and OFFL, was determined.

Differences between NRTI, OFFL and MAX-DOAS were determined. Statistical results for Athens and Bremen are summarized in **Table 5**: similar conclusions on the closeness of NRTI and OFFL are obtained for the sites De Bilt and Cabauw.

Table 5 – Statistics on the comparison of the common subset of L2_HCHO NRTI, L2_HCHO RPRO+OFFL and co-located MAX-DOAS, for the sites Bremen and Athens. (*: unit of $Pmolec/cm^2$). Numbers updated using data from the validation server at 2019-08-27.

	Bremen 276 col			Athens 136 col		
	NRTI-OFFL	NRTI-MXD	OFFL-MXD	NRTI-OFFL	NRTI-MXD	OFFL-MXD
Mean(diff)*	0.20	-2.42±0.20	-2.61±0.20	0.12	-1.38±0.33	-1.50±0.33
Median(diff)*	0.15	-1.49	-1.68	0.10	-0.09	-0.25
Std(diff)*	0.9	3.4	3.3	0.5	3.9	3.8
½ IP68(diff)*	0.4	2.7	2.5	0.1	2.1	2.1
Pearson R	0.91	0.62	0.64	0.99	0.77	0.79
Slope	0.90	0.30	0.31	1.02	0.49	0.48

The mean difference between NRTI and OFFL is of the same order or smaller as the standard error on the mean difference of NRTI-MAX-DOAS and OFFL-MAX-DOAS. Therefore, the bias difference between NRTI and OFFL is not statistically significant. Also the difference dispersion between NRTI and OFFL is small compared to the difference dispersion between either NRTI or OFFL on one hand and MAX-DOAS on the other hand. The good match between NRTI and OFFL is also demonstrated by the high Pearson R value and the near unity slope of the linear regression.

7   Validation Results: L2_HCHO

7.1   L2_ HCHO products and requirements

This section reports on the validation of the following geophysical variables of the S5P TROPOMI L2_HCHO product identified in **Table 1**: the HCHO total column. Validation results are discussed with respect to the product quality targets outlined in **Table 3**. The NRTI and OFFL processors producing very similar data products, only validation of the L2_HCHO OFFL product is reported hereafter. Subsection 0 demonstrates evidence that NRTI and OFFL data do not differ significantly and that their respective validations yield similar conclusions

Notes:
- The operational (E2) phase for the S5P TROPOMI mission starts with orbit #02818.
- The L2_HCHO NRT product has been released in Oct. 2018 with version 01.01.02.
- The L2_HCHO OFFL product has been released in Dec. 2018 with version 01.01.05.
- Version 01.01.05 starts on 5 Dec. 2018 (processing date), both for NRT and OFFL.
- The L2_HCHO RPRO product 01.01.05 has been delivered in May 2019, covering the period from 15 May to Dec. 2018.

7.1.1   Recommendations for data usage followed

In order to avoid misinterpretation of the data quality, as recommended, only those TROPOMI pixels associated with a qa_value above 0.5 (no error flag, cloud radiance fraction at 340 nm<0.5, SZA<=70°, surface albedo<=0.2, no snow/ice warning, air mass factor>0.1) have been used.

For further details, including how to apply the averaging kernel and a priori profile in comparisons, data users are encouraged to read the Product User Manual (PUM) and Algorithm Theoretical Basis Document (ATBD) associated with this data product, which are available on https://sentinels.copernicus.eu/web/sentinel/technical-guides/sentinel-5p/products-algorithms.

7.2   Validation approach

7.2.1   Ground-based networks

S5P L2_HCHO data are validated routinely through comparisons with respect to ground-based measurements acquired by NDACC MAX-DOAS UV-visible and FTIR instruments performing network operation in the framework of NDACC. For S5P validation purposes those measurements are collected either automatically through EVDC or manually through S5PVT AO projects (e.g., CESAR AO ID 28596, and NIDFORVAL AO ID 208607).

Fourier Transform Infrared Spectrometers

S5P TROPOMI L2_HCHO formaldehyde column data are compared to reference measurements acquired at over 20 NDACC FTIR stations. FTIR measurements have a bias of maximum 17% and a precision better than 10% (Vigouroux et al., 2018).

MAX-DOAS UV-Visible Spectrometers

S5P TROPOMI L2_HCHO formaldehyde column data are routinely compared to reference measurements acquired by MAX-DOAS UV-Visible spectrometers. At the present stage of S5P routine operation, two MAX-DOAS stations have contributed data routinely to the VDAF Automated Validation Server. Nine others might be available in the future through the NIDFORVAL project. MAX-DOAS HCHO column data have a bias of maximum 20% and a precision better than 30%.

7.2.2   Satellites

S5P TROPOMI L2_HCHO formaldehyde column data are also compared to similar data from the MetOp-A and B GOME-2 data (version GDP 4.8) and to EOS-Aura Ozone Monitoring Instrument (OMI). Two versions of the OMI L2 HCHO product are considered (1) the NASA L2 product (10.5067/Aura/OMI/DATA2015), (2) the QA4ECV L2 product (http://doi.org/10.18758/71021031). The first has the advantage of being operational and completely independent from TROPOMI retrievals. The second offers the advantage to be produced by the same European consortium as the TROPOMI product; the results can be directly compared because the algorithms have been made as consistent as possible.

7.2.3   Field campaigns and modelling support

Nothing in this report.

7.3   Validation of L2_ HCHO

7.3.1   Recommendations for data usage followed

7.3.2   Status of validation

This section presents a summary of the key validation results obtained by the Validation Data Analysis Facility (VDAF) of the S5P Mission Performance Centre (MPC). It takes into account results obtained by S5P Validation Team (S5PVT) AO projects CESAR and NIDFORVAL. Up-to-date validation results and consolidated validation reports are available through the MPC VDAF Portal at http://mpc-vdaf.tropomi.eu. Up-to-date validation results and consolidated validation reports are available through the MPC VDAF Portal at http://mpc-vdaf.tropomi.eu.

Comparisons of OFFL (RPRO processor version 01.01.05 + OFFL processor version 01.01.05 to 01.01.07) with MAX-DOAS at sites De Bilt and Cabauw were taken from the VDAF Automated Validation Server (VDAF-AVS, consulted at 26/08/2019). The distance between both sites is about 30 km with De Bilt being nearer to the city. The time period extends from 15th of May 2018 (in the period 2018/04/30 to 2018/05/14 S5p HCHO is artificially enhanced due to a problem with the background correction; these data points are not taken into account here) to 17th of July 2019 (last orbit 9110).

Comparison of TROPOMI OFFL (RPRO processor version 01.01.05 + OFFL processor version 01.01.05 to 01.01.07, covering one full year from the phase E2 and the operational phase) with OMI QA4ECV product (Nov.2004 - Dec.2018) offer 15 years of afternoon observations with consistent algorithms, sharing the same auxiliary datasets (except for the cloud products).

Table 6 summarizes the statistics (correlation, slope, bias) of the OMI-TROPOMI comparison for a selection of regions. Numbers are given from phase E2 and forward.

Region	Latitudes limits [degree]		Longitude limits [degree]		Correlation	Slope	Bias [%]	Dispersion of difference [Pmolec.cm^{-2}]
Europe	35.00	50.00	0.00	40.00	0.86	1.24	25	1.4
Southeastern US	30.00	40.00	-95.00	-75.00	0.92	1.20	20	1.9
Western US	34.00	44.00	-125.00	-110.00	0.84	1.27	27	2.0
Central US	30.00	44.00	-110.00	-95.00	0.83	1.26	26	1.9
Central Siberia	60.00	70.00	50.00	80.00	0.57	0.87	-1.0	2.4
Mexico	15.00	20.00	-103.00	-88.00	0.48	1.03	1.6	1.9
Guatemala	12.50	17.50	-95.00	-85.00	0.40	1.01	1.7	2.1
Amazonia	-10.00	5.00	-75.00	-50.00	0.84	1.04	2.6	1.3
Western Amazonia	-10.00	2.00	-75.00	-65.00	0.81	1.06	4.6	1.8
Northern Africa	5.00	12.00	-14.00	12.00	0.78	0.96	-2.4	1.3
Southern Africa	-15.00	-5.00	10.00	30.00	0.86	1.03	3.7	1.3
Equatorial Africa	-5.00	5.00	14.00	28.00	0.63	1.07	7.4	1.9
Southern China	24.00	33.00	108.00	121.00	0.63	1.12	13.2	2.3
Northern China	29.00	37.00	112.00	121.00	0.54	1.12	13.3	4.0
South Asia	12.00	20.00	98.50	107.50	0.60	1.00	0.6	2.1
Indonesia	-5.00	5.00	98.00	118.00	0.44	0.93	-7.2	1.1
India	15.00	24.00	75.00	85.00	0.70	0.99	0.0	2.1
Northern India	20.00	28.00	77.00	92.00	0.79	1.04	4.5	1.9
Northern Australia	-20.00	-12.50	125.00	145.00	0.64	0.99	-0.9	1.5

Table 6 – Summary of the OMI-TROPOMI comparison statistics (correlation, slope, bias) for a selection of regions. Numbers are given from phase E2 and forward.

7.3.3   Bias

The bias (mean difference) with respect to MAX-DOAS is -2.1 Pmolec cm^{-2} (median relative difference -33%) at Cabauw and -3.1 Pmolec cm^{-2} (median relative difference -43%%) at De Bilt. This is within the mission requirement of the 80% bias.

As can be seen in **Table 6**, the bias between OMI and TROPOMI is below 30% in all 19 regions, below 10% in 13 regions, and even lower than 5% in 11 regions. The regions characterized by the larger biases are mid-latitude regions (Europe, US, China). Differences can be attributed to the background-corrected slant columns, and to a lesser extent, to the cloud correction in China.
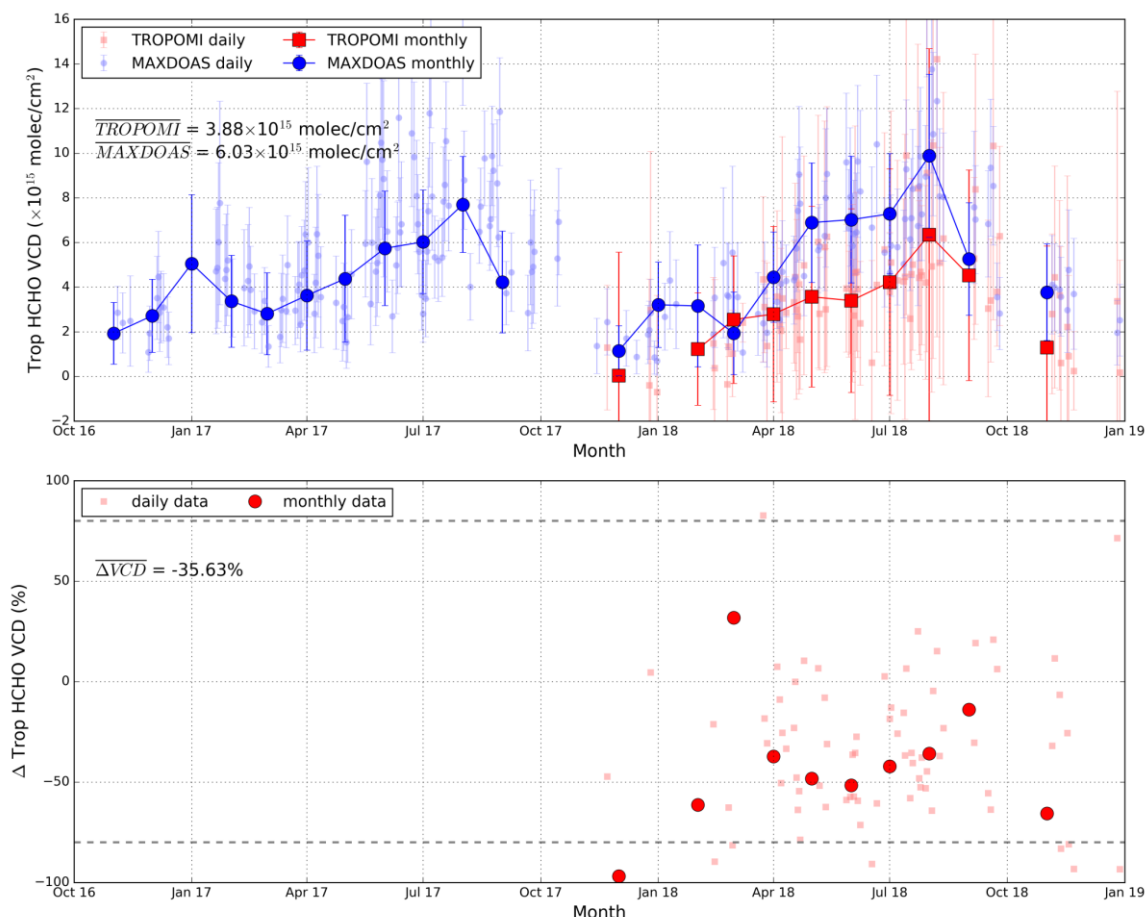
Figure 32: Time series of HCHO column measured by S5P TROPOMI and by the MAX-DOAS in Munich (Germany).

The TROPOMI TROPOMI HCHO columns are also compared to the HCHO VCDs reported from the MAX-DOAS station in Munich, Germany. Time series of the HCHO columns measured by TROPOMI and the MAX-DOAS are shown in **Figure 32**. The comparison results shows that TROPOMI observations are in general ~35% lower that the MAX-DOAS data.

7.3.4   Dispersion

The dispersion (standard deviation) of the difference of S5P with respect to MAX-DOAS is 8 Pmolec/cm^2 at Cabauw and 9 Pmolec/cm^2 at De Bilt. This is within the mission requirement of precision of 12 Pmolec/cm^2.

As reported in **Table 8**, the dispersion of the daily difference between OMI and TROPOMI is generally ranging from 1 to 2 Pmolec.cm^{-2}, with the exception of Northern China (4 Pmolec.cm^{-2}). Low dispersion is related to the large number of observations included in the averages. The standard deviation of individual OMI and TROPOMI observations is respectively about 7 and 4 Pmolec.cm^{-2} in remote regions with no local emissions.

7.3.5   Dependence on influence quantities

Nothing to report.

7.3.6   Short term variability

Overall, the short term variability seen in the MAXDOAS measurements is nicely reproduced by S5P TROPOMI. In July 2018, a HCHO peak value measured by the MAX-DOAS at De Bilt is largely underestimated by S5P (**Figure 33**).
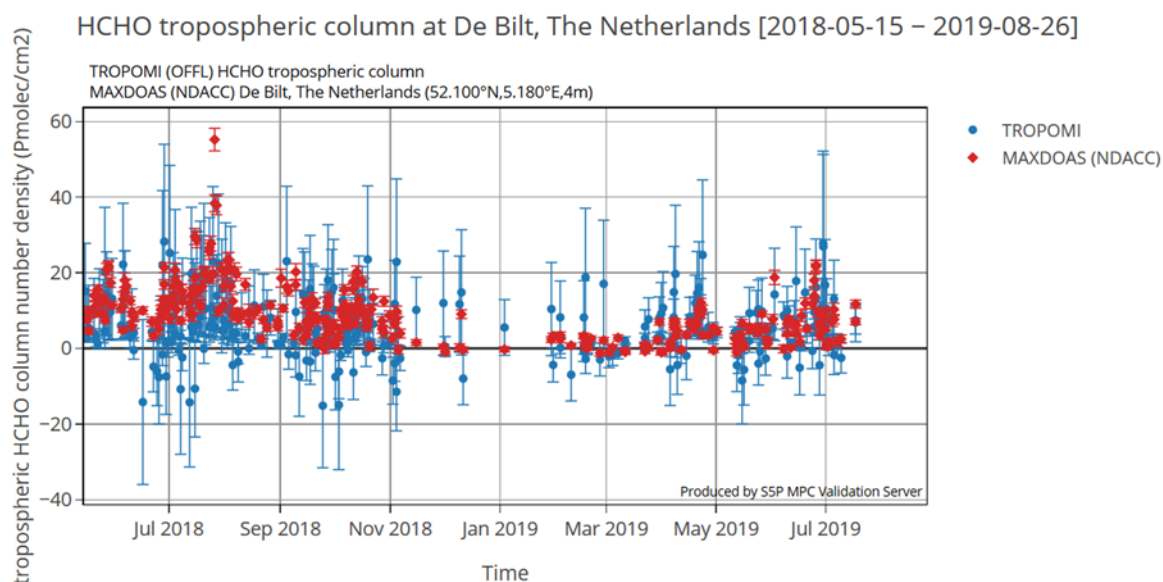
Figure 33: Comparison of S5P HCHO tropospheric column with MAXDOAS measurements in De Bilt.

7.3.7   Geographical patterns

The S5P_L2_HCHO data are seasonally averaged for spring (March-May 2018) and summer (June-August 2018) and compared to OMI (González Abad et al., 2015, 2016) and GOME-2. The comparison results are shown in **Figure 34** and **Figure 35**. The results show similar spatial patterns of HCHO columns for the three satellites. Compared to OMI, TROPOMI observations show higher HCHO columns over India and Sahara desert. GOME-2 reports similar HCHO column values as TROPOMI in the same regions.
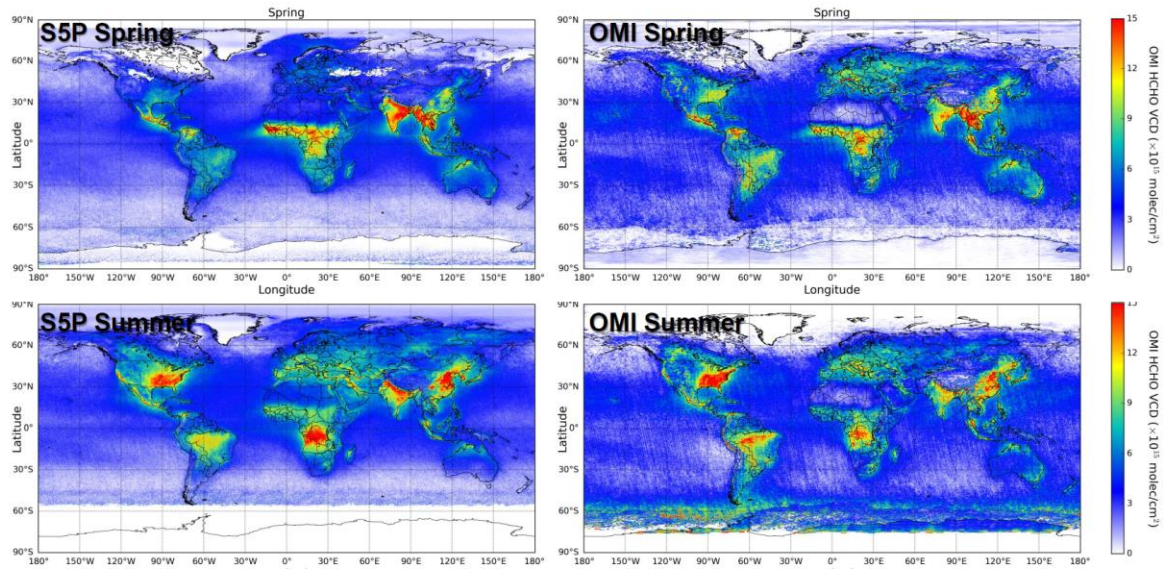
Figure 34: Seasonal average of HCHO VCDs for TROPOMI and OMI.
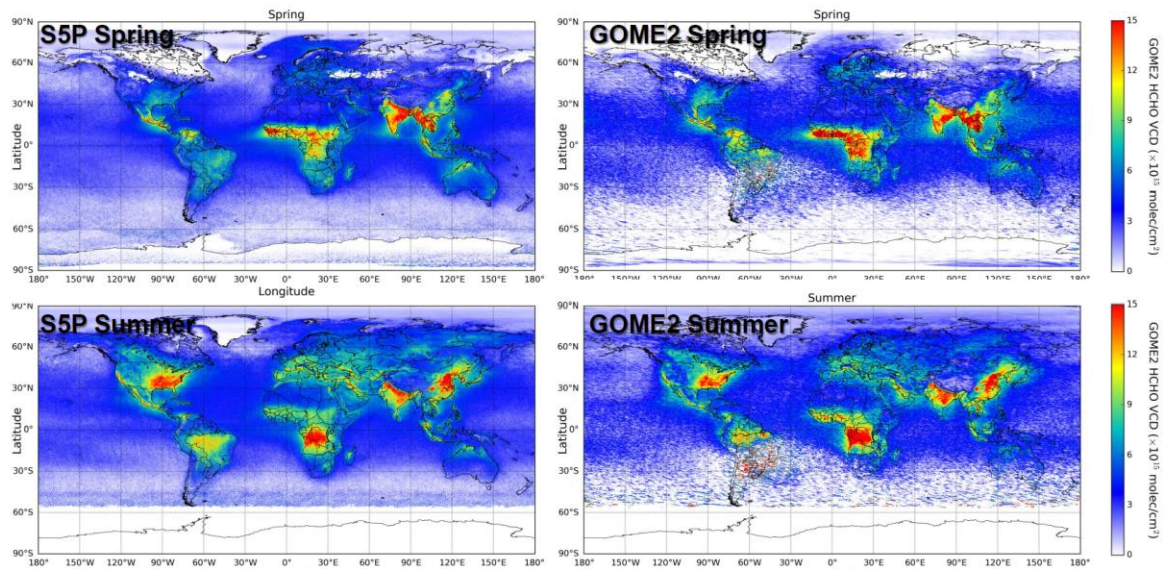
Figure 35: Seasonal average of HCHO VCDs for TROPOMI and GOME 2.

7.3.8   Other features

Nothing to report.

7.4   Equivalence of L2_HCHO NRTI and OFFL products

We demonstrate the closeness of L2_HCHO NRTI and OFFL products at the MAX-DOAS sites De Bilt and Cabauw. L2_HCHO NRTI (processor version 01.01.02 to 01.01.07) and L2_HCHO OFFL (RPRO processor version 01.01.05 + OFFL processor version 01.01.05 to 01.01.07), each co-located with MAX-DOAS, were obtained from the VDAF Automated Validation Server. The subset of pixels, common to both NRTI and OFFL, was determined and differences between NRTI, OFFL and MAX-DOAS were determined. The statistical results are summarized in **Table 7.**

Table 7 – Statistics on the comparison of the common subset of L2_HCHO NRTI, L2_HCHO RPRO+OFFL and co-located MAX-DOAS, for the sites Cabauw and De Bilt. (*: unit of Pmolec cm^{-2}).

Cabauw: 125 common co-locations
RPRO+OFFL orbits range from 4839 (2018-09-19) to 9110 (2019-07-17)

	NRTI vs OFFL	NRTI vs MXD	OFFL vs MXD
Mean(diff)±sem*	-0.16	-2.41±0.59	-2.25±0.59
Median(diff)*	-0.04	-2.90	-2.48
Std(diff)*	1.7	7.9	7.9
1/2 IP68(diff)*	1.4	6.7	6.9
Pearson R	0.98	0.30	0.29
Slope	0.98	0.52	0.51

De Bilt: 125 common co-locations
RPRO+OFFL orbits range from 4839 (2018-09-19) to 9110 (2019-07-17)

	NRTI vs OFFL	NRTI vs MXD	OFFL vs MXD
Mean(diff)±sem*	-0.10	-0.73±0.57	-0.64±0.58
Median(diff)*	0.12	-1.22	-1.04
Std(diff)*	2.1	7.5	7.6
1/2 IP68(diff)*	1.6	7.1	7.2
Pearson R	0.96	0.29	0.29
Slope	0.93	0.43	0.45

7.4.1   Bias

At the MAX-DOAS sites, the bias (both mean and median difference) of L2_HCHO NRTI vs. L2_HCHO OFFL is smaller than that of either L2_HCHO NRTI or L2_HCHO OFFL with respect to MAX-DOAS (see **Table 7**). More importantly, the bias of NRTI vs. OFFL is smaller than the standard error on the mean difference of either NRTI or OFFL with respect to MAX-DOAS. The difference in bias between NRTI and OFFL is therefore not statistically significant.

7.4.2   Dispersion

Standard deviation and the ½ 68% interpercentile (1/2 IP68) of the NRTI-OFFL differences are much smaller than that between either NRTI and MAX-DOAS or OFFL and MAX-DOAS, indicating a much smaller dispersion between NRTI and OFFL. This is also indicated by the near-unity Pearson R correlation coefficient and slope of NRTI vs OFFL, which are much smaller than for NRTI vs MAX-DOAS and for OFFL vs MAX-DOAS

8   Validation Results: L2_SO2

8.1   L2_SO2 products and requirements

This section reports on the validation of the following geophysical variables of the S5P TROPOMI L2_SO2 product identified in **Table 1**: the sulphur dioxide total column. Validation results are discussed with respect to the product quality targets outlined in **Table 3**. The NRTI and OFFL processors producing very similar data products, only validation of the L2_SO2 NRTI product is reported hereafter. Subsection 0 demonstrates evidence that NRTI and OFFL data do not differ significantly and that their respective validations yield similar conclusions.

8.2   Validation approach

8.2.1   Ground-based networks

Boundary layer pollution (SO$_2$ total)

S5P TROPOMI L2_SO2 sulphur dioxide column data are compared to ground-based MAX-DOAS UV-visible observations. However, currently the number of available stations in strongly polluted regions is very rare. Outside strongly polluted regions, the SO$_2$ column is below the detection limit of both the MAX-DOAS and satellite measurements. For the validation of the S5P TROPOMI L2_SO2 sulphur dioxide column data MAX-DOAS measurements at Xianghe (China), Greater Noida (India), and Basra (Iraq) were used so far.

Volcanic plumes (SO2 enhanced)

S5P TROPOMI L2_SO2 sulphur dioxide column data are compared to MAX-DOAS UV-visible measurements collected from the Network for Observation of Volcanic and Atmospheric Change (NOVAC) [ER_NOVAC]. Because of the strong SO$_2$ concentration gradients in volcanic plumes, the comparison is not performed using the SO$_2$ columns but rather using the derived SO$_2$ fluxes.

8.2.2   Satellites

S5P TROPOMI L2_SO2 sulphur dioxide column data are compared to similar data from EOS-Aura OMI and Suomi-NPP OMPS.

8.2.3   Field campaigns and modelling support

S5P TROPOMI L2_SO2 sulphur dioxide column data are compared to car MAX-DOAS measurements performed in Lahore.

8.2.4   Test of the expectation of zero SO$_2$ SCDs (within detection limit) outside volcanic plumes and strongly polluted regions

Outside strongly polluted regions and volcanic plumes, the atmospheric SO$_2$ concentrations are very low and the corresponding SO$_2$ columns are below the detection limit of S5P TROPOMI. Thus S5P TROPOMI measurements outside strongly polluted regions and volcanic plumes are used to check the consistency of the S5P TROPOMI L2_SO2 sulphur dioxide column data with the assumption of SO$_2$ slant column densities (SCD) of zero. From this test, also the spread of the S5P TROPOMI L2_SO2 sulphur dioxide column data is quantified.

8.3   Validation of L2_SO2 NRTI

8.3.1   Recommendations for data usage followed

The quality of the observations depends on many factors which are taken into account in the definition of the `qa_value`. While it is a handy way of filtering observations of less quality, the "quality assurance value" should also be considered with caution, as it is a compromise to take into account several aspects, such as: processing errors, presence of clouds or snow/ice, observations affected by sun glint, South Atlantic Anomaly, possible contamination by volcanic SO_2, absence of background correction, and important variables out of range (importantly the AMF).

The `qa_value` is a continuous variable, ranging from 0 (error) to 1 (all is well). In order to avoid misinterpretation of the data quality, it is recommended at the current stage to only use those TROPOMI pixels associated with a `qa_value` above 0.5.

For further details, data users are encouraged to read the Product Readme File (PRF), Product User Manual (PUM) and Algorithm Theoretical Basis Document (ATBD) associated with this data product, all available on https://sentinels.copernicus.eu/web/sentinel/technical-guides/sentinel-5p/products-algorithms

8.3.2   Status of validation

So far the validation of the S5P TROPOMI L2_SO2 sulphur dioxide column data is mainly based on satellite to satellite comparisons, for which good agreement is found with OMI and OMPS measurements. Validation for polluted regions using ground based MAX-DOAS data is limited to two stations in polluted regions (Xianghe, China, Greater Noida, close to New Delhi, India, and Basra, Iraq) and to one field campaign in Lahore (Pakistan). Also here in general good agreement was found. However, it should be noted that for these comparisons the SO_2 columns were mostly close to or below the detection limit of S5P TROPOMI.

S5P TROPOMI L2_SO2 sulphur dioxide column data were also compared to ground based MAX-DOAS measurements from the NOVAC network. However, the SO_2 columns were not compared directly, because of the strong gradients across volcanic plumes. Instead the derived SO_2 fluxes were compared, for which good agreement was found.

Outside strongly polluted regions and volcanic plumes, the atmospheric SO_2 SCDs were found to be consistent with the assumption of zero within the measurement uncertainties.

From these comparisons (details are shown below) the following conclusions are drawn:

- over polluted regions the requirements are fulfilled;

- over volcanic plumes the bias requirement is fulfilled, but the random requirement is often not fulfilled. Here it should be noted that the random requirement is very strict (0.15 – 0.3 DU). For the often very high SO_2 columns in volcanic plumes it is unrealistic that the random requirement can strictly be fulfilled, and it is recommended that the random requirement should be reconsidered;

- from the time series of averaged SO_2 SCDs (and their errors and standard deviations) it is concluded that the requirements are fulfilled. The bias and spread are typically below 0.2 DU.
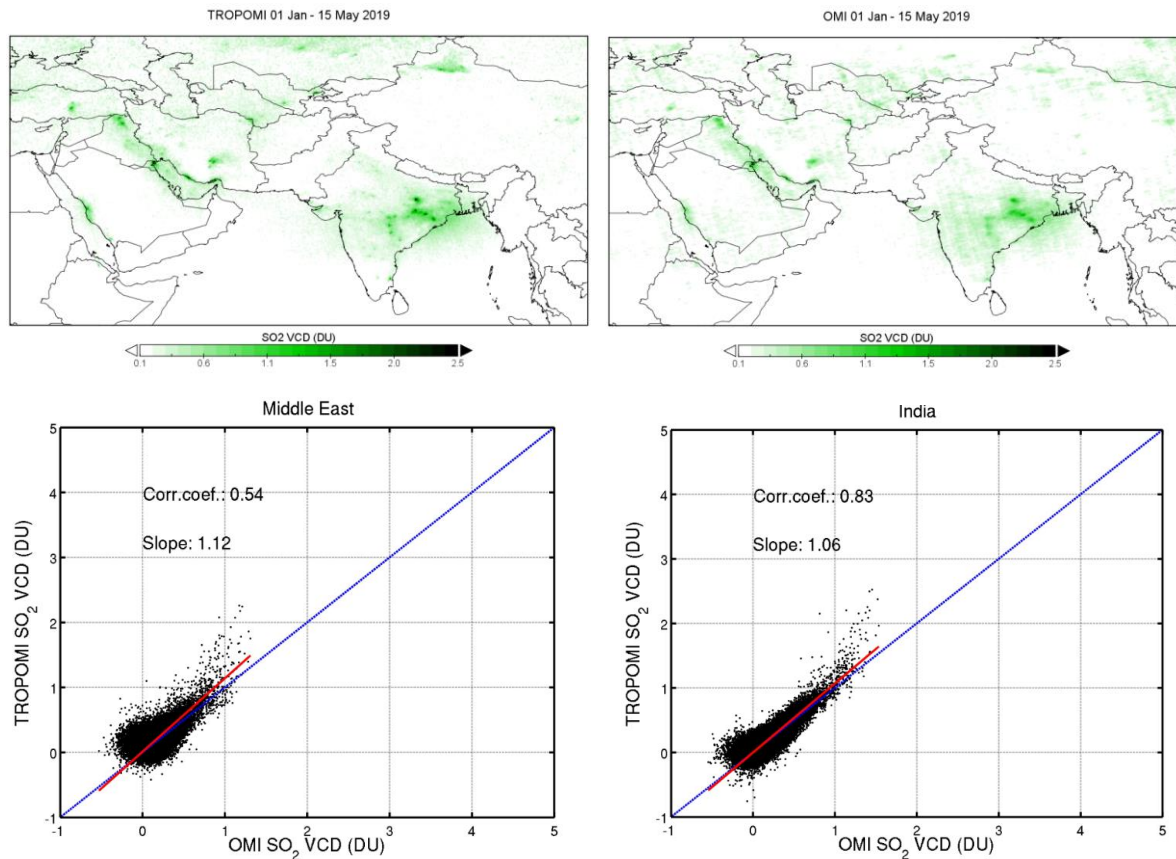
Figure 36: Top: Comparison of the average distribution (01 Jan 2019 – 15 May 2019) of the SO$_2$ VCDs derived from TROPOMI and OMI over regions with strong air pollution. Both data sets show very good agreement. Bottom:Correlation plots TROPOMI versus OMI over the Middle East and India. Note that a fixed AMF of 0.4 was used for both retrievals to exclude the effect of different profile assumptions. Courtesy of Nicolas Theys, BIRA-IASB.
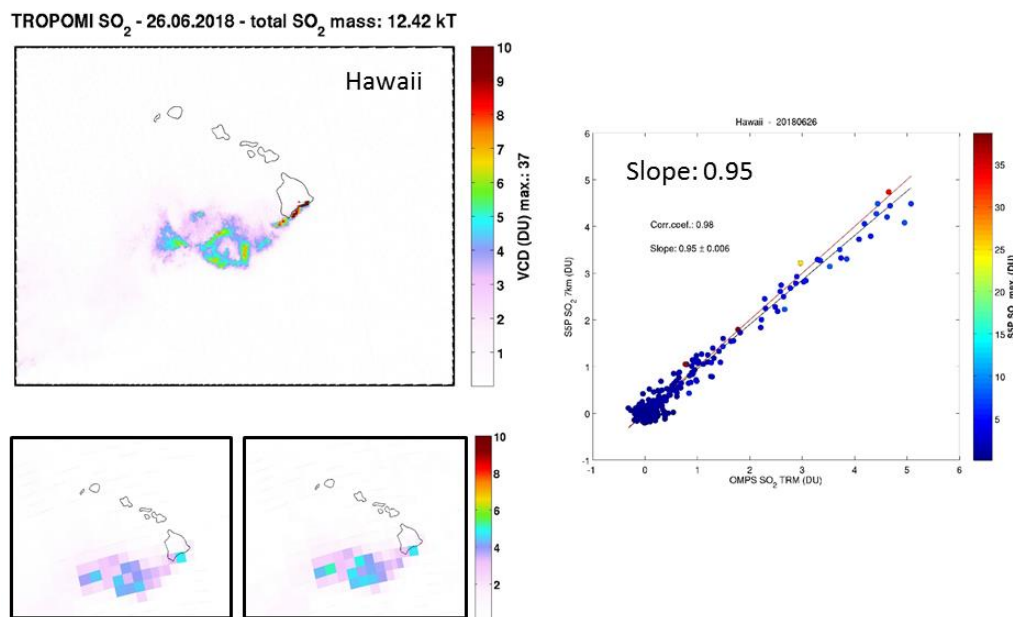
Figure 37: Comparison of TROPOMI and OMPS measurements of the volcanic plume of Kilauea on 26 June 2018. The large figure shows the original TROPOMI data. The two small figures show the spatially degraded TROPOMI data and the OMPS data. The figure right shows the correlation plot of the degraded TROPOMI data versus the collocated OMPS data. Courtesy of C. Li and N. Krotkov, NASA/GSFC.
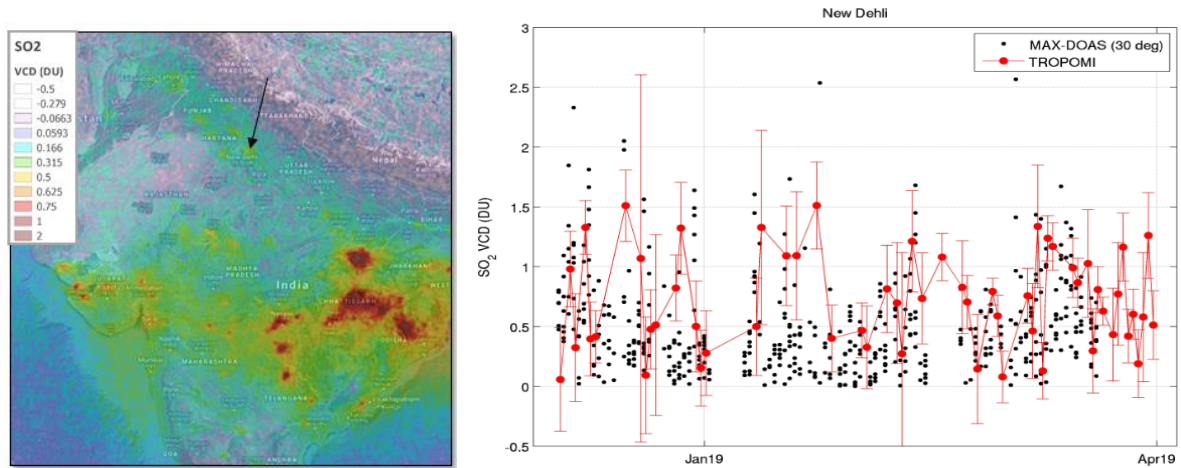
Figure 38: Comparison of TROPOMI SO$_2$ VCDs to MAX-DOAS measurements at Greater Noida (close to New Delhi, India). The following selection criteria were applied: distance < 15km, CF<0.2, AMF>0.2, MAX-DOAS +/- 1h around S5P overpass. Courtesy of M. Sharma (Sharda University, India) S. Donner, S. Dörner, T. Wagner (MPIC), N. Theys (BIRA-IASB).
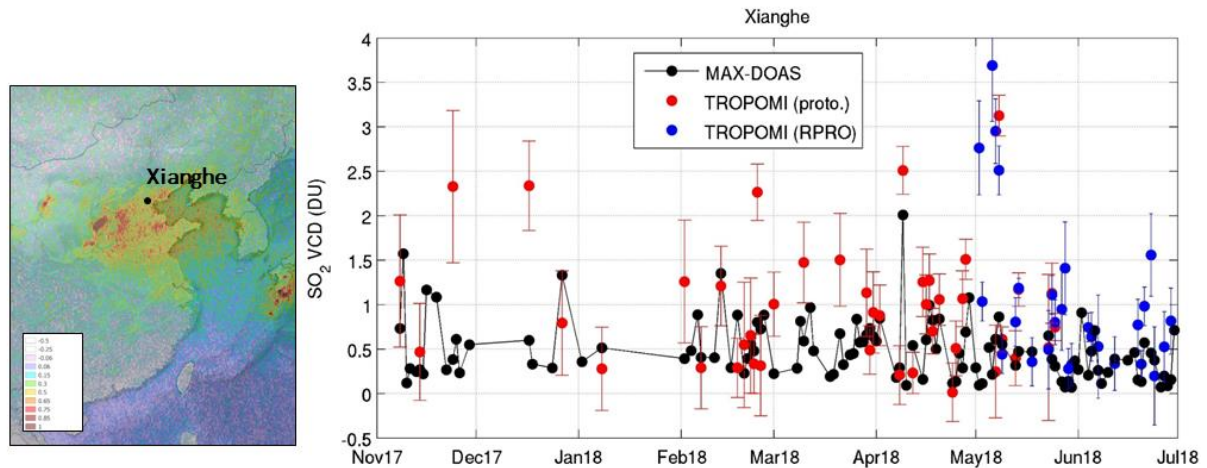
Figure 39: Comparison of TROPOMI SO$_2$ VCDs to MAX-DOAS measurements (daily means) at Xianghe (China). The following selection criteria were applied: distance < 15km, CF<0.2, AMF>0.2, number of observations >10. Courtesy of N. Theys (BIRA-IASB).
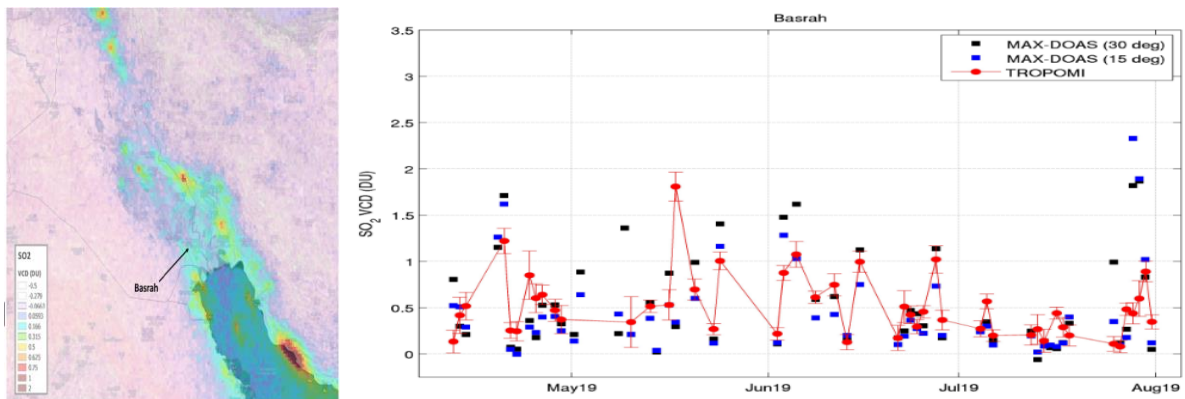
Figure 40: Comparison of TROPOMI SO$_2$ VCDs to MAX-DOAS measurements (daily means) at Basra (Iraq). The following selection criteria were applied: distance < 25km, CF<0.2, AMF>0.2, time window +/- 1h around overpass. Courtesy of N. Theys (BIRA-IASB), data provided by Nayyef Almaliki, Mustafa Aldossary, Ali Almasoudii, Sebastian Donner, Steffen Dörner, Thomas Wagner.

8.3.3   Bias

The bias is well within requirements for observations of volcanic plumes and boundary pollution. From the time series of averaged SO_2 SCDs it is estimated that the bias is within 0.2 DU.

8.3.4   Dispersion

The dispersion is well within requirements for observations boundary pollution. For observations of strong volcanic plumes the dispersion is slightly above the requirements. However, here it should be noted that the requirements (0.15-0.3 DU) are quite strict and should be reconsidered. The slightly larger dispersion over strong volcanic plumes is not seen as a substantial restriction of the data quality. From the time series of the standard deviation of the SO_2 SCDs it is estimated that the dispersion is within 0.2 DU.
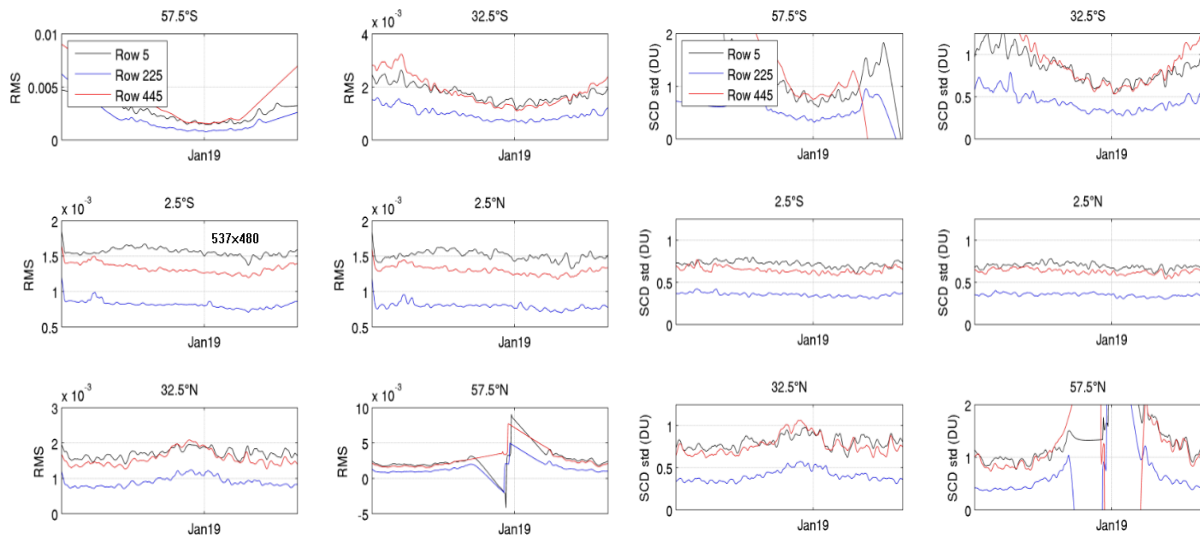
Figure 41: Temporal evolution of the measurement error (left) and the standard deviation (right) for selected 5° latitude bands and 3 detector rows from December 2018 to August 2019. Good qualitative agreement between both quantities is found indicating that the random uncertainty is well characterized by the measurement error. Larger errors (and standard deviations are found at the edges of the detector and towards high latitudes. Courtesy of N. Theys (BIRA-IASB).
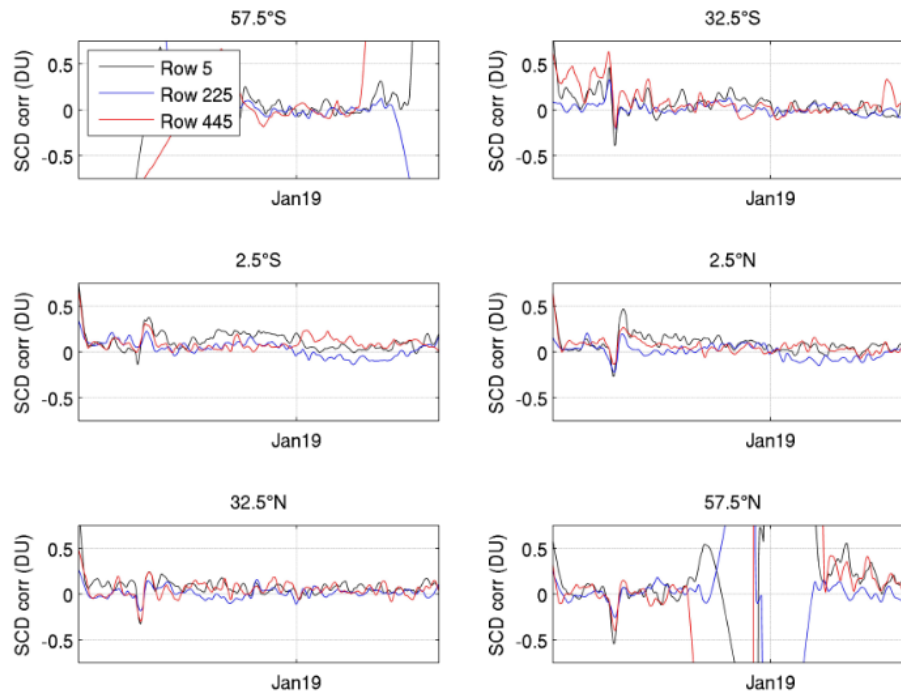
Figure 42: Temporal evolution of the averaged SO_2 SCD for selected 5° latitude bands and 3 detector rows from December 2018 to August 2019. The values are close to zero and show relatively small day to day variations. The larger variations in August are caused by strong volcanic eruptions.

8.3.5   Dependence on influence quantities

Slightly larger bias and dispersion are found towards higher SZA.

8.3.6   Short term variability

The short term variability can be estimated from the time series of averaged SO_2 SCDs (outside periods with strong volcanic eruptions). It is estimated to below about 0.1 DU.

8.3.7   Geographical patterns

Slightly larger bias and dispersion are found at higher latitudes, likely as an effect of high solar zenith angles.

8.3.8   Other features

None to report.

8.4   Equivalence of L2_SO2 NRTI and OFFL products

The NRT and offline SO_2 products are very similar, as illustrated by the comparison of the SO_2 SCDs of both data versions hereafter. Thus, the validation activities performed for the OFFL data product (see above) are also representative for the NRTI data product.
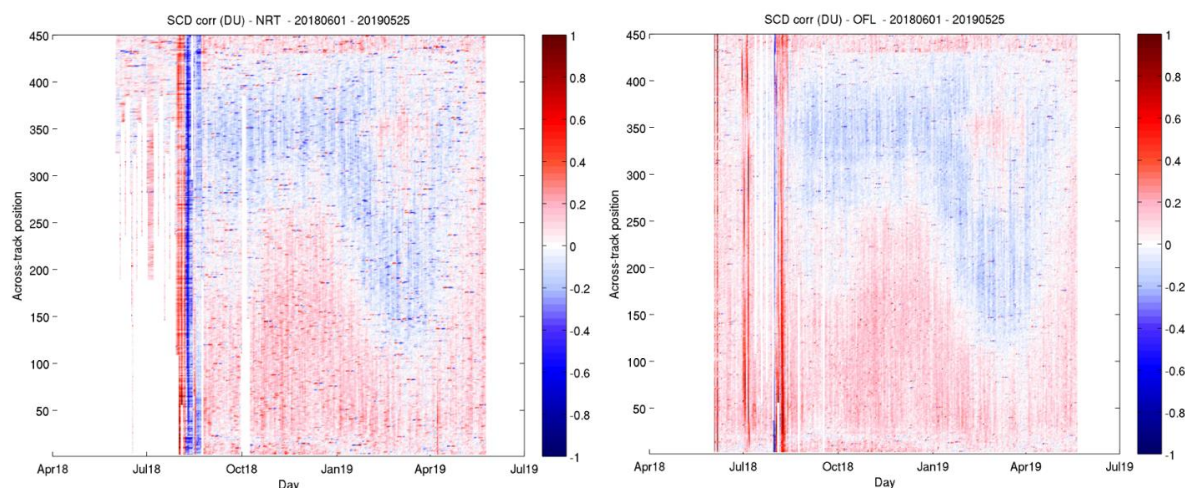
Figure 43: Comparison of the NRT (left) and offline (right) SO$_2$ data products. Shown are the time series of background corrected SO$_2$ SCDs for all 450 detector rows from June 2018 to August 2019. Courtesy of Nicolas Theys, BIRA-IASB.

9   Validation Results: L2_CO

9.1   L2_CO products and requirements

This section reports on the validation of the following geophysical variables of the S5P TROPOMI L2_CO product identified in **Table 1**: the carbon monoxide total column. Validation results are discussed with respect to the product quality targets outlined in **Table 3**. The NRTI and OFFL processors using different approaches, their respective validation is reported in separate subsections.

9.2   Validation approach

9.2.1   Ground-based networks

S5P TROPOMI L2_CO carbon monoxide column data are routinely compared to reference measurements obtained from FTIR spectrometers performing network operation in the context of the Network for the Detection of Atmospheric Composition Change (NDACC, http://ndacc.org) and the Total Carbon Column Observing Network (TCCON, https://tccondata.org). **Figure 44** displays the geographical distribution of the NDACC and TCCON sites. Near-infrared TCCON measurements provide CO column averaged (xCO) data with typical uncertainty values of 2% for the bias and 1% for the precision. Solar infrared NDACC measurements provide CO total column data with a typical total uncertainty of 3%.
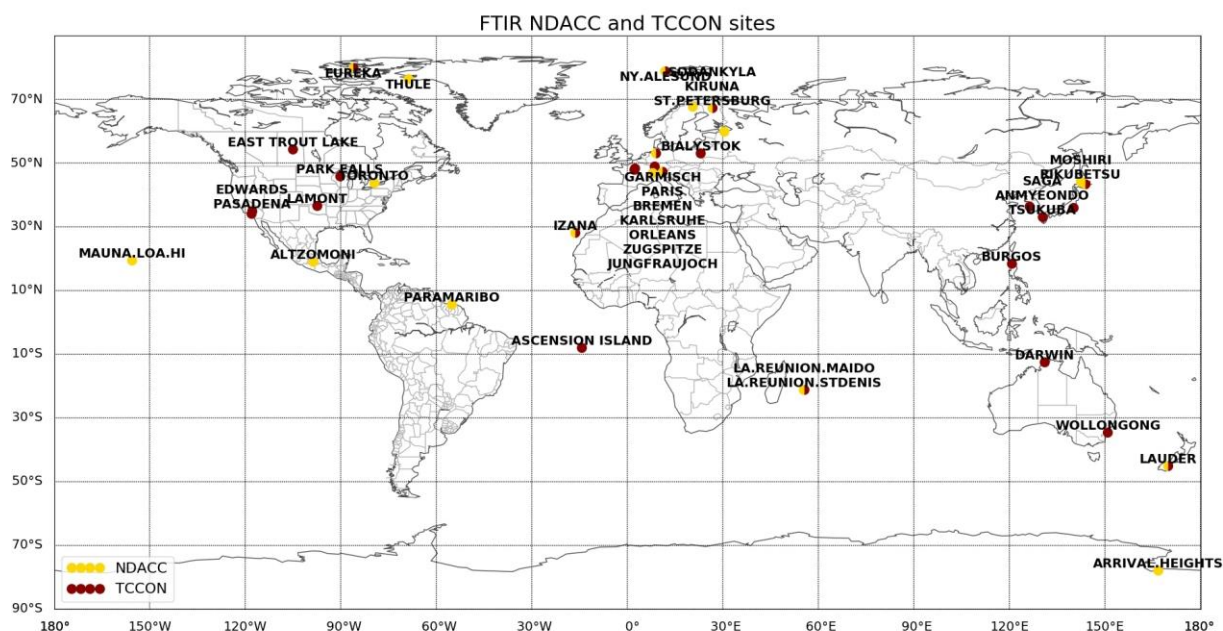
Figure 44: Geographical distribution of NDACC and TCCON FTIR stations measuring atmospheric carbon monoxide column data. Some sites contribute to both networks.

9.2.2   Satellites

None for this report.

9.2.3   Field campaigns and modelling support

None for this report.

9.3   Validation of L2_CO NRTI

9.3.1   Recommendations for data usage followed

The Product Readme File (PRF) recommends the use of only S5P data with a `qa_value` above 0.5. The validation results reported hereafter are obtained by filtering the pixels using the parameters mentioned in the PRF, distinguishing three cases based on cloud filtering:

1. Clear sky: cloud height below 500 m and cloud optical depth below 0.5 (`qa_value=1`);
2. Cloud: cloud height below 5000 m and cloud optical depth above 0.5 (`qa_value=0.7`);
3. All: cloud height below 5000 m.

For further details, data users are encouraged to read the Product Readme File (PRF), Product User Manual (PUM) and Algorithm Theoretical Basis Document (ATBD) associated with this data product, all available on https://sentinels.copernicus.eu/web/sentinel/technical-guides/sentinel-5p/products-algorithms.

9.3.2   Status of validation

This section presents a summary of the key validation results obtained by the MPC VDAF and by S5PVT AO projects. It is based on the validation methodology used at the S5P First Public Release Validation Workshop (ESA/ESRIN, June 25-26, 2018). Up-to-date validation results and consolidated validation reports are available through the MPC VDAF Portal at http://mpc-vdaf.tropomi.eu.

Current conclusions are based on the S5P and reference measurements available at the time of this analysis, which yield comparison pairs from May 2018 through June 2019. Routine validation is done using the Automated Validation Server of the MPC VDAF, the CO validation system operated at BIRA-IASB, and the HARP toolset.

TROPOMI observations co-located with the TCCON measurements are found by selecting all filtered TROPOMI pixels within a radius of 50 km around each station and with a maximal time difference of 1h for TCCON and 6h for NDACC observations. The 1 hour interval can be justified by noting that TCCON instruments acquire only one type of spectra, while NDACC instruments are supposed to measure different type of spectra, making the CO observations more sparse. In the TCCON comparison, the apriori in the TCCON measurements have been substituted with the S5P CO apriori (Rodgers 2003). The validation setup for both the NDACC and TCCON columns adapts the TROPOMI CO column to the altitude of the groundbased FTIR instrument.

9.3.3 Bias

The systematic difference between daily mean co-locations is on average 9% for the NDACC and 14% for the TCCON network. At some sites this is exceeded typically because of the currently limited amount of co-locations or geographical colocation issues (e.g., mountain stations). This bias value falls well within the mission requirements. **Figure 46** (NDACC) and **Figure 47** (TCCON) display the mean biases for the full time period (May 2018 – June 2019) sorted by latitude. It seems that there is no latitudinal dependence of the bias. **Figure 45** does not show any significant degradation in bias in time (note that the longer time period covers different processor versions). **Figure 45** also shows a slight increase of bias during local winter, but due to the limited time period it is too early to make conclusions on seasonal cycle of the bias.
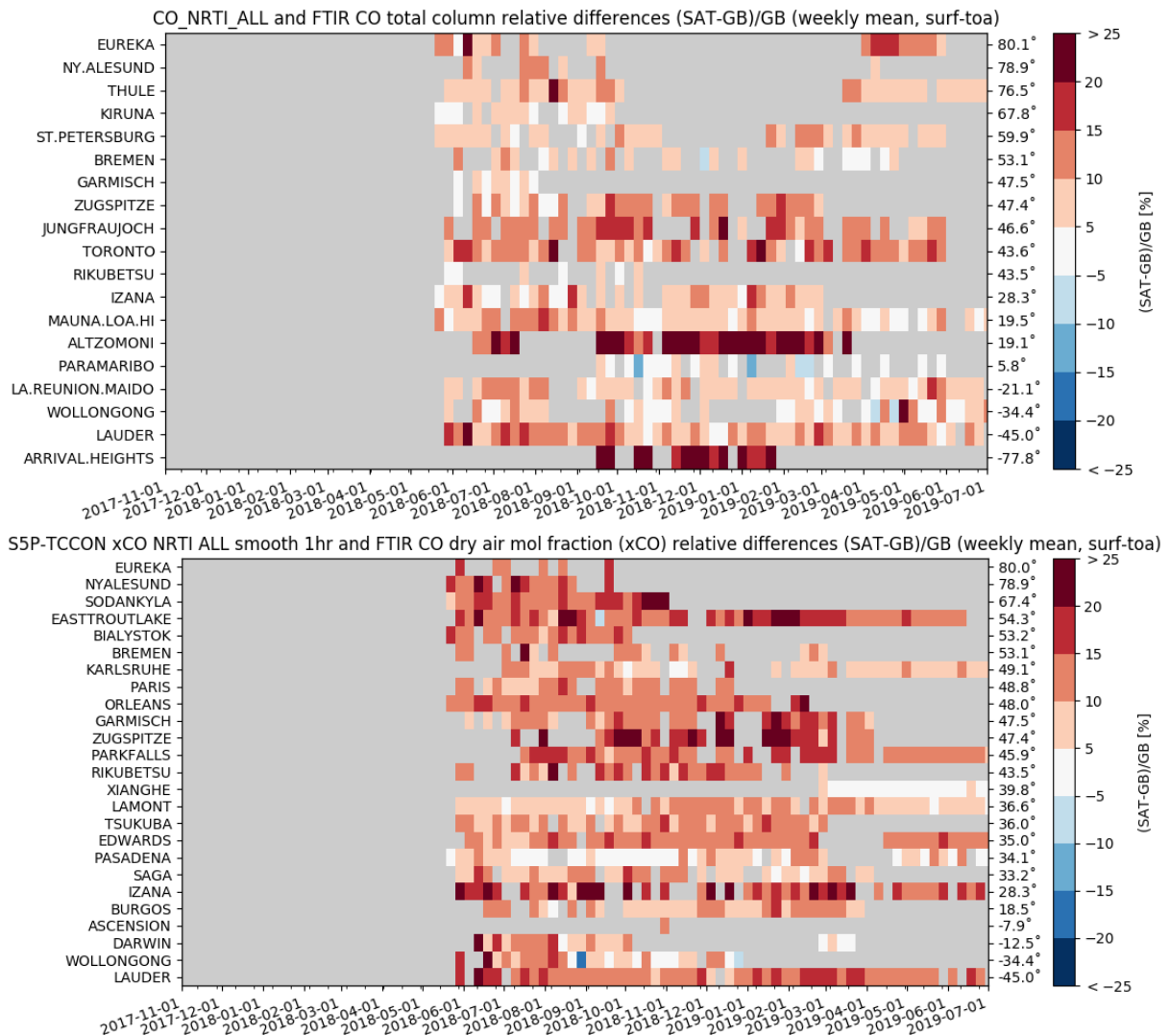
Figure 45: Mosaic plots of relative biases between S5P L2_CO NRTI and NDACC (top) and TCCON (bottom) FTIR measurements. The plots do not show a clear meridian dependence or temporal change in the biweekly averaged biases for the time period May 2018 – March 2019.
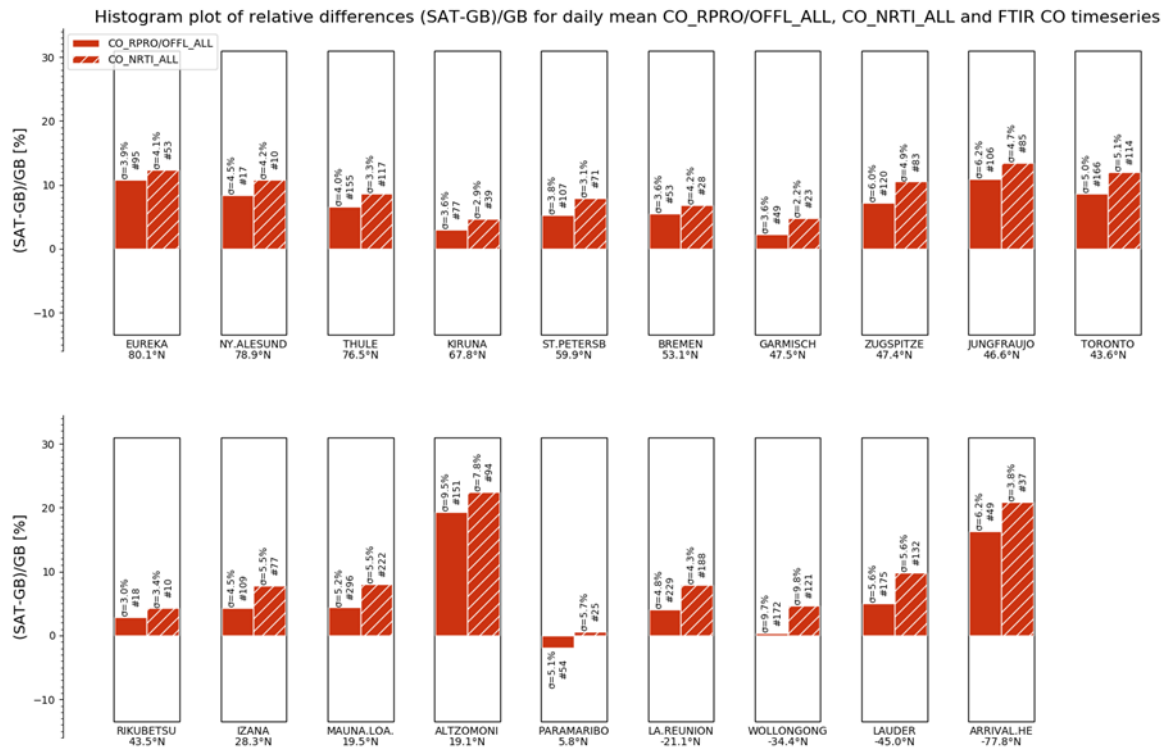
Figure 46: Bar chart of relative mean difference for 19 NDACC FTIR sites for all data within the time range from May 2018 till June 2019 showing NRTI against RPRO/OFFL . The sites are sorted with decreasing latitude. All biases are below 15% except at Altzomoni, which is a mountain city near Mexico City: the higher bias is due to the chosen pixel selection criteria, here higher concentration pixels near the city are taken into account in the average. Arrival Height (Antarctic) also shows an increased bias.
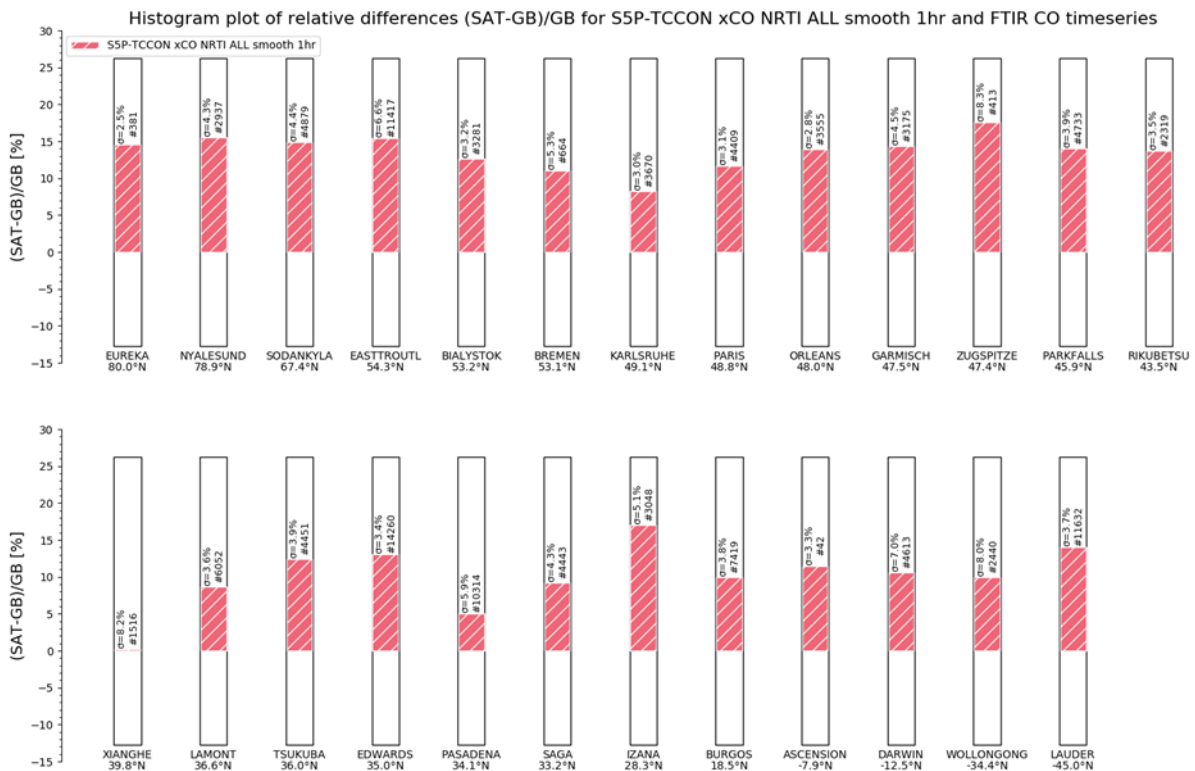
Figure 47: Bar chart of relative mean difference for 25 TCCON sites for all data within the time range May 2018 till June 2019. The sites are sorted with decreasing latitude. All biases are below 15%. Xianghe station lies in a polluted region where we see almost zero bias.

9.3.4   Dispersion

The 1σ dispersion of the relative mean bias around its mean is of the order of 5%. The individual values for the different sites are indicated in **Figure 46** and **Figure 47.** This dispersion can be considered as an upper boundary of the random uncertainty of the satellite data.

9.3.5   Dependence on influence quantities

At this stage, the evaluation of potential dependence of the S5P bias and spread on the Solar Zenith Angle (SZA) does not reveal any significant variation.
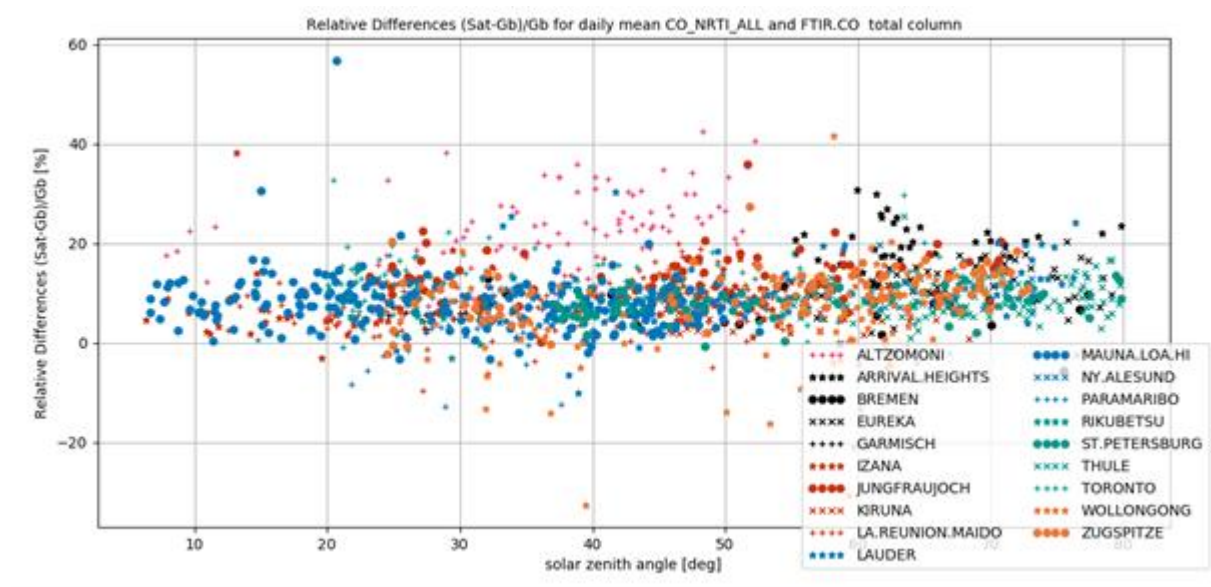
Figure 48: Relative difference (daily mean) between S5P L2_CO NRTI and NDACC carbon monoxide total column as a function of the TROPOMI solar zenith angle, in the 'all' case.

9.3.6   Short term variability

For all the NDACC and TCCON stations, short scale temporal variations in the CO column as captured by ground-based instruments are reproduced very similarly by S5P L2_CO NRTI. This overall good agreement is confirmed by individual Pearson correlation coefficients well above 0.6 and on average reaching almost 0.9.

Taylor diagram for daily mean CO_NRTI_ALL and FTIR.CO timeseries

1: CO_NRTI_ALL
2: EUREKA (53)
3: NY.ALESUND (10)
4: THULE (117)
5: KIRUNA (39)
6: ST.PETERSBURG (71)
7: BREMEN (28)
8: GARMISCH (23)
9: ZUGSPITZE (83)
10: JUNGFRAUJOCH (85)
11: TORONTO (114)
12: RIKUBETSU (10)
13: IZANA (77)
14: MAUNA.LOA.HI (222)
15: ALTZOMONI (94)
16: PARAMARIBO (25)
17: LA.REUNION.MAIDO (188)
18: WOLLONGONG (121)
19: LAUDER (132)
20: ARRIVAL.HEIGHTS (37)

Taylor diagram for S5P-TCCON xCO NRTI ALL smooth 1hr and FTIR.CO timeseries

1: S5P-TCCON xCO NRTI ALL smooth 1hr
2: EUREKA (381)
3: NYALESUND (2937)
4: SODANKYLA (4879)
5: EASTTROUTLAKE (11417)
6: BIALYSTOK (3281)
7: BREMEN (664)
8: KARLSRUHE (3670)
9: PARIS (4409)
10: ORLEANS (3555)
11: GARMISCH (3175)
12: ZUGSPITZE (413)
13: PARKFALLS (4733)
14: RIKUBETSU (2319)
15: XIANGHE (1516)
16: LAMONT (6052)
17: TSUKUBA (4451)
18: EDWARDS (14260)
19: PASADENA (10314)
20: SAGA (4443)
21: IZANA (3048)
22: BURGOS (7419)
23: ASCENSION (42)
24: DARWIN (4613)
25: WOLLONGONG (2440)
26: LAUDER (11632)

Figure 49: Taylor diagrams for daily mean differences between S5P L2_CO NRTI and network CO data: NDACC (top) and TCCON (bottom) for our all case of pixel selection criteria. Poor correlation is observed at Wollongong (see below); Paramaribo and Ascension (few co-locations).
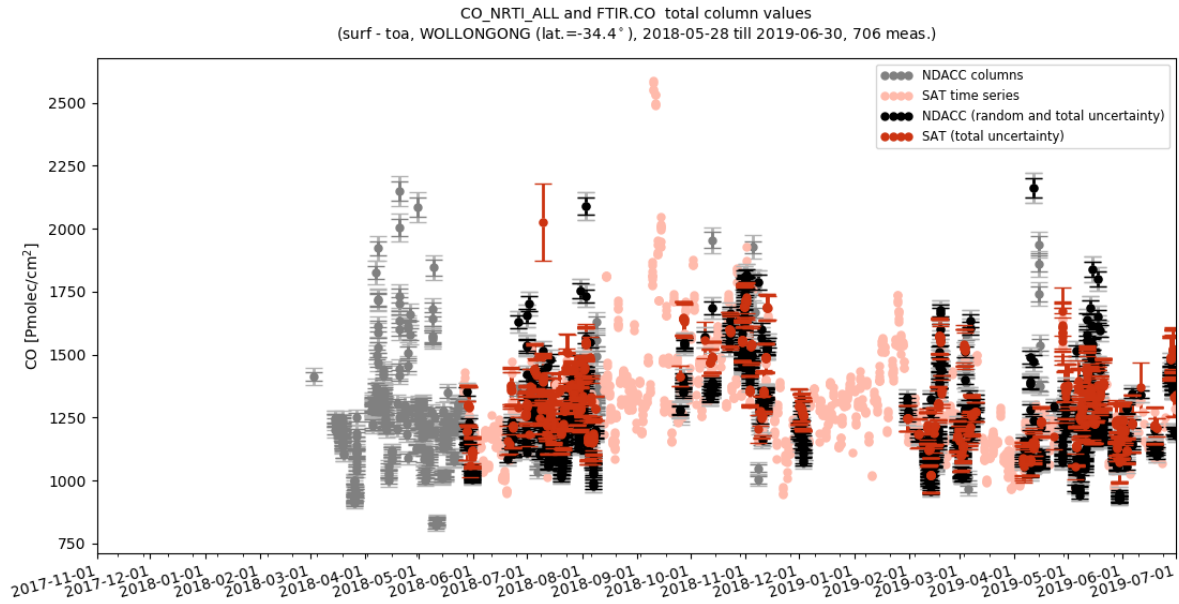
Figure 50: Wollongong time series. Lower correlation values are due to outlying satellite CO columns and some higher concentration values not observed by the NRTI product after April 2019. This may be caused by the higher tolerance in time difference between observations and satellite overpass (6h).

9.3.7 Geographical patterns

See section 9.4.7

9.3.8 Other features

NRTI granules from one S5P orbit have overlapping pixels. In order to avoid duplicated pixels in the validation statistics, pixels from the first 12 scanlines have been filtered.

9.4 Validation of L2_CO OFFL

9.4.1 Recommendations for data usage followed

The Product Readme File (PRF) recommends the use of only S5P data with a `qa_value` above 0.5. The validation results here are obtained by filtering the pixels using the parameter mentioned in the PRF, distinguishing three cases based on cloud filtering:

4. Clear sky: cloud height below 500 m and cloud optical depth below 0.5 (`qa_value=1`);
5. Cloud: cloud height below 5000 m and cloud optical depth above 0.5 (`qa_value=0.7`);
6. All: cloud height below 5000 m

For further details, data users are encouraged to read the Product Readme File (PRF), Product User Manual (PUM) and Algorithm Theoretical Basis Document (ATBD) associated with this data product, all available on https://sentinels.copernicus.eu/web/sentinel/technical-guides/sentinel-5p/products-algorithms.

### 9.4.2 Status of validation

This section presents a summary of the key validation results obtained by the MPC VDAF and by S5PVT AO projects. It is based on the validation methodology used at the S5P First Public Release Validation Workshop (ESA/ESRIN, June 25-26, 2018). Individual contributions to the workshop are archived in https://nikal.eventsair.com/QuickEventWebsitePortal/sentinel-5p-first-product-release-workshop/sentinel-5p, while up-to-date validation results and consolidated validation reports are available through the MPC VDAF Portal at http://mpc-vdaf.tropomi.eu.

Current conclusions are based on the amount of reference measurements available at the time of this analysis, yielding comparison pairs from November 2017 through June 2019. The more basic validation is done using the Automated Validation Server of the MPC VDAF, the CO validation system operated at BIRA-IASB, and the HARP toolset.

For the comparison TROPOMI observations are co-located with the TCCON measurements by selecting all filtered TROPOMI pixels within a radius of 50 km around each station and with a maximal time difference of 1h for TCCON and 6h for NDACC observations. The 1 hour interval can be justified by noting that TCCON instruments acquire only one type of spectra, while NDACC instruments are supposed to measure different type of spectra, making the CO observations more sparse. In the TCCON comparison, the apriori in the TCCON measurements have been substituted with the S5P CO apriori (Rodgers 2003). The validation setup for both the NDACC and TCCON columns adapts the TROPOMI CO column to the altitude of the groundbased FTIR instrument.

9.4.3 Bias

The systematic difference between daily mean co-locations is on average 6% for NDACC and 9% for the TCCON network. At some sites this is exceeded typically because of geographical colocation issues (mountain stations, …). This bias value falls well within the mission requirements. **Figure 52** and **Figure 53** show the biases for the full time period (Nov 2017 – June 2019) sorted by latitude. Given the restricted time period, it seems that there is no latitudinal dependence of the bias. **Figure 51** does not show any significant degradation in bias in time (note that the longer time period covers different processor versions). **Figure 51** also shows a slight increase of bias during local winter, but due to the limited time period it is too early to make conclusions on seasonal cycle of the bias
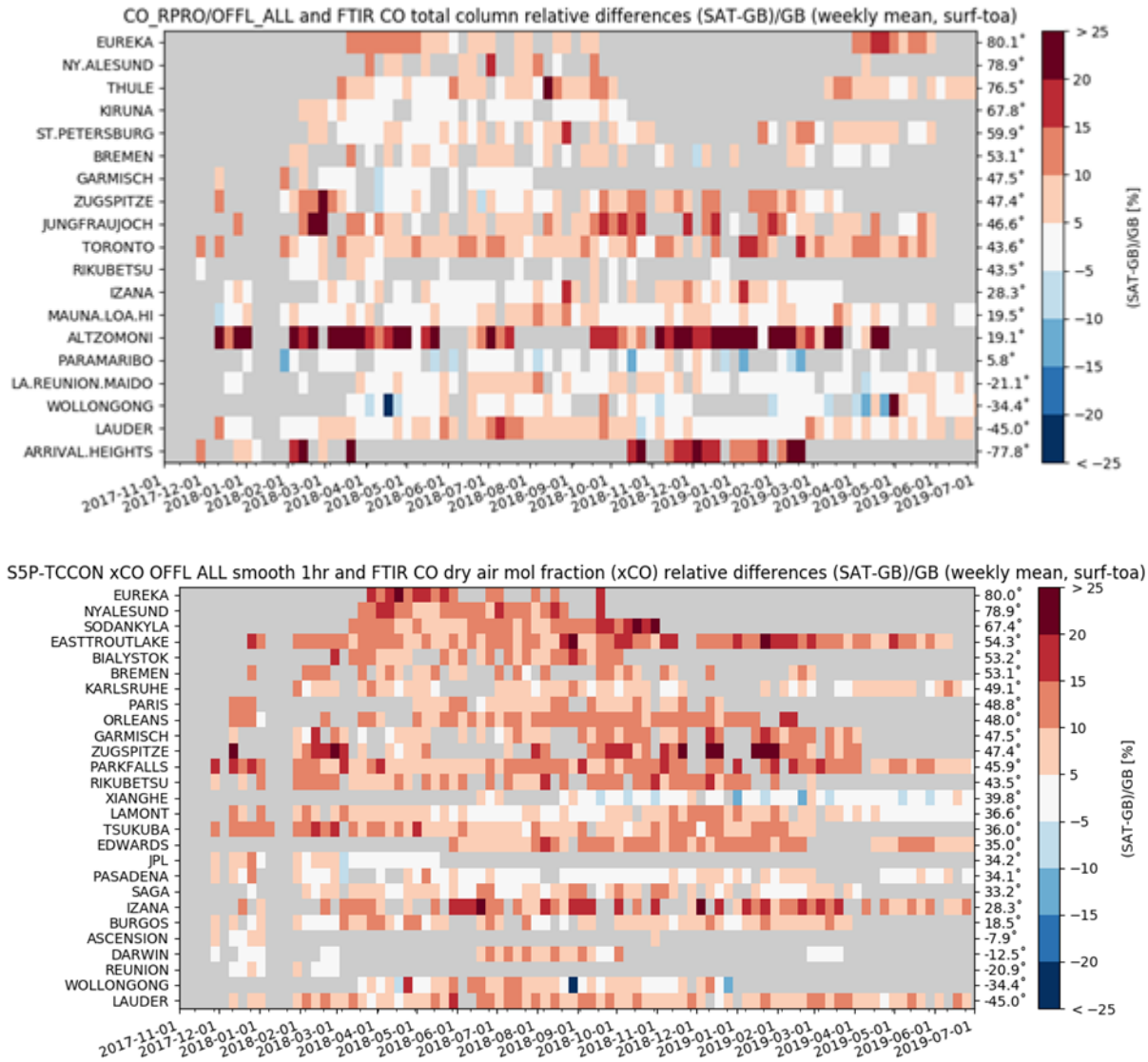
Figure 51: Mosaic plots of relative biases between S5P L2_CO OFFL and ground-based CO column data at NDACC (top) and TCCON (bottom) stations. Over the Nov. 2017 – June 2019 time period the plots do not show a clear meridian dependence or temporal change in the weekly averaged biases.
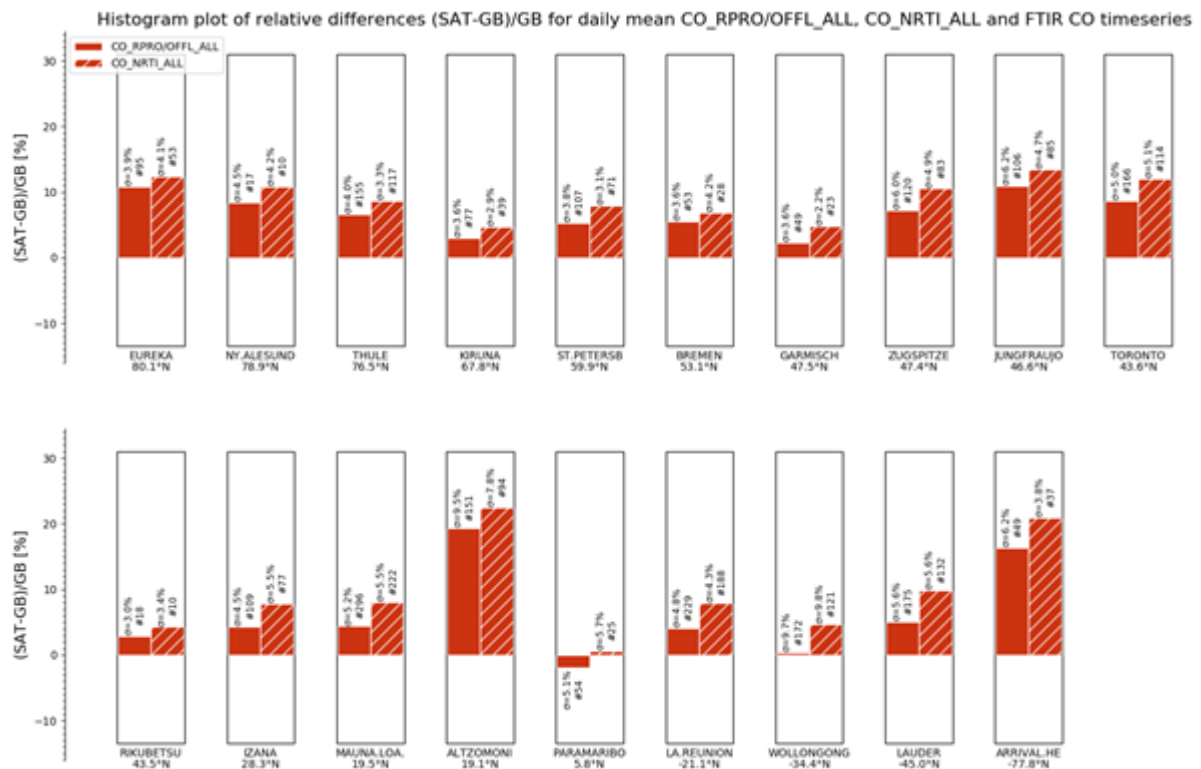
Figure 52: Bar chart of relative mean difference for 19 NDACC FTIR sites for all data within the time range from May 2018 till June 2019 showing NRTI against RPRO/OFFL . The sites are sorted with decreasing latitude. All biases are below 15% except at Altzomoni, which is a mountain city near Mexico City: the higher bias is due to the chosen pixel selection criteria, here higher concentration pixels near the city are taken into account in the average. Arrival Height (Antarctic) also shows an increased bias.
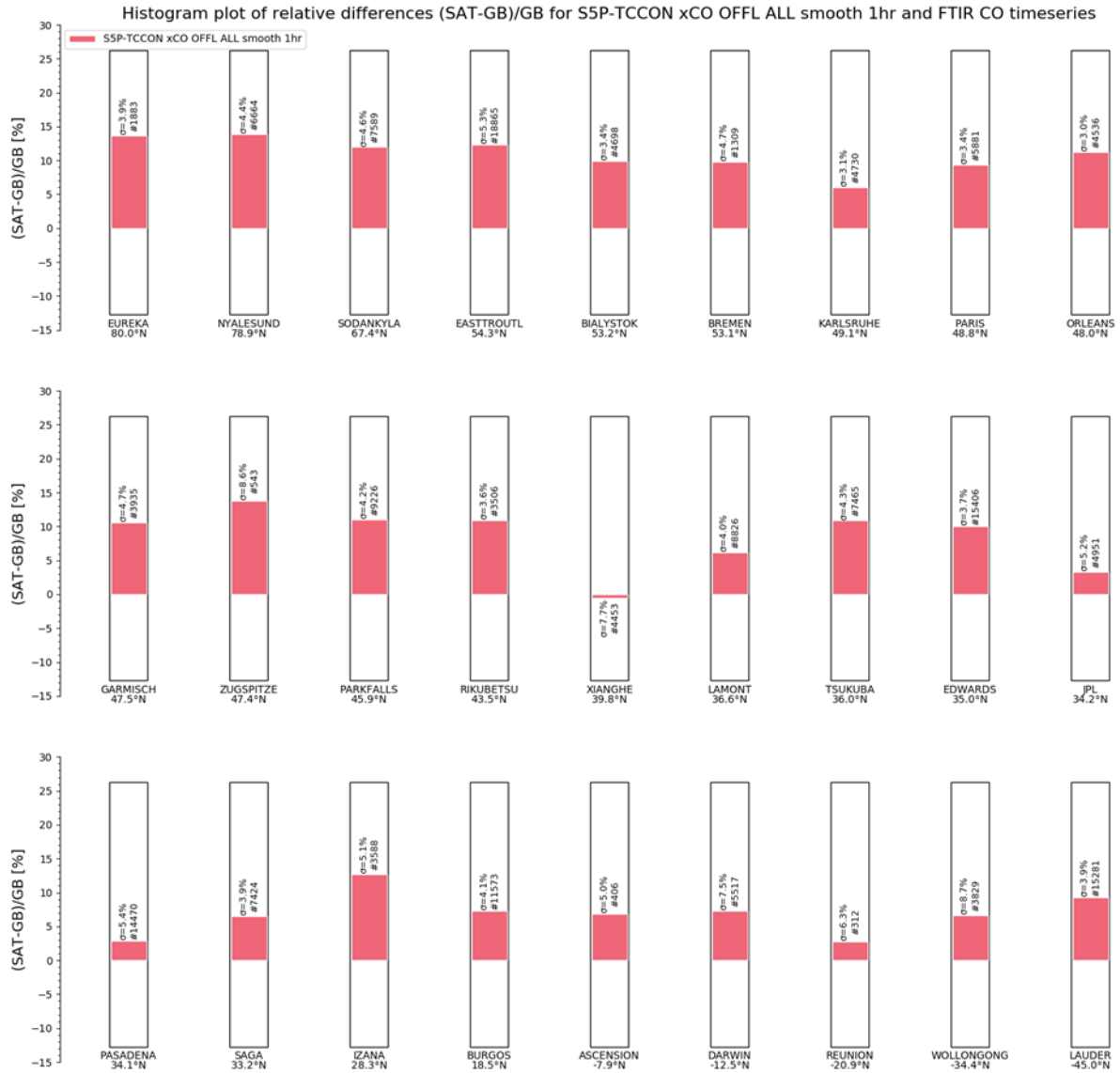
Figure 53: Bar chart of relative mean difference between S5P and FTIR CO column data at 27 TCCON sites for all data within the time range Nov 2017 till June 2019. The sites are sorted with decreasing latitude. The majority of the biases are below 10% except in the Arctic where the bias is slightly above 10%. Xianghe station lies in a polluted region where we see almost zero bias.

9.4.4   Dispersion

The 1σ dispersion of the relative mean bias around its mean is of the order of 5%. The individual values for the different sites are indicated in **Figure 52** and **Figure 53.** This dispersion can be considered as an upper boundary of the random uncertainty of the satellite data.

9.4.5   Dependence on influence quantities

At this stage, the evaluation of potential dependence of the S5P bias and spread on the Solar Zenith Angle (SZA) shows an increase of the relative bias with the solar zenith angle of about 5% between 10deg and 80deg. A more precise estimate will be made when more measurement data is available.
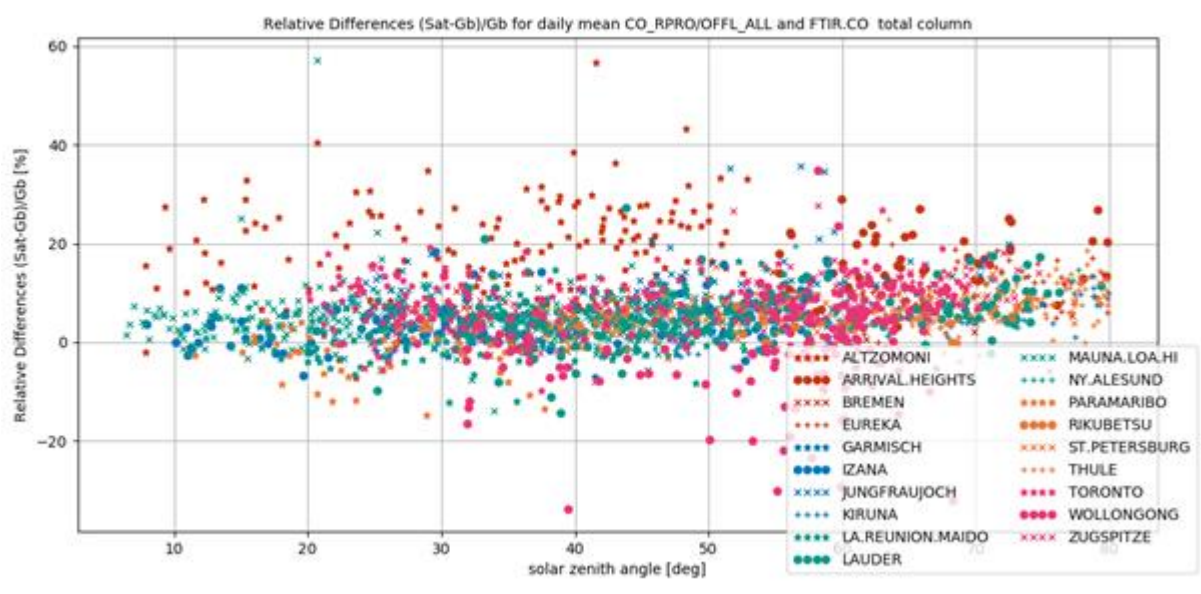
Figure 54: Bar Relative difference (daily mean) between S5P L2_CO RPRO/OFFL and NDACC carbon monoxide total column as a function of the TROPOMI solar zenith angle, in the 'all' case.

9.4.6   Short term variability

For all the NDACC and TCCON stations, short scale temporal variations in the CO column as captured by ground-based instruments are reproduced very similarly by S5P L2_CO OFFL. This overall good agreement is confirmed by individual Pearson correlation coefficients well above 0.6 and on average reaching almost 0.9 (**Figure 55**).
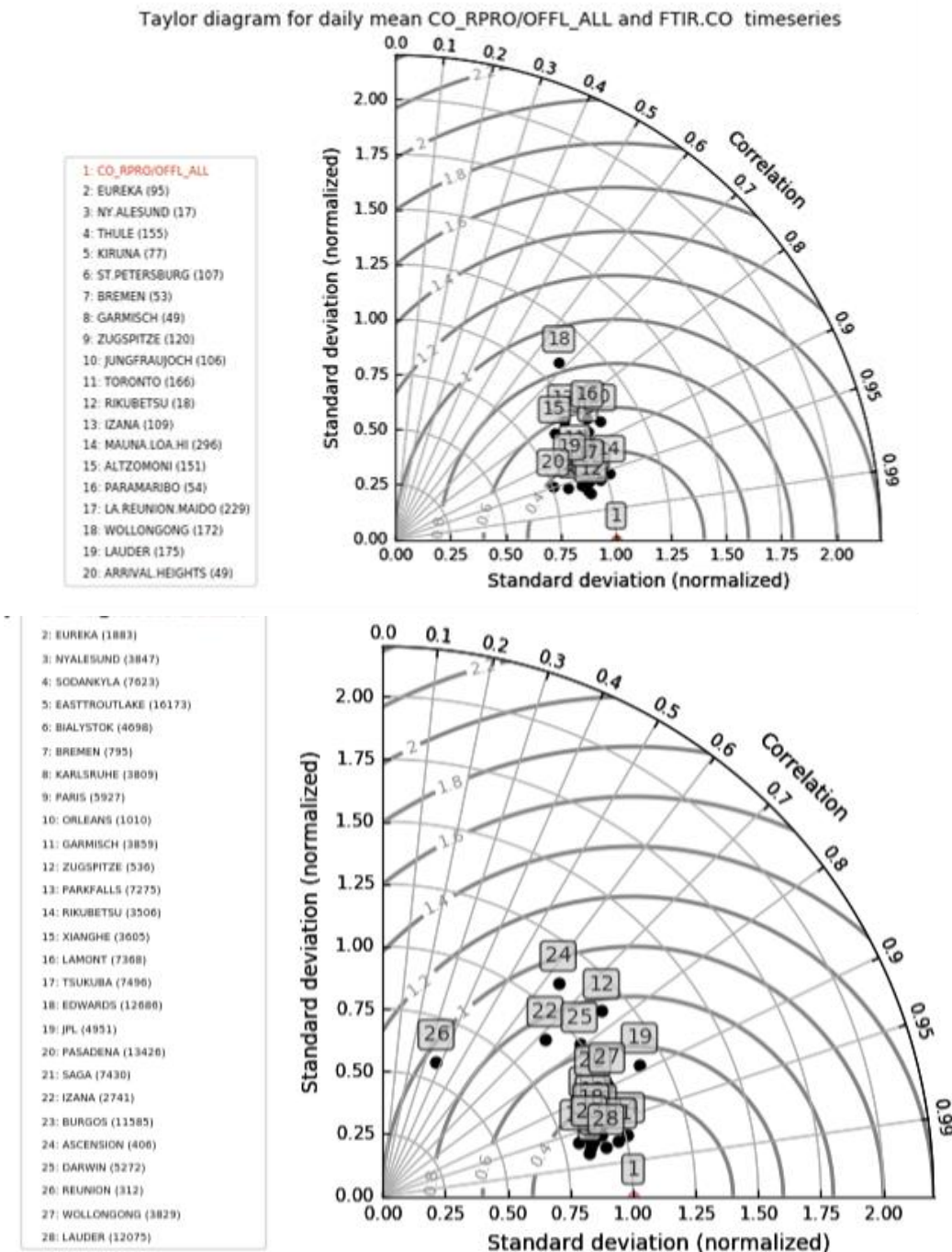
Figure 55: Taylor diagrams for daily mean differences between S5P L2_CO OFFL and ground-based networks CO data: NDACC (top) and TCCON (bottom) for our all case of pixel selection criteria.

9.4.7 Geographical patterns

Single TROPOMI overpasses show stripes of erroneous CO values < 5% in the flight direction, probably due to calibration issues of TROPOMI, see **Error! Reference source not found.** below. This data quality issue is known but not covered by the quality flags, and should be kept in mind when looking at the carbon monoxide data product and also at preliminary validation results. How this can be removed from the data is discussed in the PRF and is subject to further investigation in the framework of instrument calibration.
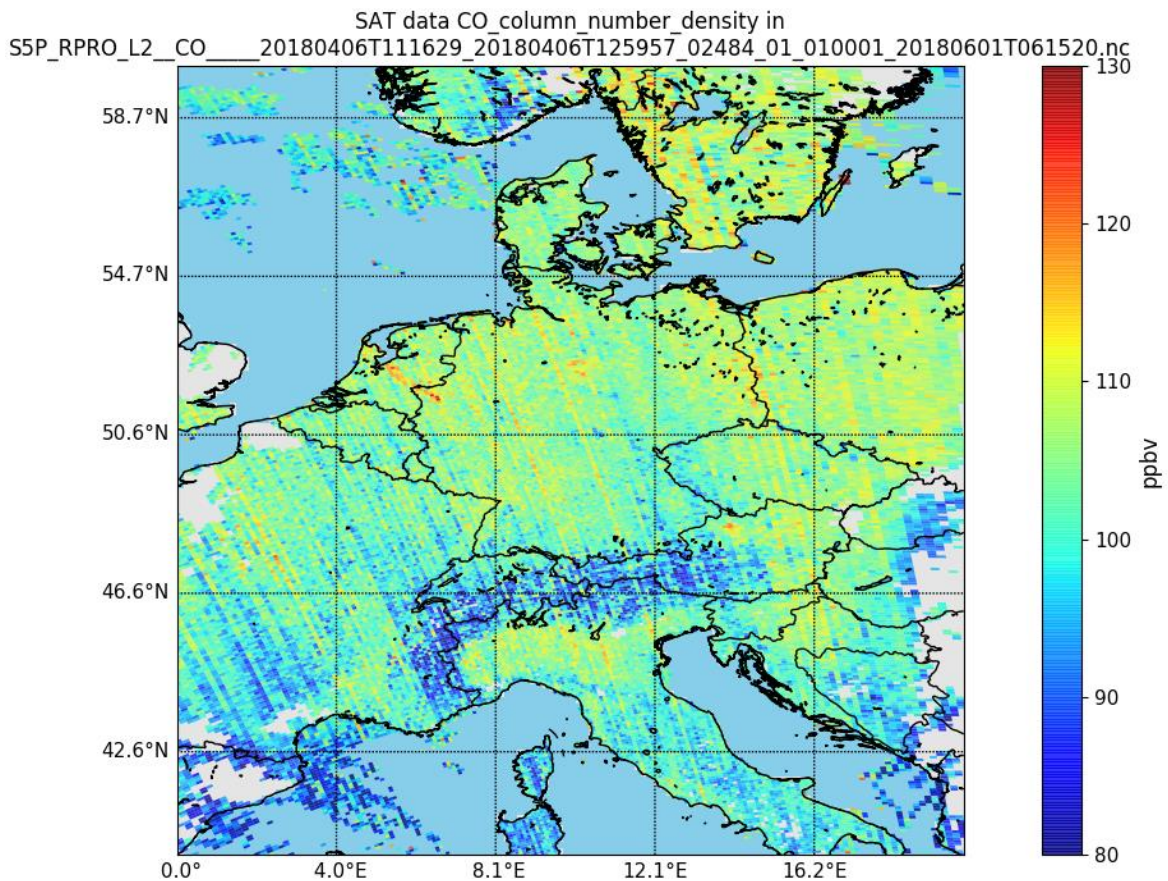
Figure 56: Example of stripe patterns in L2_CO OFFL data along a S5P orbit above Europe.

9.4.8 Other features

None to report.

10   Validation Results: L2_CH4

10.1   L2_CH4 products and requirements

This section reports on the validation of the following geophysical variables of the S5P TROPOMI L2_CH4 product identified in **Table 1**: the methane total column. Validation results are discussed with respect to the product quality targets outlined in **Table 3**.

10.2   Validation approach

10.2.1   Ground-based networks

S5P TROPOMI L2_CH4 methane column data are routinely compared to reference measurements obtained from FTIR spectrometers performing network operation in the context of the Network for the Detection of Atmospheric Composition Change (NDACC, http://ndacc.org) and the Total Carbon Column Observing Network (TCCON, https://tccondata.org). **Figure 44** displays the geographical distribution of the NDACC and TCCON sites. Near-infrared TCCON measurements provide calibrated methane column averaged (xCH_4) data with typical uncertainty values of 0.5% for the precision and 0.2% for the accuracy. Solar infrared NDACC measurements provide CH_4 total column data with a lower accuracy (typically 3%) and precision (1.5%). The required accuracy (<1.5%) and precision (<1%) for S5P implies that we mainly focus on the validation with TCCON measurements.

10.2.2   Satellites

None for this report.

10.2.3   Field campaigns and modelling support

None for this report.

10.3   Validation of L2_CH4 OFFL

10.3.1   Recommendations for data usage followed

The Product Readme File (PRF) recommends the use of only S5P data with a `qa_value` above 0.5.

The S5P L2 data contains two xCH_4 column values: the standard retrieved product and a bias corrected product. Both products are validated separately, but only the bias corrected is mentioned in the quality indicators in **Table 2**.

For further details, data users are encouraged to read the Product Readme File (PRF), Product User Manual (PUM) and Algorithm Theoretical Basis Document (ATBD) associated with this data product, all available on https://sentinels.copernicus.eu/web/sentinel/technical-guides/sentinel-5p/products-algorithms.

10.3.2 Status of validation

This section presents a summary of the key validation results obtained by the MPC VDAF and by S5PVT AO projects. The results presented here are an update of the first results reported at the S5P acceptance review meeting in February 2019 that are available through the MPC VDAF Portal at http://mpc-vdaf.tropomi.eu.

TROPOMI observations co-located with the TCCON measurements are found by selecting all filtered TROPOMI pixels within a radius of 100 km around each station and with a maximal time difference of 1h for TCCON and 3h for NDACC observations. The 1 hour interval can be justified by noting that TCCON instruments acquire only one type of spectra, while NDACC instruments are supposed to measure different type of spectra, making the CH_4 observations more sparse. In the comparison, the apriori in the TCCON/NDACC measurements have been substituted with the S5P CH_4 apriori (Rodgers 2003). For NDACC data the method described in Rodgers (2003) is followed one step further and the FTIR CH_4 concentration profile (with the S5P prior substituted) is additionally smoothed with the S5P column averaging kernel. The validation setup for both the NDACC and TCCON columns adapts the TROPOMI CH_4 column to the altitude of the groundbased FTIR instrument.

Current conclusions are based on the S5P and reference measurements available at the time of this analysis, which yield comparison pairs from January 2018 through June 2019. Routine validation is done using the Automated Validation Server of the MPC VDAF, the CH_4 validation system operated at BIRA-IASB, and the HARP toolset and shows an up-to-date comparison.

10.3.3   Bias

The systematic difference (the mean of all relative differences) is on the average -0.8% (standard) and -0.3% (bias corrected), well within the mission requirements. Only at a few TCCON sites the bias is slightly higher than 1.5% for the standard S5P methane column.
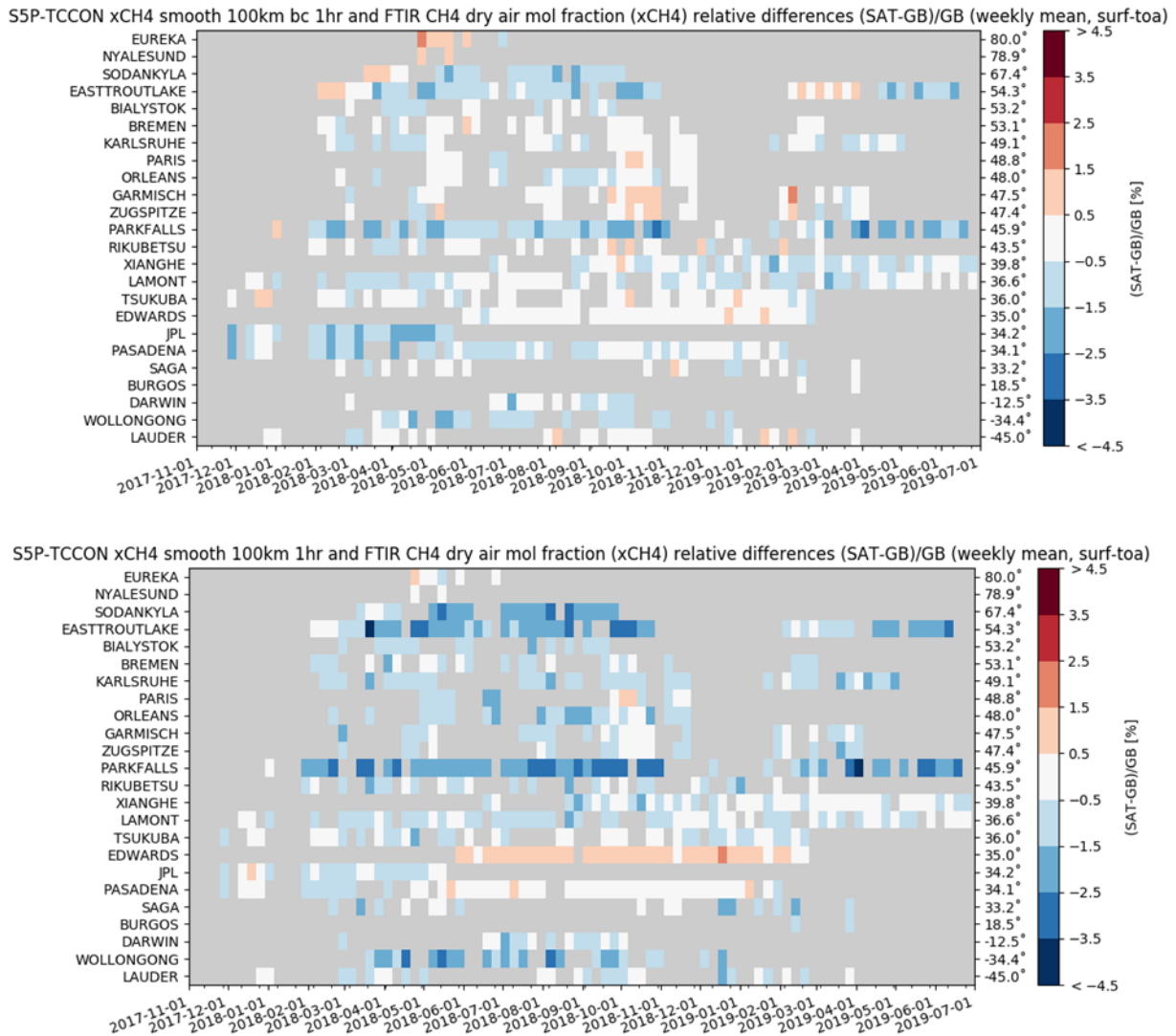
Figure 57: Mosaic plots of relative biases between S5P L2_CH4 RPRO+OFFL and ground-based CH_4 TCCON column data for the bias corrected (top) and standard (bottom) methane products. Over the Dec. 2017 – June 2019 time period the plots do not show a clear meridian dependence or temporal change in the biweekly averaged biases.
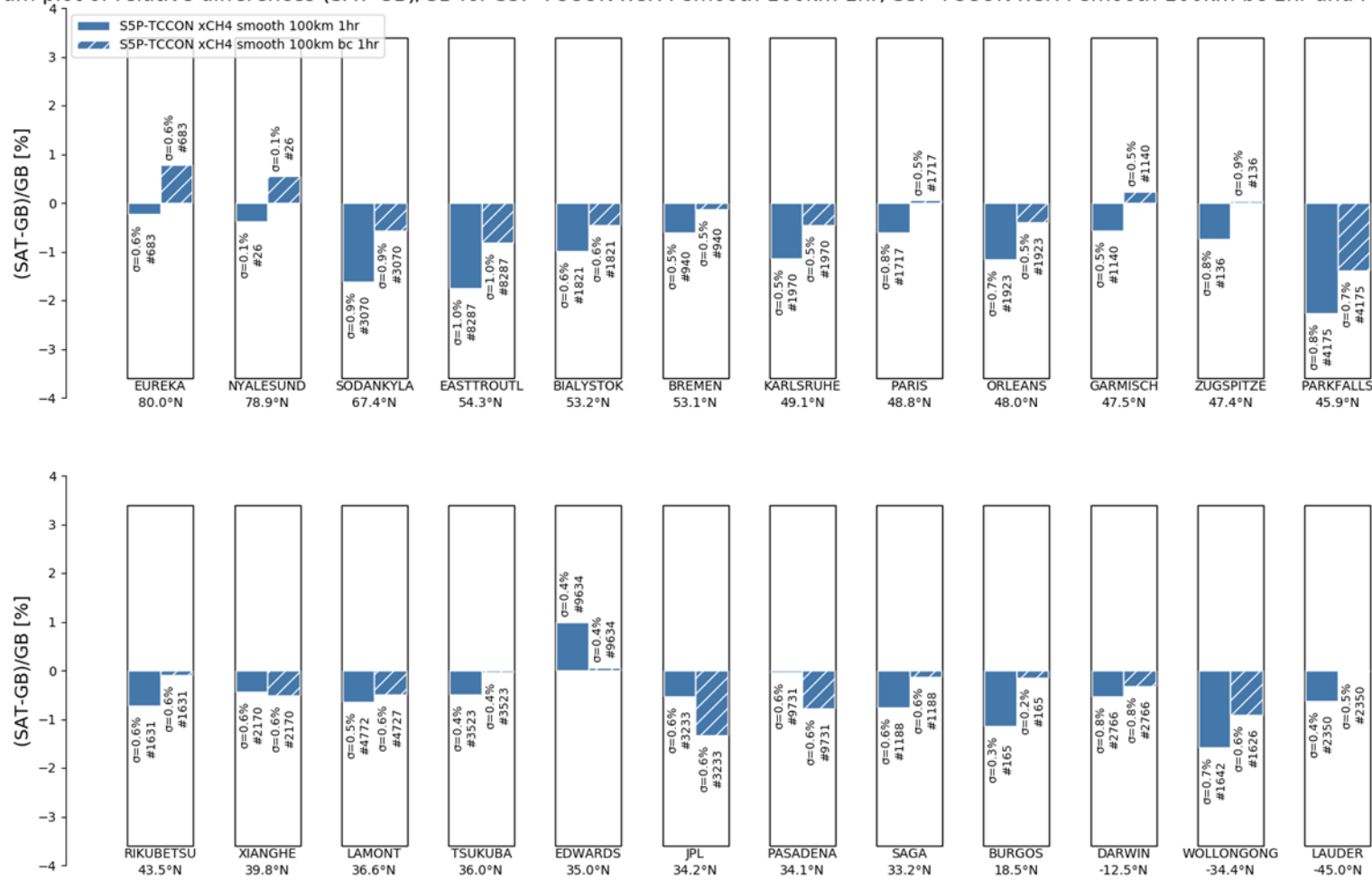
Figure 58: Bar chart of relative mean difference between S5P and FTIR CH$_4$ column data at 24 TCCON sites within the time range Nov 2017 till June 2019. The sites are sorted with decreasing latitude. The relative mean difference of the standard XCH4 product slightly exceeds the mission requirements (bias below 1.5%) only at a few TCCON sites (i.e. Sodankylä, East Trout Lake, Parkfalls and Wollongong). However, it never exceeds the mission requirements for the bias corrected product.

site	#	rel. NDACC std	correlation	rel diff bias(%)	rel diff std(%)	#	rel. NDACC std	correlation	rel diff bias(%)	rel diff std(%)	lat
			S5P-NDACC xCH4 smooth 100km 3hr					S5P-NDACC xCH4 smooth 100km bc 3hr			
NY.ALESUND	4	2.7	0.89	3.57	1.07	4	2.7	0.97	4.54	1.02	78.9
THULE	52	0.9	0.74	3.52	0.75	52	0.9	0.76	4.52	0.73	76.5
KIRUNA	61	0.8	0.16	-0.51	1.41	61	0.7	0.18	0.49	1.44	67.8
SODANKYLA	72	0.9	0.21	-0.56	1.16	72	0.9	0.26	0.48	1.15	67.4
ST.PETERSBURG	73	1.1	0.31	-0.51	0.94	73	1.2	0.4	0.4	0.86	59.9
BREMEN	26	1.1	0.61	0.88	0.62	26	1.2	0.63	1.44	0.6	53.1
GARMISCH	17	1.1	0.73	-0.39	0.54	17	1.1	0.76	0.48	0.52	47.5
ZUGSPITZE	33	0.9	0.75	-0.12	0.6	33	0.9	0.74	0.72	0.64	47.4
JUNGFRAUJOCH	16	0.8	0.81	-0.62	0.51	16	0.7	0.79	0	0.56	46.6
ALTZOMONI	41	1	0.32	2.69	0.72	41	0.9	0.53	2.48	0.63	19.1
LAUDER	37	1.3	0.68	0.09	0.66	37	1.2	0.65	0.63	0.69	-45
ARRIVAL.HEIGHTS	9	0.6	0.42	1.57	1.07	9	0.6	0.27	2.42	1.07	-77.8
		1.1	0.55	0.8	**0.84**		1.1	0.58	1.55	**0.83**	

Table 8 – Overview of statistics for the co-located NDACC and S5P time series. Due to the lower accuracy of the NDACC data, only conclusions can be drawn on precision (std on the rel. diff.).

10.3.4   Dispersion

The 1σ spread of the relative difference (between the S5P and the TCCON) around the mean value is below the mission requirements (precision <1%) for both the bias corrected and standard products. The individual values for the different sites are indicated in **Figure 58**.

10.3.5   Dependence on influence quantities

At this stage, the evaluation of potential dependence of the S5P bias and spread on the Solar Zenith Angle (SZA) is hard to evaluate: at Sodankylä, the bias during spring and autumn (both seasons have high SZA) changes sign.

The relative differences shows a dependence on the surface albedo, which is corrected in the bias corrected product. The relative difference of the bias corrected product shows a remaining weak dependence in low albedo case (which corresponds to the shape and 'goodness' of the polynomial fit used to determine the S5P bias correction factor).
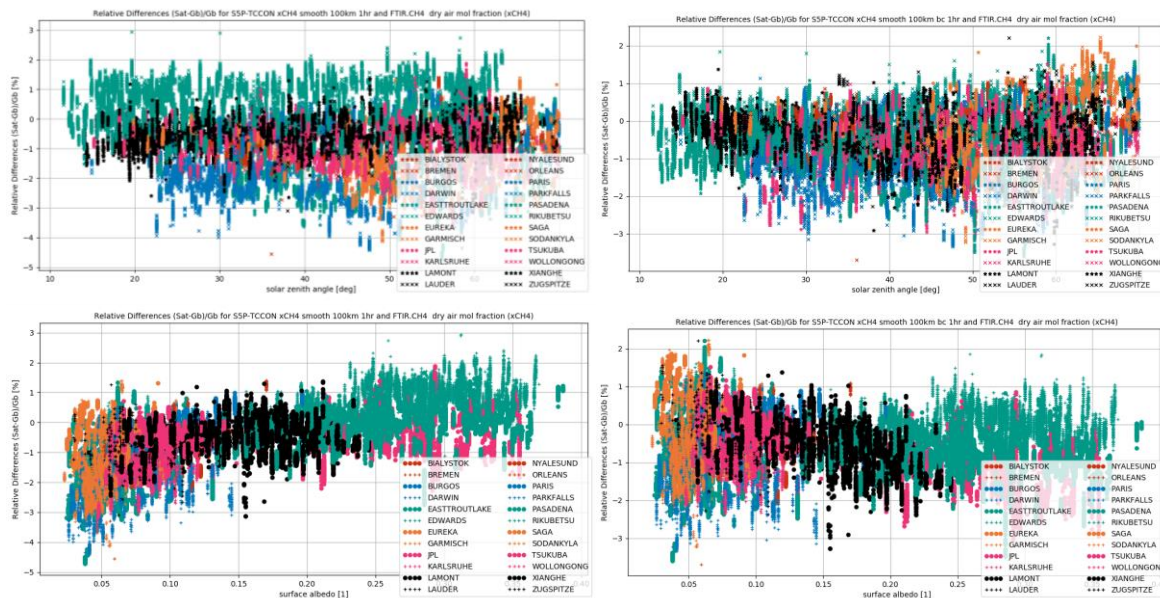
Figure 59: Dependence of the S5P-TCCON relative difference on solar zenith angle (top) and surface albedo (bottom). The left column shows the standard S5P product and the right column the bias corrected S5P product. The bias correction removes the surface albedo dependence of the standard S5P product.

10.3.6 Short term variability

For all the NDACC and TCCON stations, short scale temporal variations in the CH_4 column as captured by ground-based instruments are reproduced very similarly by S5P L2_CH4 OFFL. The individual Pearson correlation coefficients are on average 0.6, see **Figure 60**. At some sites the correlations are very low (e.g. Sodankylä, Burgos, Darwin). This is probably due to the `qa_value` filtering which, at some sites, does not filter all bad pixels, see also Section 10.3.8.
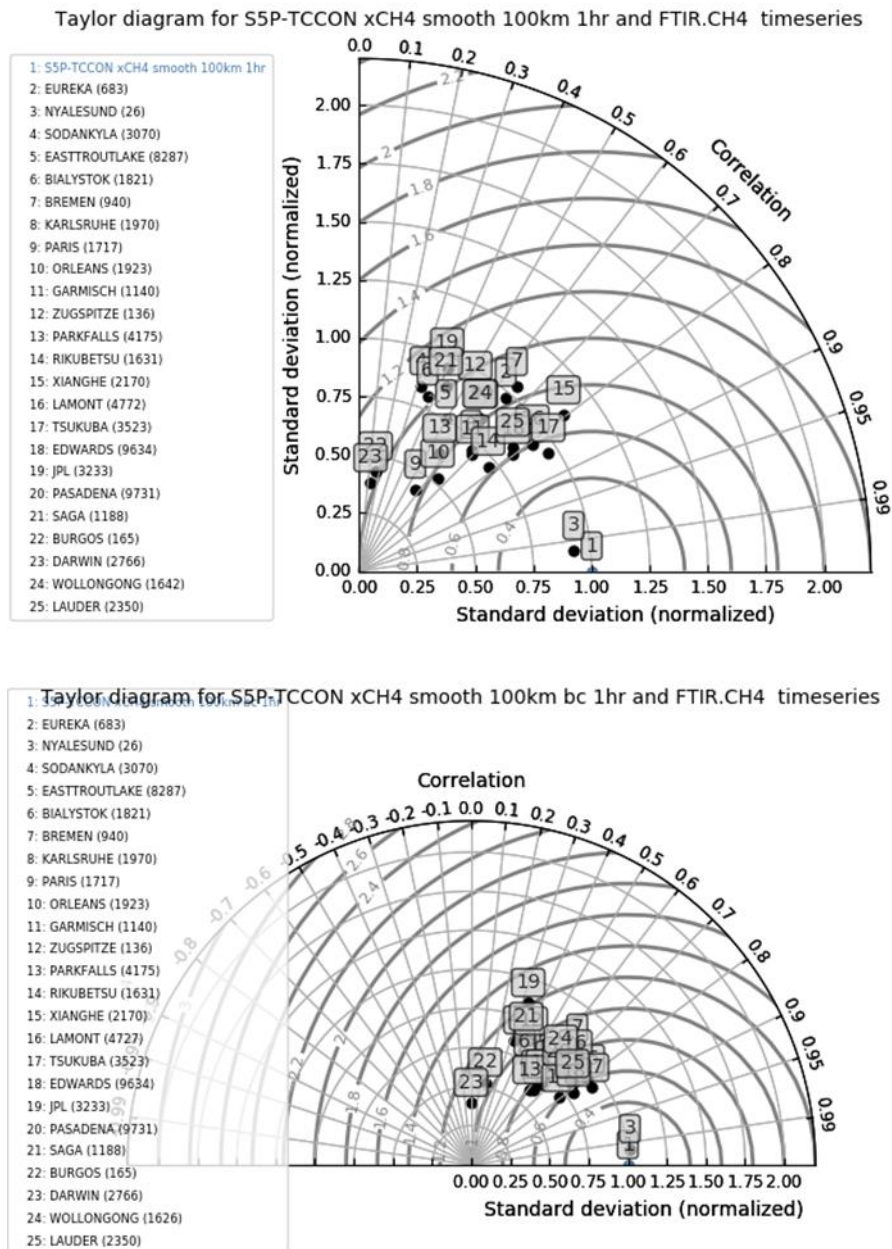
Figure 60: Taylor diagrams for differences between S5P L2_CH4 RPRO/OFFL and TCCON data: standard (top) and bias corrected (bottom) S5P methane columns. At almost all sites the variability of the S5P column data is higher compared to the variability in the TCCON data.

10.3.7   Geographical patterns

Single TROPOMI overpasses show stripes of erroneous CH$_4$ values in the flight direction (see **Figure 61** left). For orbits before orbit 7644 (April 5 2019) not all pixels above inland water are filtered with the `qa_value` flag, see **Figure 61** (right, above Caspian sea).
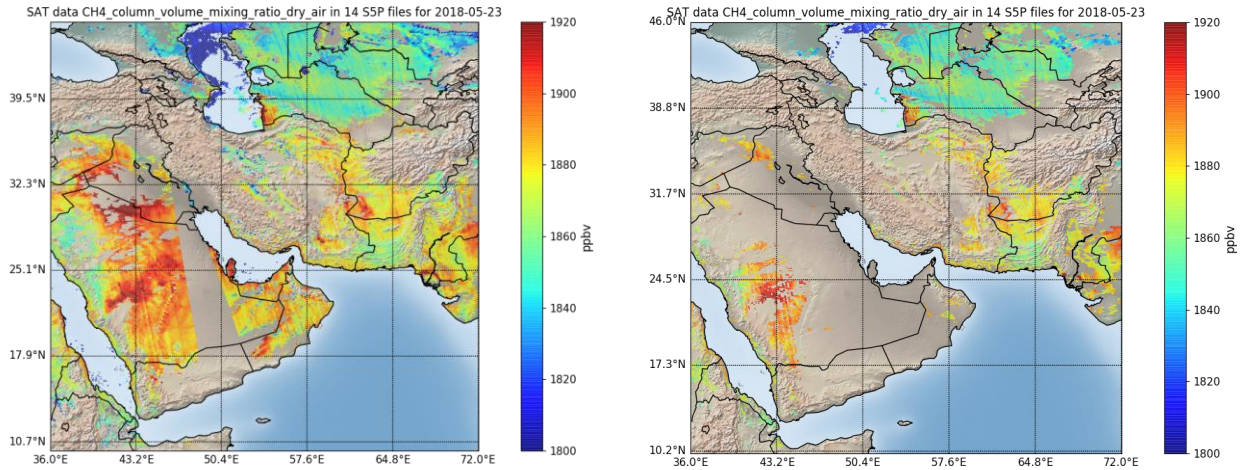
Figure 61: Maps showing XCH$_4$ concentrations above the Middle East measured on May 23 2018. The left panel shows all available pixels, the right panel shows only pixels with qa_value>0.5. The left panel shows the presence of stripes in the flight direction and the right panel shows the presence of filtered pixels above inland water (Caspian Sea).

10.3.8   Other features

Filtering on qa value >0.5 does not remove all pixels considered bad. Some pixels with too low and too high methane concentrations are still present**.**
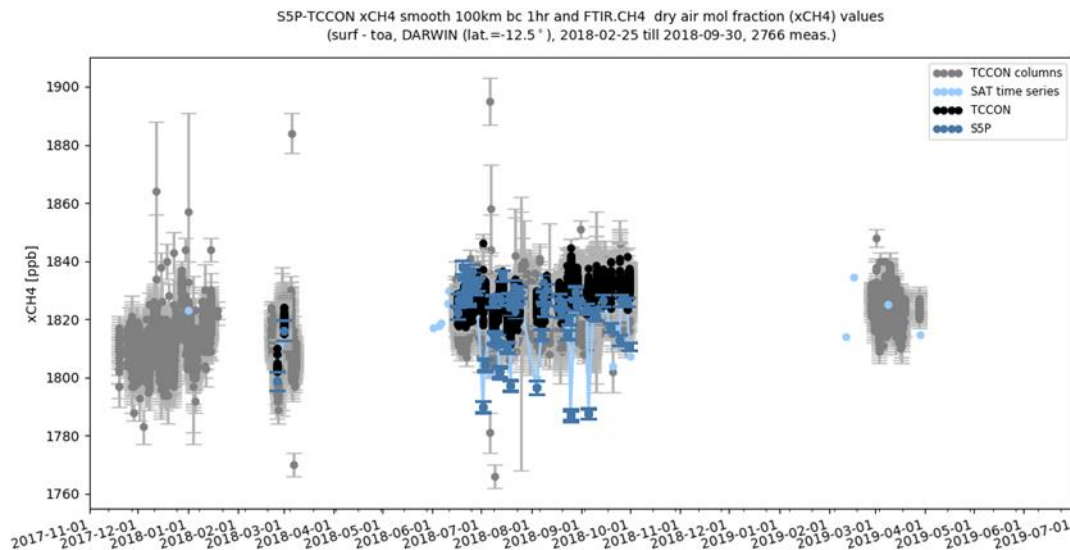
Figure 62: S5P XCH$_4$ time series over Darwin where low values of XCH$_4$ are observed for several days.

11   Validation Results: L2_CLOUD

11.1   L2_CLOUD products and requirements

This section reports on the validation of the following geophysical variables of the S5P TROPOMI L2_CLOUD product identified in **Table 1**: the Cloud Fraction (CF), the Cloud Height (CH), and the Cloud Optical Thickness (COT). Validation results are discussed with respect to the product quality targets outlined in **Table 3**. The NRTI and OFFL processors are currently based on the same algorithm and are producing very similar data products; therefore, only validation of the L2_CLOUD OFFL product is reported hereafter. Subsection 11.4 demonstrates evidence that NRTI and OFFL data do not differ significantly and that their respective validations yield similar conclusions

11.2   Validation approach

11.2.1   Ground-based networks

S5P TROPOMI L2_CLOUD cloud data have been routinely compared at 13 ground-based stations (**Table 9**) to reference lidar/radar data from the cloud target classification product of the CLOUDNET and ARM ground-based networks [ER_Cloudnet]. Cloud base height, cloud top height and a vertical cloud classification profile (resolution <100 m) are provided each 30 s, typically.

Station	Location	Network	Latitude (N)	Longitude (E)
Ny-Ålesund	Svalbard	CLOUDNET	78.932	11.921
Summit	Greenland	CLOUDNET	72.60	-38.42
Mace Head	Ireland	CLOUDNET	53.325	-9.9
Lindenberg	Germany	CLOUDNET	52.211	14.13
Leipzig	Germany	CLOUDNET	51.35	12.43
Chilbolton	United Kingdom	CLOUDNET	51.145	-1.437
Jülich	Germany	CLOUDNET	50.909	6.413
Palaiseau	France	CLOUDNET	48.713	2.208
Munich	Germany	CLOUDNET	48.15	11.57
Schneefernerhaus	Germany	CLOUDNET	47.42	10.98
Potenza	Italy	CLOUDNET	40.6	15.72
Graciosa	Azores	ARM	39.092	-28.026
Iquique	Chile	CLOUDNET	-20.54	-70.18

Table 9 – List of ground-based stations providing the cloud classification data product, and used in this study: 8 CLOUDNET sites and 1 ARM (Atmospheric Radiation Measurement) site. Data is collected from EVDC.

For the comparisons between S5P and CLOUDNET data, two approaches were tested.

First approach: S5P TROPOMI pixels are selected if `qa_value` > 0.5, `cloud_fraction` > 0.5, the pixel encompasses the CLOUDNET site, and the cloud is not multilayered according to the CLOUDNET classification. Per S5P overpass, the closest co-location pair in time (within a time interval of 600 s) only is kept. This approach was routinely used in the previous ROCVR validation reports, but the constraints to high cloud fractions and monolayer cloud limited the scope of the validation.

Second approach: S5P TROPOMI pixels are selected if `qa_value` > 0.5, `cloud_fraction` > 0.1, the pixel encompasses the CLOUDNET site, the site is cloud covered (according to CLOUDNET) at least 50% of the 1200 s temporal interval centered at the TROPOMI overpass time, and the standard deviation of CLOUDNET cloud height is smaller than 0.5 km within this temporal interval. Note that there is no filtering of multilayer clouds. The average cloud height or cloud top height is calculated from CLOUDNET cloud types 1-7. Although with this second approach generally a higher bias is obtained, correlative properties also improve or are comparable. Given the broader scope of this second approach, it is selected here.

11.2.2   Satellites

S5P TROPOMI L2_CLOUD cloud data (internal UPAS product, comparable to the operational OFFL 01.01.05 product) have also been compared to MODIS L3 data (https://ladsweb.modaps.eosdis.nasa.gov/missions-and-measurements/products/MYD08_D3/) and VIIRS NASA non-operational product[1]. The comparison with MODIS allows only for daily means validation whereas the comparison against VIIRS offers a pixel-by-pixel validation of the product.

For the comparisons between S5P L2_CLOUD and VIIRS data, the following exclusion filters were applied: TROPOMI with `qa_value` < 0.5 were rejected; snow/ice scenes as well; VIIRS geometrical cloud fraction < 0.9 (to mitigate regridding artefacts); CTH > 15 km (as the S5P L2_CLOUD algorithm does not retrieve above this value); COT < 1 (as the S5P L2_CLOUD algorithm does not retrieve below this value), and COT > 150 (as this is the maximum VIIRS value after regridding).

11.2.3   Alternative S5p cloud algorithms

The support product S5P TROPOMI FRESCO cloud height is also compared to CLOUDNET observations. This helps to judge if discrepancies between S5P CLOUD CRB and CLOUDNET are specific to the adopted cloud retrieval algorithm or are of more general nature.

11.2.4   Field campaigns and modelling support

None for this report.

---

[1] The VIIRS cloud datasets were obtained from a pre-production code run specifically for limited S5P team analysis. The VIIRS cloud algorithm is based on the MODIS Collection 6 algorithms [https://modis-atmosphere.gsfc.nasa.gov/documentation/collection-6; Platnick et al. (2017). The CLDPROP data have been released in Feb. 2019 and described here: https://modis-atmos.gsfc.nasa.gov/sites/default/files/ModAtmo/EOSSNPPCloudOpticalPropertyContinuityProductUserGuidev1.pdf. Those operational publicly available data might have some differences compared to the limited data provided by the NASA group directly to DLR.

11.3   Validation of L2_CLOUD OFFL

11.3.1   Recommendations for data usage followed

As recommended, only those TROPOMI ground pixels associated with a `qa_value` above 0.5 have been assessed here. The `qa_value` summarizes the quality of the product by taking into consideration several aspects like the spectral channel quality flags from L1B data, geometry limitations (e.g. not reliable retrievals for SZA>75°), inhomogeneous scene warnings, high residual of the fitting process etc.

Some of the known data quality issues are not covered by the quality flags and have been considered when interpreting the validation results reported hereafter (see also the Product Readme File (PRF)). Those issues are:

1. instrumental feature: spatial mis-registration between TROPOMI bands 3-4 (OCRA, UV trace gas fitting window) and band 6 (ROCINN fitting window),
2. insensitivity to very thin clouds,
3. treatment of multi-layer clouds,
4. treatment of ice clouds,
5. snow/ice conditions,
6. unknown straylight impact in the NIR,
7. saturation (note that the L1B flagging works well, only blooming isn't flagged correctly yet),
8. NRTI data gaps northern hemisphere,
9. some ground pixels contain cloud-height values close to the a-priori. This behavior is related to the current setting of the inversion algorithm. This bug is resolved from version 01.01.06 onwards.
10. Version 01.01.06 had an inconsistency in cloud parameters; for pixels with a priori cloud fraction below 0.05, the cloud height and other properties were set to fill values which caused data gaps in the ozone product. This problem is corrected in 01.01.07 by setting cloud fractions below 0.05 to 0.0 in the retrieval. The original a priori cloud fraction is maintained in the variable `cloud_fraction_apriori`.

For further details, data users are encouraged to read the Product Readme File (PRF), Product User Manual (PUM) and Algorithm Theoretical Basis Document (ATBD) associated with this data product, all available on https://sentinels.copernicus.eu/web/sentinel/technical-guides/sentinel-5p/products-algorithms.

11.3.2   Status of validation

This section presents a summary of the key validation results obtained by the MPC VDAF and by S5PVT AO projects. It is based on several updates of the results reported at the S5P First Public Release Validation Workshop (ESA/ESRIN, June 25-26, 2018). Individual contributions to the workshop are archived in https://nikal.eventsair.com/QuickEventWebsitePortal/sentinel-5p-first-product-release-workshop/sentinel-5p, while up-to-date validation results and consolidated validation reports are available through the MPC VDAF Portal at http://mpc-vdaf.tropomi.eu.

Current conclusions are based on the limited amount of reference measurements available at the time of this analysis, resulting in a limited amount of comparison pairs. The validation vs. CLOUDNET

ground-based data uses S5P L2_CLOUD RPRO+OFFL 01.01.07 data. This covers the time period from 2018-04-30 till 2019-08-06. CLOUDNET data from 13 sites were considered in this analysis.

11.3.3   Bias

Comparison vs. CLOUDNET

L2_CLOUD CAL cloud top height is generally below the CLOUDNET cloud top height. A typical case is provided for the CLOUDNET site at Jülich (Figure 63, Figure 64). The monthly mean S5P CAL CTH generally follows the trend of the CLOUDNET cloud top height (Figure 63). This is corroborated by the high Pearson correlation coefficient of 0.8 (Figure 64). In absolute scale terms, the overestimation is higher for high clouds (Figure 64). On the other hand, Figure 64 makes clear that the 20% upper limit requirement on the bias becomes very strict for low clouds. Note that with the second validation approach, there are more near-surface CLOUD CAL CTH values.
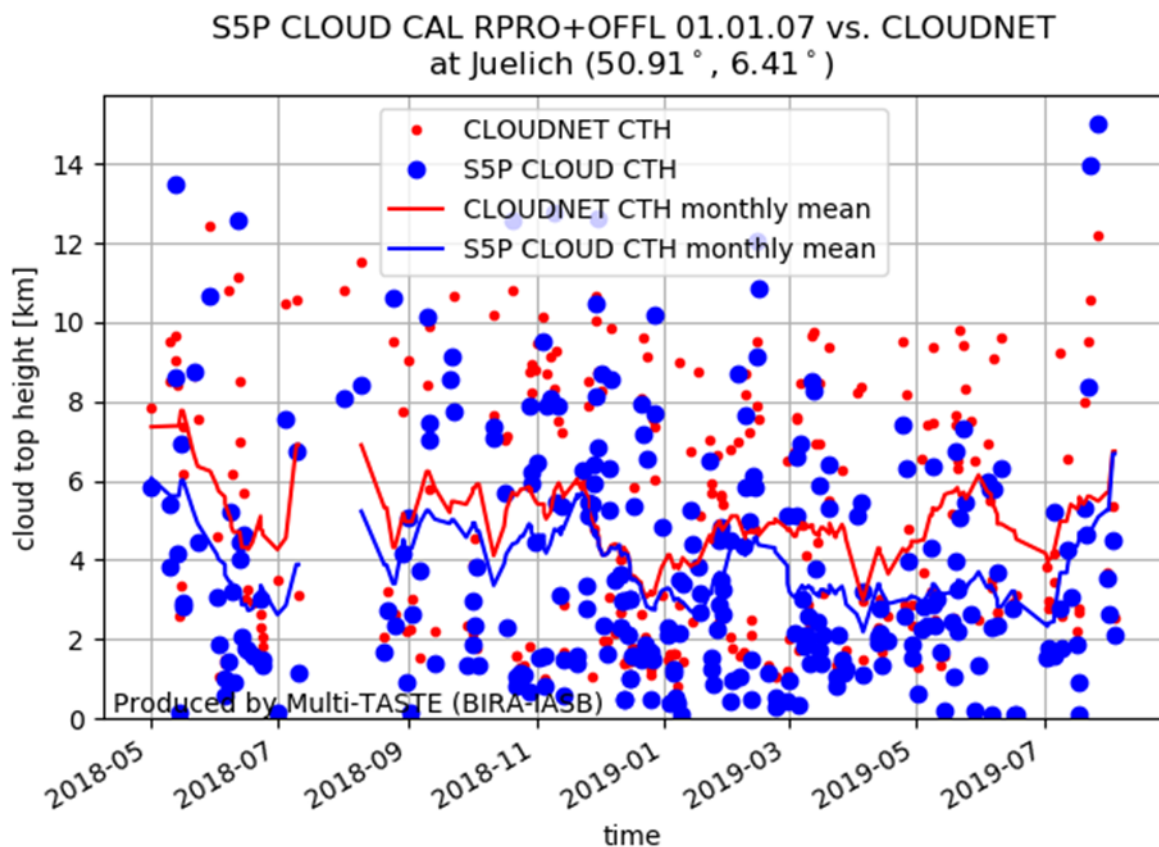

Figure 63: Time series of S5P CLOUD CAL (RPRO and OFFL, processor version 01.01.07) CTH vs. CLOUDNET CTH at Jülich. The monthly mean of both is also provided. Sensing times considered between 2018-04-30 (start RPRO 01.01.07) and 2019-08-06.
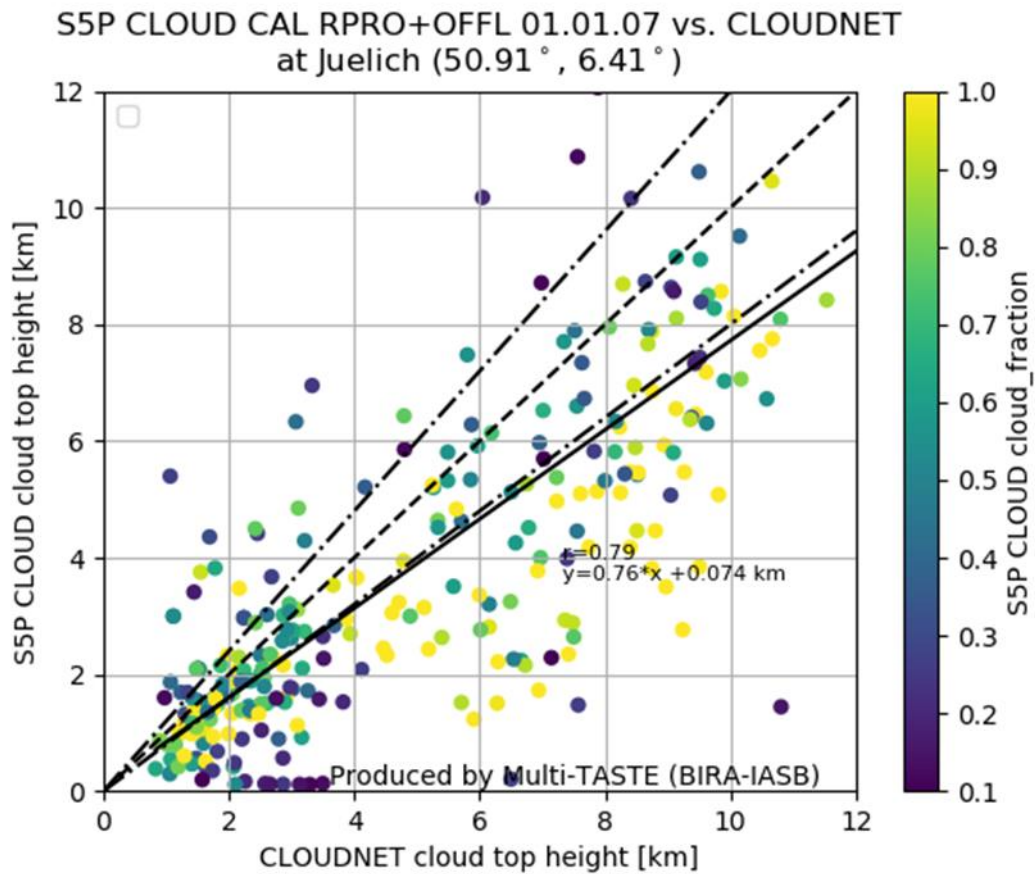
Figure 64: Correlation plot of S5P L2_CLOUD CAL (RPRO+OFFL, processor version 01.01.07) CTH vs. CLOUDNET CTH at Jülich. The colour indicates the S5P L2_CLOUD cloud fraction. Dashed line is the 1:1 line and dash-dotted line the 20% bias requirement. See note about data versions and sensing times in the caption of Figure 63.

At most of the sites, the S5P L2_CLOUD CAL top height is lower than the CLOUDNET top height, as depicted in **Figure 65**.
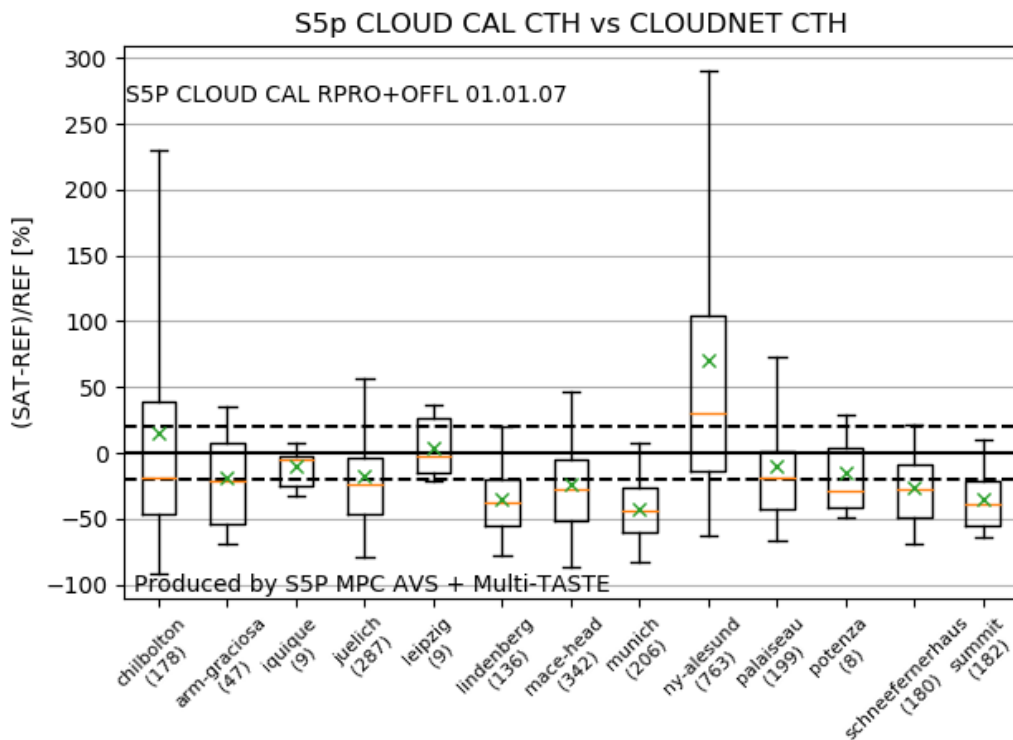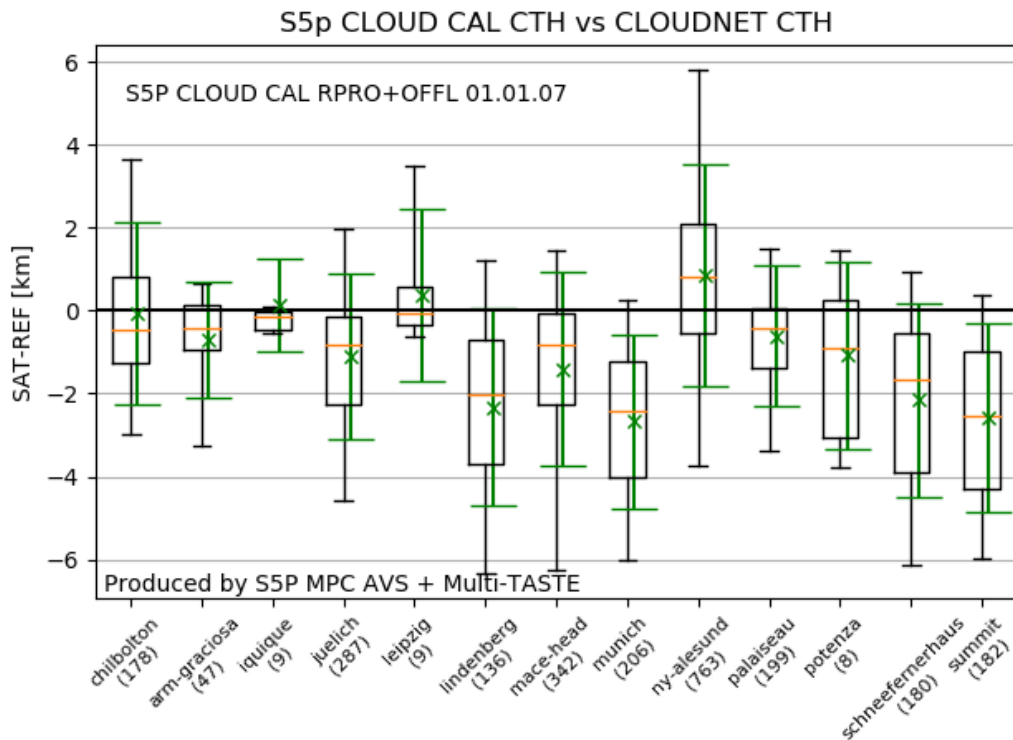
Figure 65: Upper panel: Boxplots of S5P L2_CLOUD CAL CTH minus CLOUDNET CTH, per site. Boxplot conventions: box bounds are at first and third quartile. Orange line is median. Whiskers are at 5 and 95 percentiles. Slightly offset green cross is mean, with error bar ±the standard deviation. Lower panel: Similar as upper panel but now for the relative difference, and without indication of the standard deviation. See also note about data versions and sensing times in the caption of Figure 63.

The mean relative difference is in about half of the cases lower than the bias upper limit requirement of 20%. Inspection of the individual cases (not shown here) lead to the following conclusions:

- The bad agreement at Summit can be ascribed to the occurrence of snow and ice cover (a known problem for satellite retrieval), resulting in retrieving the surface height as the cloud top height.
- The bad agreement at Schneefernerhaus is due to the specific orography; the CLOUDNET station is at a mountain, and the S5P surface altitude for co-located pixels is approximately 1 km below the CLOUDNET station. S5P CLOUD (as well as the other UPAS and also the KNMI products) takes its surface altitude from the DEM GMTED2010, but averaged within a radius of 5 km.
- The large positive bias at Ny-Ålesund is caused mainly by a cluster of low CLOUDNET CTH values, with a high retrieved CLOUD CTH and a low retrieved CLOUD CF. Possibly snow/ice cover also plays a role here. This should be further investigated.
- Regarding Chilbolton, there is a large discrepancy between the mean relative difference (+15%) and the median relative difference (-20%). The large mean relative difference is caused by the presence of a limited amount of comparison pairs where CLOUDNET reports a low cloud top height (< 1 km) while S5P L2_CLOUD CAL reports a much higher cloud top height (several km). Differently from the Ny-Ålesund case, there is no clear link with retrieved CLOUD CF. This should be further investigated.
- The cause of the exceptional large deviations for Munich and Lindenberg has to be further investigated (e.g., role of orography, cloud type, land cover…).

CLOUD CRB cloud height is generally below the CLOUDNET cloud height. A typical case is provided for the CLOUDNET site at Jülich (Figure 66, Figure 67). The monthly mean S5P CRB CH generally follows the trend of the CLOUDNET cloud mean height (Figure 66). This is corroborated by the high Pearson correlation coefficient of 0.77 (Figure 67). Figure 67 indicates that the 20% upper limit requirement on the bias is more easily met for high-lying clouds.
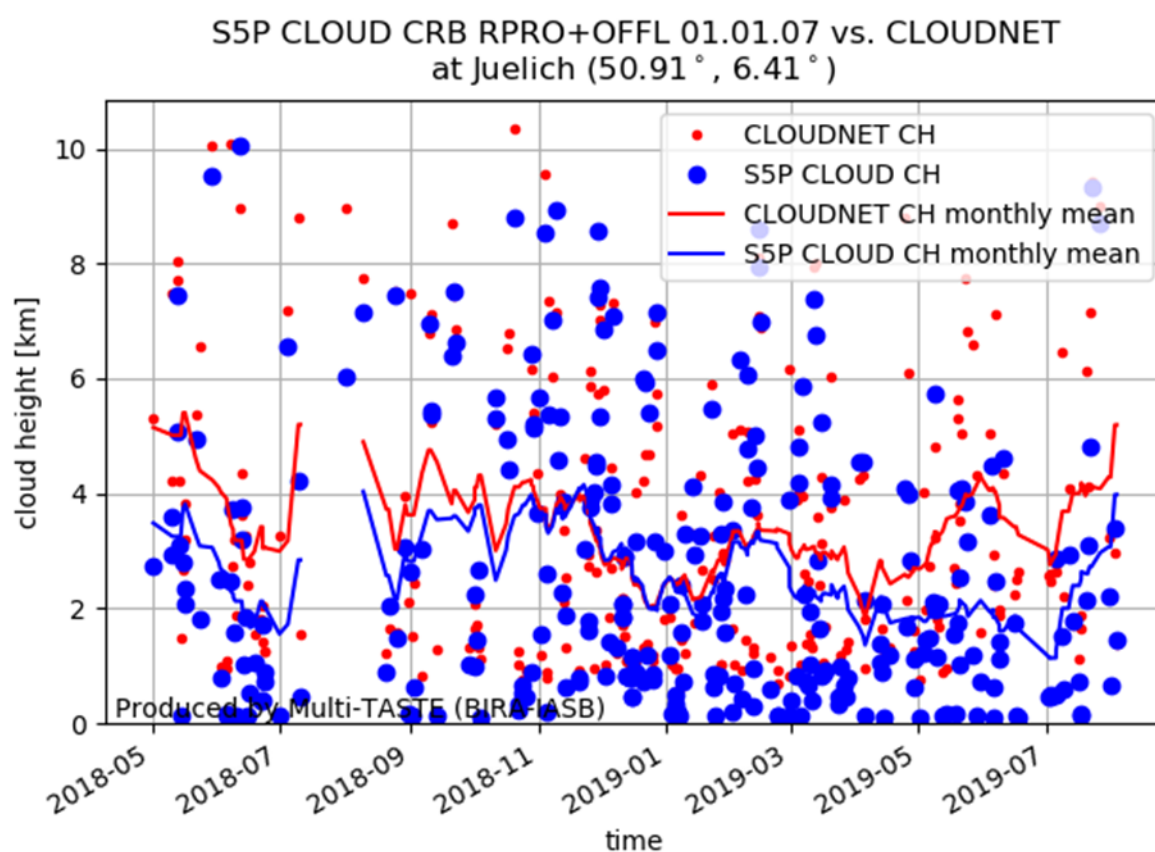
Figure 66: Time series of S5P L2_CLOUD CRB (RPRO and OFFL, processor version 01.01.07) CH vs. CLOUDNET CH at Jülich. The monthly mean of both is also provided. See note about data versions and sensing times in the caption of Figure 63.
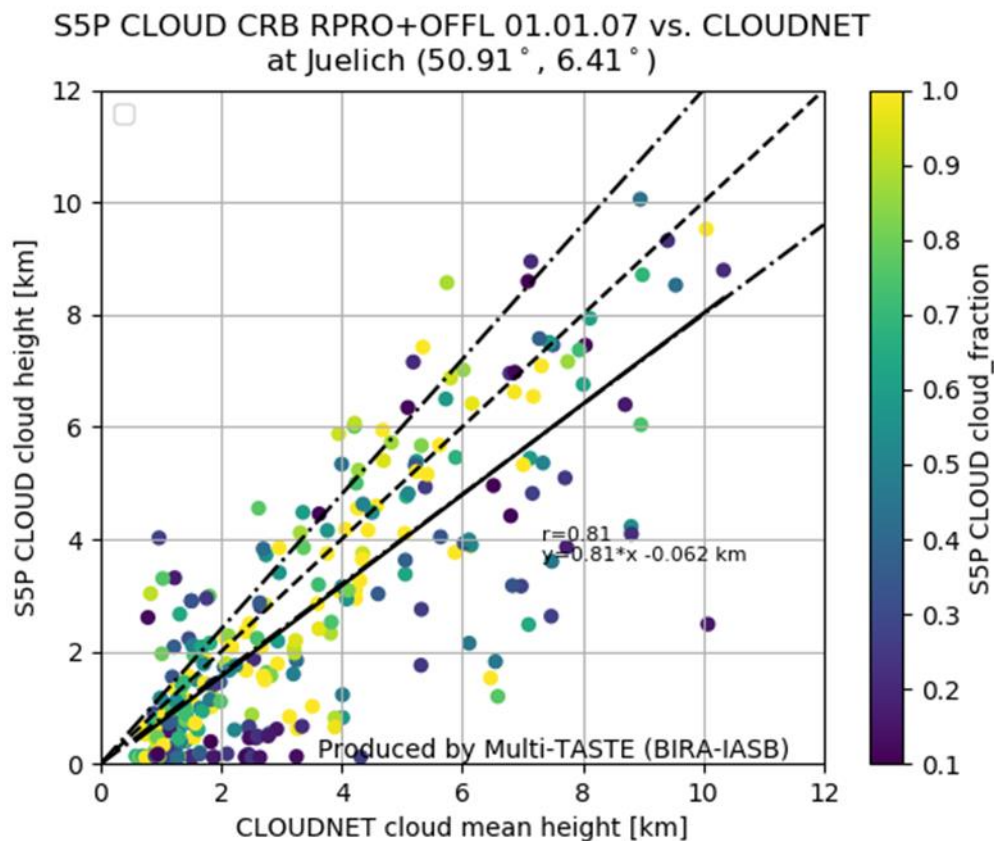
Figure 67: Correlation plot of S5P L2_CLOUD CRB (RPRO and OFFL, processor version 01.01.07) CH vs. CLOUDNET cloud mean height at Jülich. The colour indicates the S5P CLOUD cloud fraction. Dashed line is the 1:1 line and dash-dotted line the 20% bias requirement. See note about data versions and sensing times in the caption of Figure 63.

At most of the sites the S5P L2_CLOUD CRB CH is lower than the CLOUDNET mean height. At most sites the bias is below 750 m. The 20% limit is exceeded in almost all cases. The outliers at Schneefernerhaus and Summit are due to orography and snow/ice cover (see the discussion for CAL CTH bias). Other exceptions (e.g., Munich, Lindenberg) deserve further investigation. Roughly similar biases are seen for the S5P support product FRESCO vs. CLOUDNET, indicating that the discrepancies are not specific to a particular cloud retrieval algorithm.
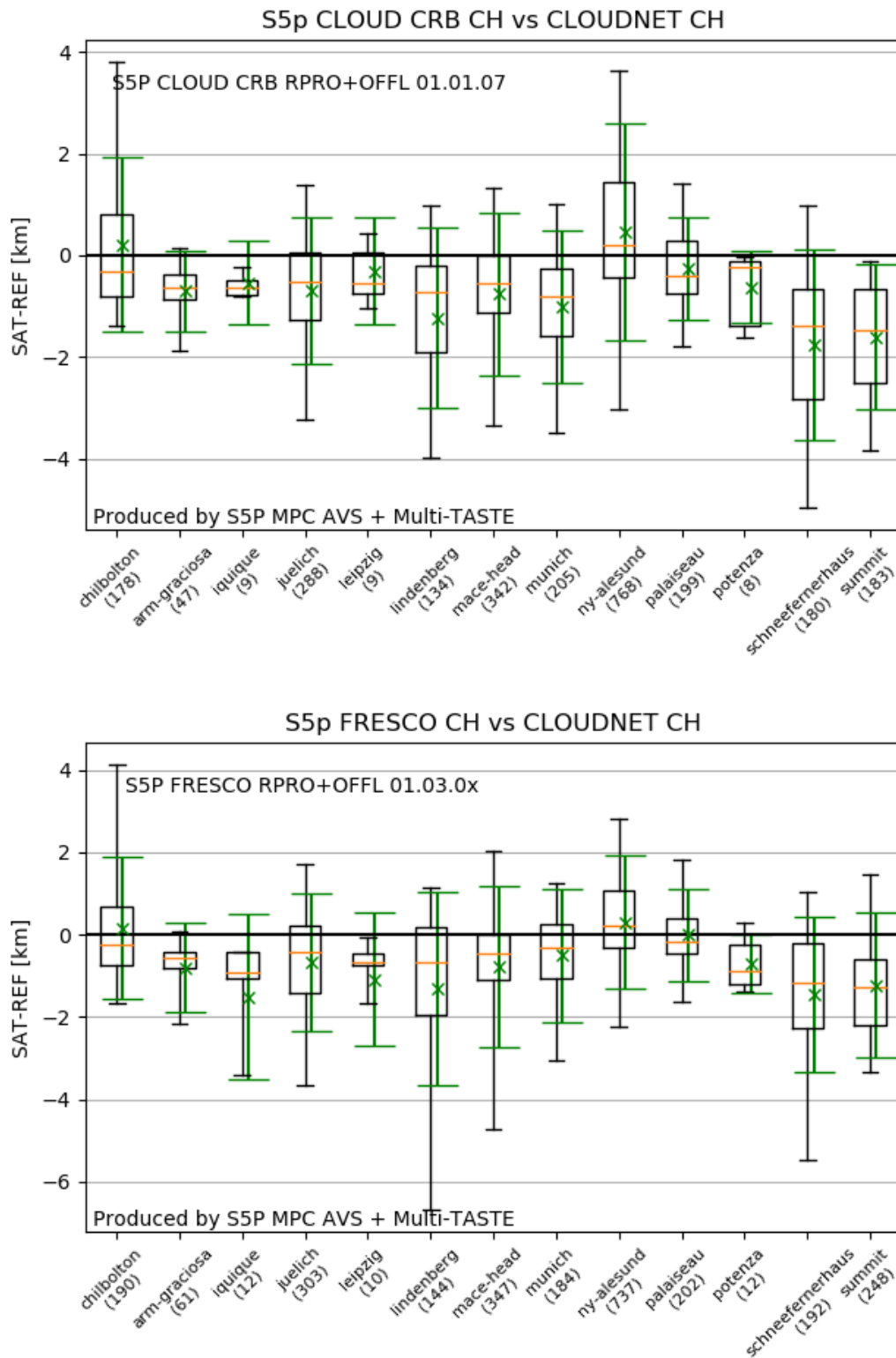
Figure 68: Upper panel: Boxplots of S5P L2_CLOUD CRB CH minus CLOUDNET CH, per site. Lower panel: The same but now for the S5P Support product FRESCO RPRO 01.03.02 + OFFL 01.03.00-02. The same conventions as for **Figure 65** apply. See note about data versions and sensing times in the caption of **Figure 63**.
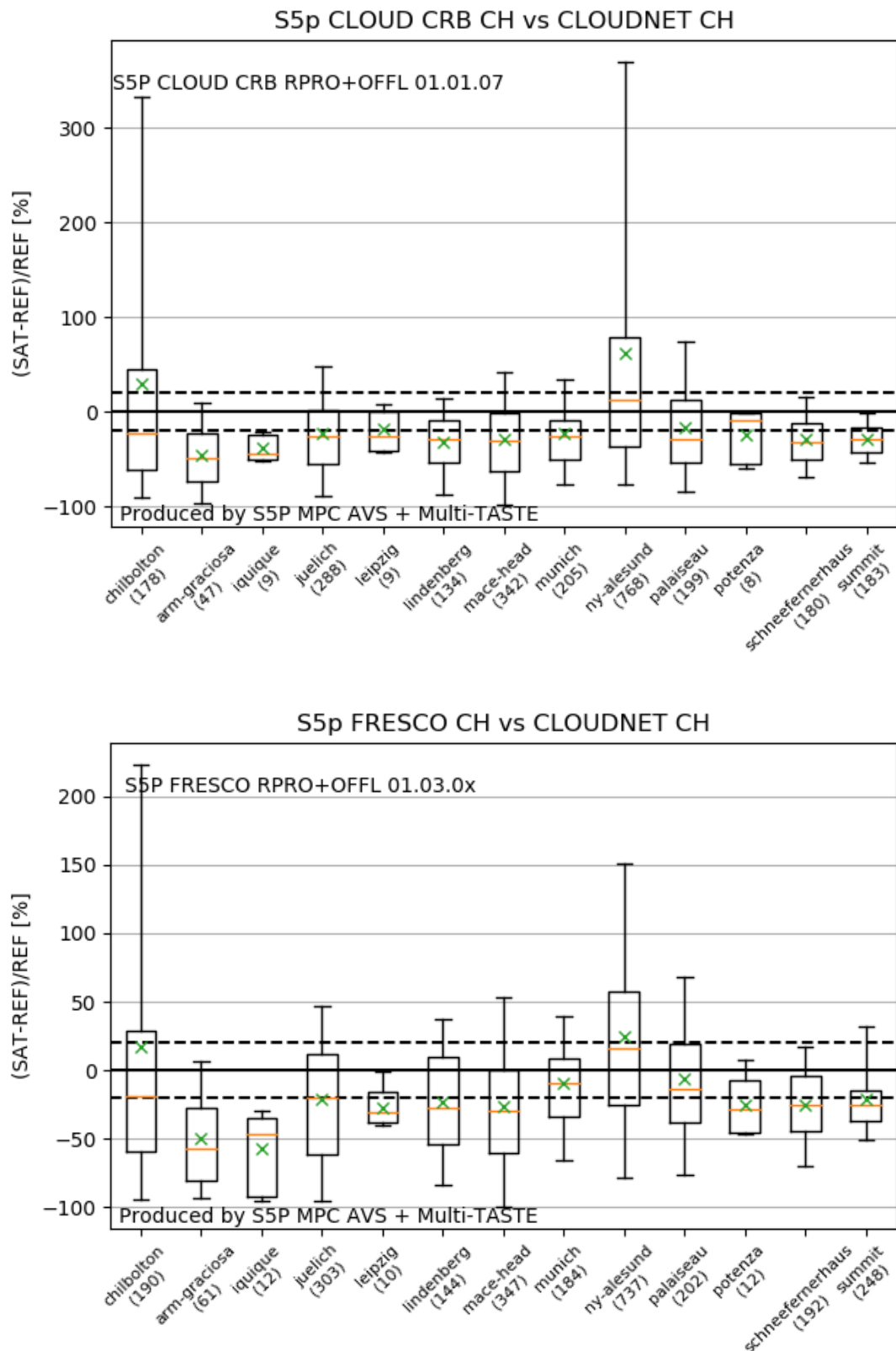
Figure 69: Upper panel: Boxplots of the relative difference of S5P L2_CLOUD CRB CH vs CLOUDNET CH, per site. Lower panel: The same but now for the S5P Support product FRESCO RPRO 01.03.02 + OFFL 01.03.00-02 vs CLOUDNET. The same conventions as for **Figure 65** apply. See note about data versions and sensing times in the caption of **Figure 63**.

Comparison vs. satellites

A negative bias (mean difference) in the cloud top height (CTH) (-1.6 km) and a positive bias (+7.9) in the cloud optical thickness (COT) with respect to VIIRS has been found. Note however that S5P L2_CLOUD and VIIRS capture the same CTH mode at 1.8 km (**Figure 70**).

A comparison of S5P L2_CLOUD with MODIS using commissioning phase data also showed a negative CTH bias (-1 km between -60ºS and +60ºS) and a positive COT bias at tropical and middle latitudes (+3.8 between -60ºS and +60ºS).

Possible bias in the cloud fraction is difficult to be identified because of the comparison of radiometric cloud fraction from TROPOMI against geometrical cloud fraction from MODIS/VIIRS.
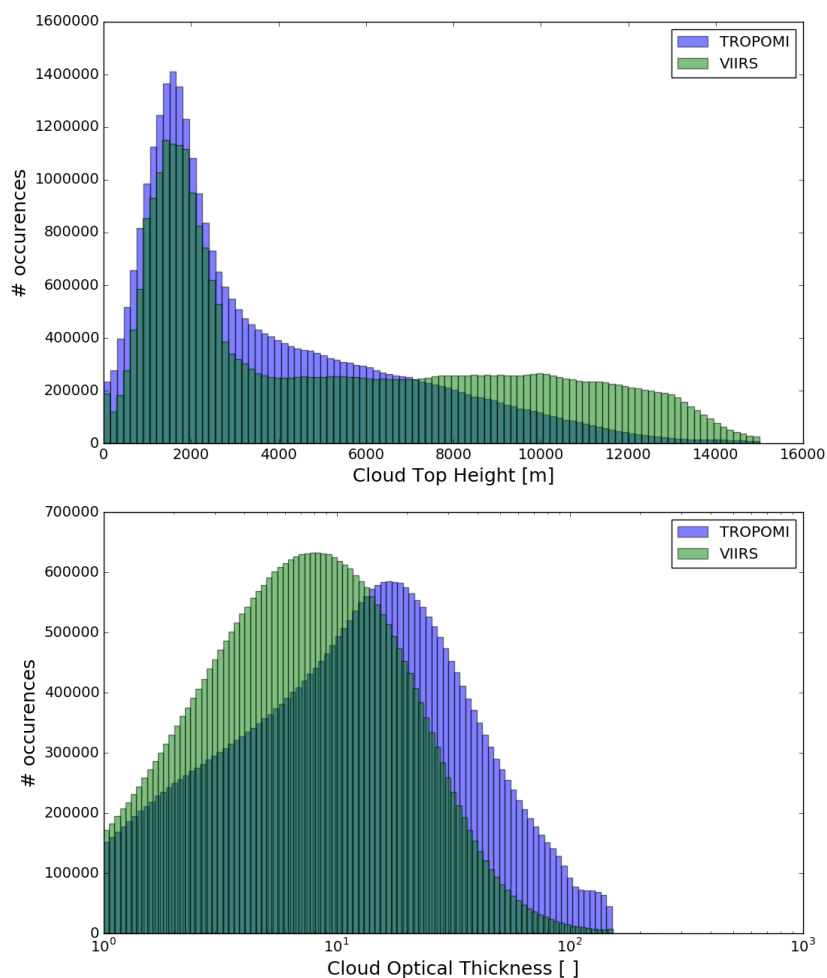
Figure 70: Upper panel: Histograms of cloud top height of S5P L2_CLOUD (internal prototype comparable to operational processing version 01.01.05) cloud top height and VIIRS cloud top height. Lower panel: Similar to upper panel but for cloud optical thickness.

11.3.4   Dispersion

Comparison vs. CLOUDNET

From **Figure 65** it can be inferred that the comparison spread (expressed as standard deviation) of S5P CLOUD CAL CTH vs. CLOUDNET CTH, exceeds the upper limit for random error dispersion (500 m). However, also CLOUDNET CTH random error, and comparison error, contribute to the comparison spread, and these contributions have not been quantified yet. The same holds for S5P CLOUD CRB CH vs. CLOUDNET CH (**Figure 68**). Roughly similar dispersions are seen for the S5P support product FRESCO vs. CLOUDNET, indicating that the discrepancies are not specific to a particular cloud retrieval algorithm.

Comparison vs. satellites

S5P L2_CLOUD CTH shows good correlation with VIIRS CTH: Pearson coefficient R = 0.74 for continental clouds and 0.86 for marine clouds. For COT, a weaker correlation is seen: Pearson R = 0.48 for continental clouds and 0.66 for marine clouds.
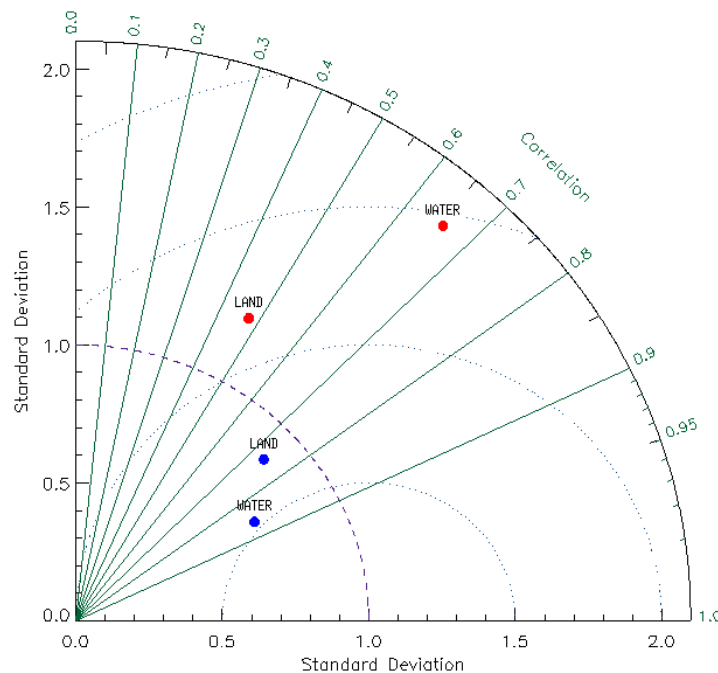
Figure 71: Taylor diagram between CTH (blue) and COT (red) of S5p CLOUD and those of VIIRS.

11.3.5   Dependence on influence quantities

The S5P L2_CLOUD cloud fraction gets unphysically high values at very large SZAs (above 85 degrees) due to very weak illumination. The other cloud parameters might also be affected for high SZAs due to limitation in the RTM treatment of spherical atmosphere.

The high surface albedo above snow and/or ice covered surfaces is a challenge for cloud retrievals. Note that a very large SZA implies a measurement above the polar region, and therefore snow-ice covered surfaces are likely.

11.3.6   Short term variability

Nothing to report.

11.3.7   Geographical patterns

The geographical patterns are closely linked to the effects of the solar zenith angle and surface albedo mentioned above.

11.3.8   Other feature: a priori bug and its fix

Prior to version 01.01.06, a bug, causing cloud (top) height values being close to its a priori value of 3.8 km for a number of pixels (see Figure 72), impacted the CLOUD product quality. In processor version 01.01.06, this bug was corrected.
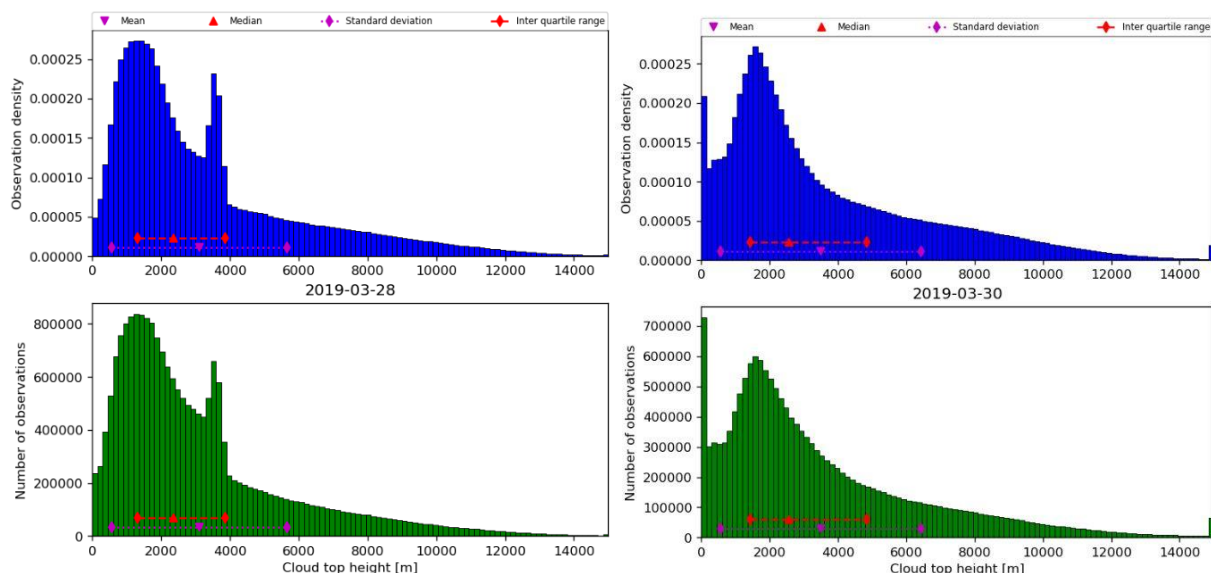
Figure 72: Histograms of cloud top height of S5P CLOUD. Left. Version 01.01.05, on the day before the version switch to 01.01.06. An artificial peak at 3.8 km, the a priori value, is visible. Right. Version 01.01.06. The peak at 3.8 km has disappeared.

11.3.9   Other feature: Switch to smaller ground pixel size

The effect of the switch to a smaller ground pixel size on 6 August 2019 on the retrieved L2_CLOUD cloud parameters was investigated by comparing histograms (**Figure 73**) and global maps (**Figure 74**) on 5 and 6 August. No obvious effect on the retrieved values is noticed. Note that, as expected, the count of the histograms has increased.

Comparisons with CLOUDNET at Jülich depicted in **Figure 75** are not noticeably affected, but it has to be noted that the temporal range after the pixel size switch is still very short.
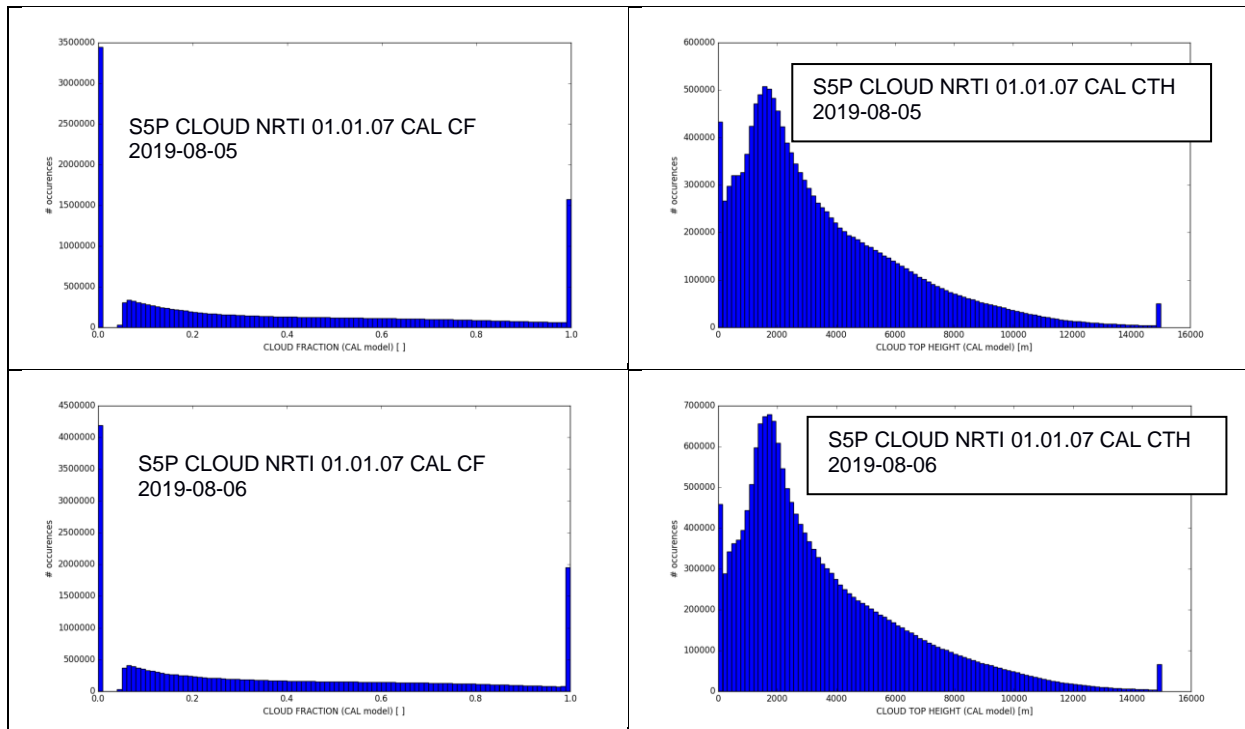
Figure 73: Histograms of S5P CLOUD NRTI 01.01.07 CAL cloud fraction (left) and CAL cloud top height (right), at 2019-08-05, before the pixel size switch (top) and at 2019-08-06, after the pixel size switch (bottom). The histograms shapes are very similar, but note that the count has increased. The same conclusion can be reached for the other CLOUD retrieved parameters.
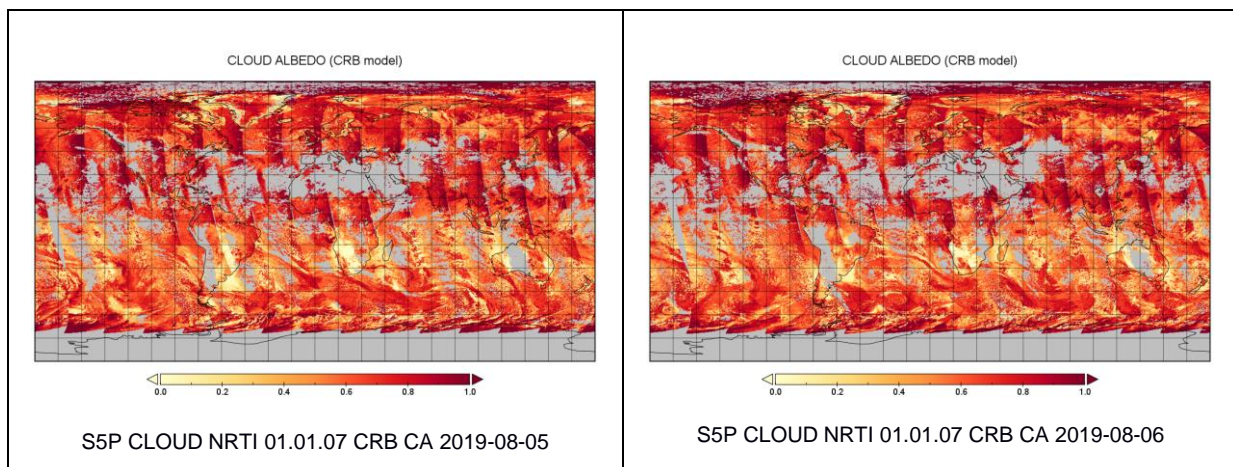
Figure 74: Global map of CLOUD NRTI 01.01.07 CRB cloud albedo at 2019-08-05 (before the pixel size switch) and at 2019-08-06 (after the switch).
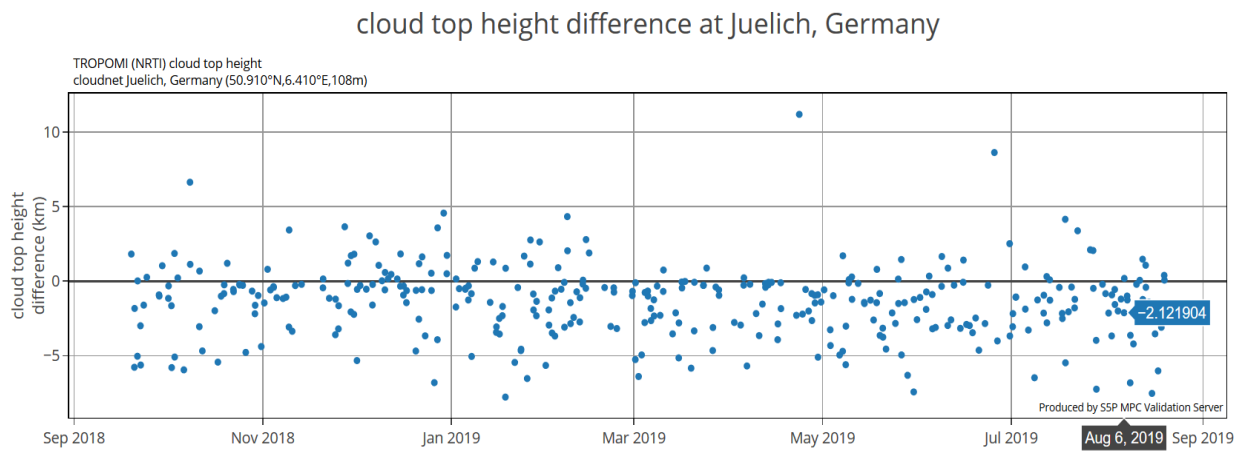
Figure 75: S5P NRTI CLOUD 01.01.01-01.01.07 CAL CTH vs CLOUDNET CTH at Jülich, as taken from the validation server at 2019-08-28. The last co-located point is on 2019-08-19.

11.4   Equivalence of L2_CLOUD NRTI and OFFL products

This section shows evidence that the L2_CLOUD NRTI and OFFL products do not differ significantly and that their respective validations yield similar conclusions.

CLOUD NRTI and OFFL use currently the same algorithm and therefore their difference is expected to be negligible. **Figure 76** shows illustrative demonstration for cloud top height, but similar conclusions apply to cloud fraction and cloud optical thickness. The difference is close to zero for the vast majority of the pixels and the mean difference over the whole granule is very small (e.g., 0.001 for cloud fraction or -19m for cloud top height).

Note that beginning with version 02.00.00, S5P L2_CLOUD OFFL and NRTI will be different because the OFFL will also incorporate VIIRS cloud mask information.

cloud_top_height
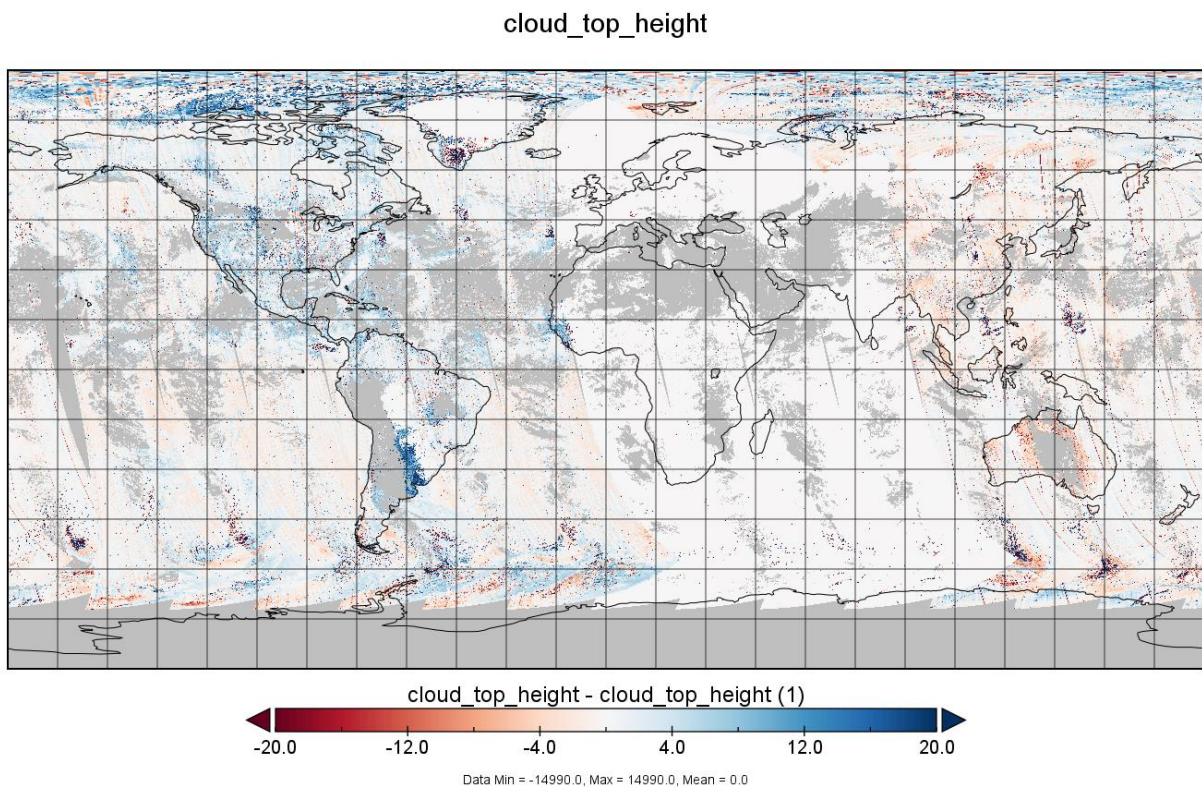
Figure 76: S5P CLOUD CAL 01.01.07 CTH NRTI-OFFL differences on 2019-08-06. CTH expressed in meter.

12 Validation Results: L2_AER_AI

12.1 L2_AER_AI products and requirements

This section reports on the validation of the following geophysical variables of the S5P TROPOMI L2_AER_AI UV aerosol absorbing index products identified in **Table 1**. Validation results are discussed with respect to the product quality targets outlined in **Table 3**. The NRTI and OFFL processors producing very similar data products, only validation of the L2_AER_AI NRTI product is reported hereafter. Subsection 0 demonstrates evidence that NRTI and OFFL data do not differ significantly and that their respective validations yield similar conclusions.

12.2 Validation approach

The UV aerosol index (UVAI) is not a geophysical quantity that can be directly compared to independent measurements from ground or to model results. The way to validate this index is to compare it to coincident satellite measurements from different sensors. For the validation of S5P TROPOMI UVAI, measurements from EOS-Aura OMI and Suomi-NPP OMPS are well suited for that purpose.

In addition to the validation using satellite observations, the S5P TROPOMI UVAI data products can also be checked for internal consistency. For example, the following tests can be performed:

a) the dependence of the UVAI on the observation geometry (in particular on the SZA and the VZA of the measurement) can be investigated;
b) the UVAI values for clear sky and low aerosol amount should be close to zero;
c) the geographical patterns of the UVAI can be compared to those of other measurements, e.g., trace gas distributions of large biomass burning plumes or volcanic plumes.

It should be noted that for S5P TROPOMI the UVAI is calculated for two wavelength pairs, 388 / 354 nm and 380 / 340 nm, the first one allowing a direct comparison to the UVAI from OMI (which is also calculated for 388 / 354 nm).

12.2.1 Ground-based networks

As stated above, satellite UVAI data cannot be directly compared to ground-based measurements.

12.2.2 Satellites

S5P TROPOMI UV aerosol index data are compared to the aerosol indices obtained from EOS-Aura OMI and Suomi-NPP OMPS. Both OMI and OMPS have similar afternoon overpass times as compared to TROPOMI. With OMI the same wavelength pair (388 / 354 nm) can be compared.

12.2.3 Field campaigns and modelling support

As stated above, no direct comparison of the UVAI to non-satellite measurements is possible.

12.3   Validation of L2_AER_AI NRTI

12.3.1   Recommendations for data usage followed

In order to avoid misinterpretation of the data quality and to avoid the effects of sun glint, it is recommended to only use those TROPOMI pixels associated with a `qa_value` above 0.8. The variables `aerosol_index_340_380_precision` and `aerosol_index_354_388_precision` can also be used to diagnose the quality of the UVAI. These are new data product fields and are under evaluation.

For further details, data users are encouraged to read the Product Readme File (PRF), Product User Manual (PUM) and Algorithm Theoretical Basis Document (ATBD) associated with this data product, all available on https://sentinels.copernicus.eu/web/sentinel/technical-guides/sentinel-5p/products-algorithms [ER_CoperATBD].

12.3.2   Status of validation

This section presents updated validation results obtained as a part of the S5P Mission Performance Centre (MPC) and by S5P Validation Team (S5PVT) AO projects. It is based on several updates of preliminary results reported at the S5P First Public Release Validation Workshop (ESA/ESRIN, June 25-26, 2018) and extends now until August 2019. Individual contributions to the workshop are archived in https://nikal.eventsair.com/QuickEventWebsitePortal/sentinel-5p-first-product-release-workshop/sentinel-5p .

The validation of S5P TROPOMI L2_AER_AI data presented here is based on comparisons with similar aerosol indices from the EOS-Aura OMI and Suomi-NPP OMPS satellite missions. Both OMI and OMPS have similar afternoon overpass times as compared to TROPOMI and with OMI the same wavelength pair (354/388 nm) can be compared. Focus is placed on several case studies for different known aerosol sources using reprocessed data from the period covered during the E1 Commissioning Phase (November 2017 to April 2018). The typical case studies identified in **Table 10** were selected to cover different types of aerosol plumes expected to be detected by TROPOMI: biomass burning smoke, desert dust, and volcanic aerosol sources. One example for desert dust is shown in **Figure 77**. The conclusions summarized hereafter need to be confirmed by a larger amount of test cases and co-locations, and extended over a full year of data, hence, a full cycle of key influence quantities, in order to enable detection and quantification of potential patterns, dependences, seasonal cycles and longer term features.

Table 10 – Case studies for different aerosol types.

| Date	Type of case	TROPOMI orbit	OMI orbit	OMPS orbit
2017-11-10	Desert dust and small Sub-Saharan fire plumes	00398	70864	31285
2017-11-27	Volcanic eruption, Bali	00636	71108	31523
2017-12-13	Large biomass burning fires, California	00858	71350	31745
2018-03-31	Long-range transport of large desert dust plumes	2397, 2398	72916, 72917	33284, 33285
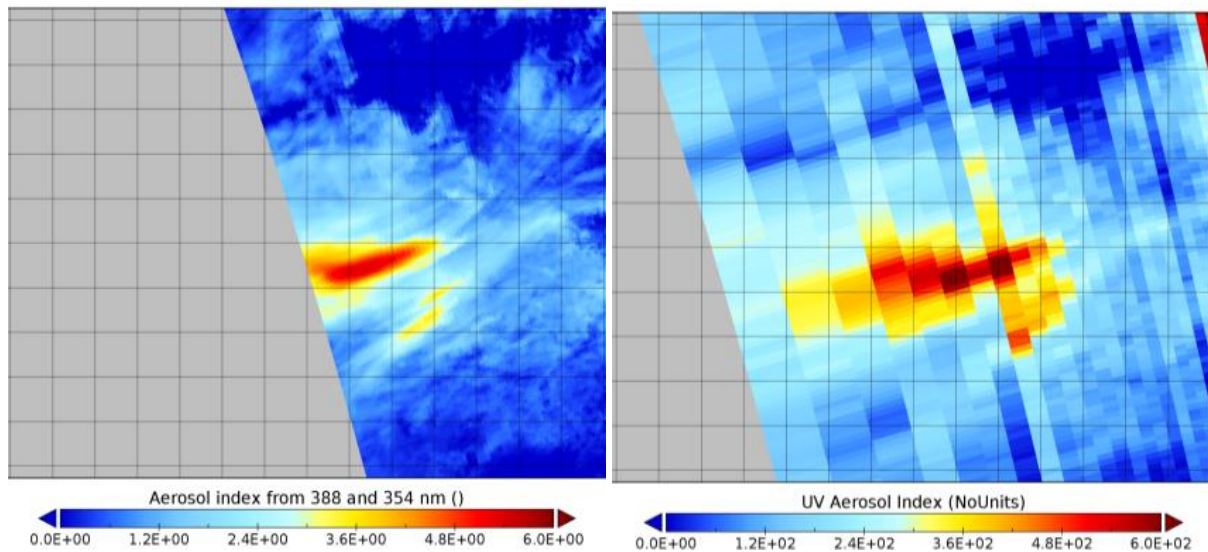
Figure 77: Comparison of S5P TROPOMI UVAI (orbit 00398, left) and OMI OMAERO UV Aerosol Index (orbit 70864, right) for Saharan dust on 10 November 2017. In general very good agreement is found (the stripes in north-south direction in the OMI data are caused by the OMI row anomaly and should be ignored).

For the selected case studies, in general very good agreement of the patterns of enhanced UVAI was found. Comparison results between S5P TROPOMI and OMPS UVAI are shown in **Figure 78** and **Figure 79** below (courtesy of Omar Torres and Changwoo Ahn, NASA-GSFC). At the beginning of TROPOMI measurements (Nov. and Dec. 2017, **Figure 78**), the patterns of enhanced UVAI agree very well. But the S5P TROPOMI UVAI is mostly negative and is systematically smaller than the OMPS results. The negative bias of the S5P TROPOMI UVAI is steadily increasing so that is now outside the requirements (bias < 1 UVAI unit). The spread of the S5P TROPOMI values is similar as the OMPS values (assuming LER clouds). From this finding it is concluded that the S5P TROPOMI UVAI is also within the requirement for random errors of 0.1 UVAI units. It should be noted that the standard deviation of the OMPS Mie product is systematically smaller due to the more realistic assumptions about clouds and surface reflectance. A second comparison is performed for measurements in August 2018 (**Figure 79**). Here again, the spatial patterns agree very well. However, the S5P TROPOMI observations now show systematically decreased UVAI values, which are mostly outside the requirements (bias < 1 UVAI unit). This may in part be related to a wavelength dependent degradation in the irradiance measurements where, shorter wavelengths are more affected. Also the spread of the S5P TROPOMI UVAI values has become broader than during the early phase of measurements (see **Figure 82**). Also the reason for this degradation of the data quality has to be further investigated.

Desert dust, 10 Nov 2017
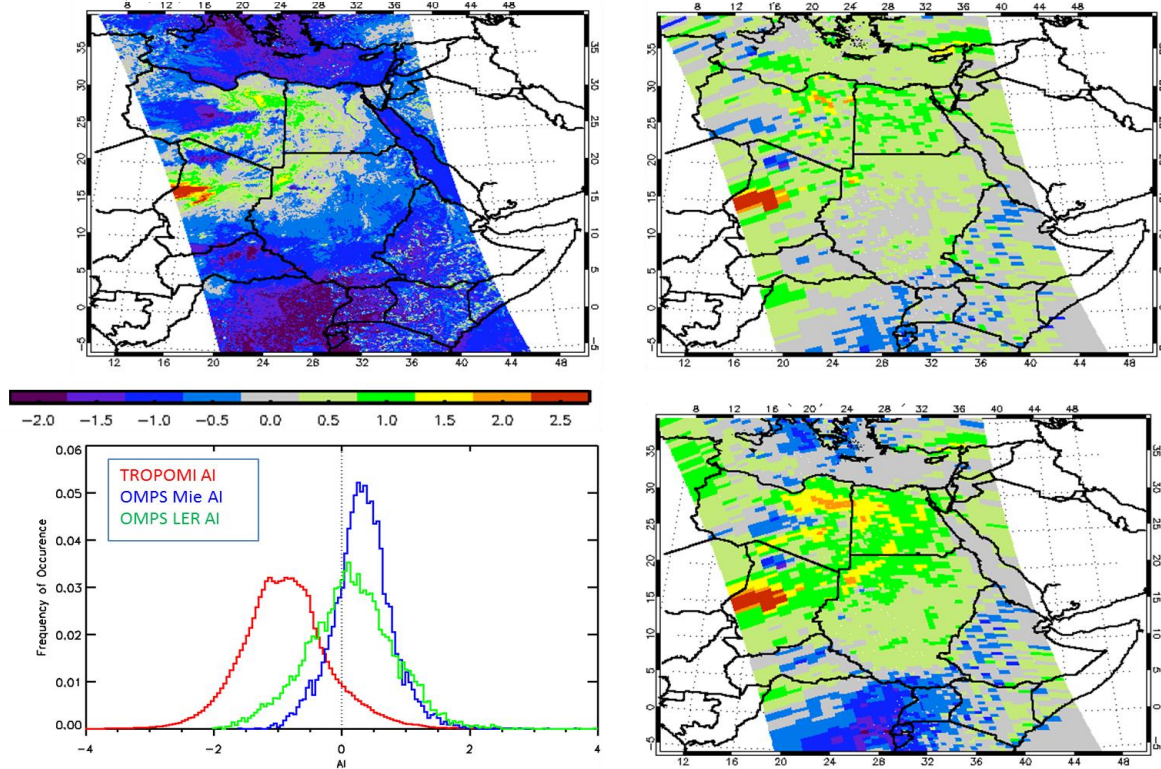
Biomass burning, 12 Dec 2017
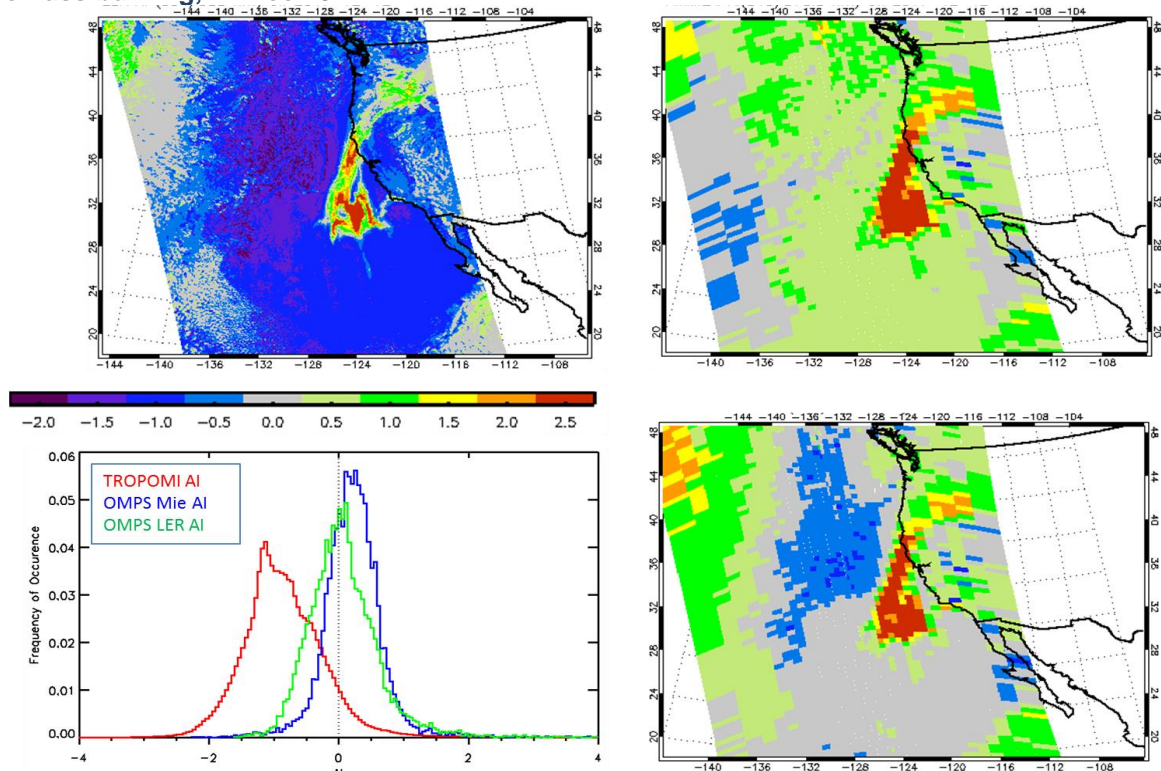
Figure 78: Comparison of UVAI from TROPOMI and OMPs for a situation with desert dust (10 Nov 2017, top) and biomass burning (12 Dec 2017, bottom). For OMPS, UVAI are calculated either assuming LER or Mie clouds. The UVAI for Mie clouds yield more consistent results. The frequency distributions indicate that S5P TROPOMI results have a similar distribution as the OMPS UVAI calculated for the LER assumption. But TROPOMI values are systematically smaller than the OMPS values (courtesy of Omar Torres and Changwoo Ahn, NASA-GSFC).
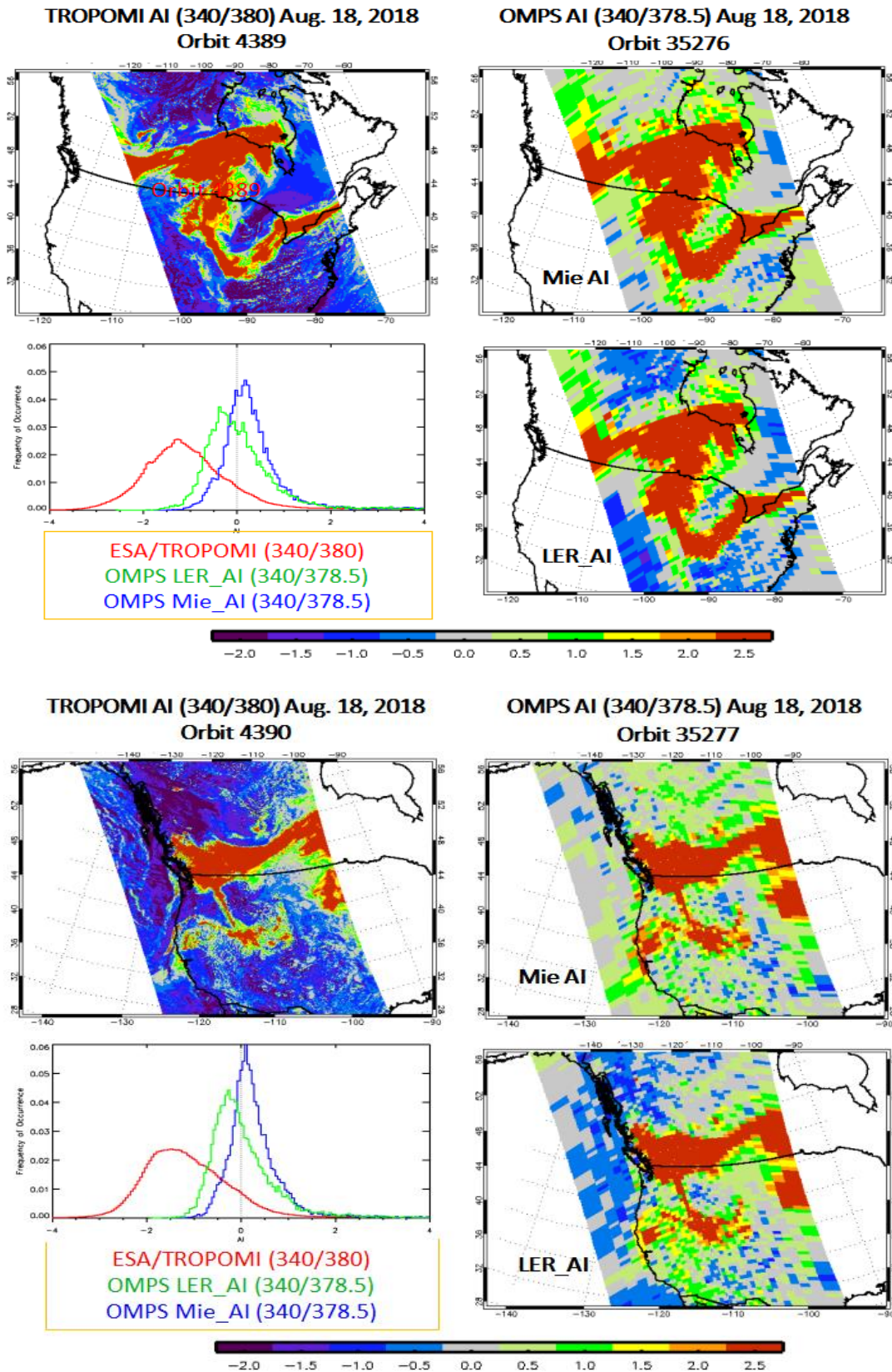
Figure 79: Comparison of UVAI from TROPOMI and OMPs for an observation of a biomass burning plume (18 Aug. 2018). For OMPS UVAI are calculated assuming either LER or Mie clouds. The UVAI for Mie clouds yields more consistent results. In contrast to early TROPOMI observations, values have systematically decreased and the spread of the UVAI values has become larger (courtesy of Omar Torres and Changwoo Ahn, NASA-GSFC).

Also comparisons with patterns from other S5P TROPOMI products are performed. **Figure 80** below shows an example of measurements of UVAI and NO_2 VCDs, for which enhanced NO_2 and UVAI are found at the same locations.
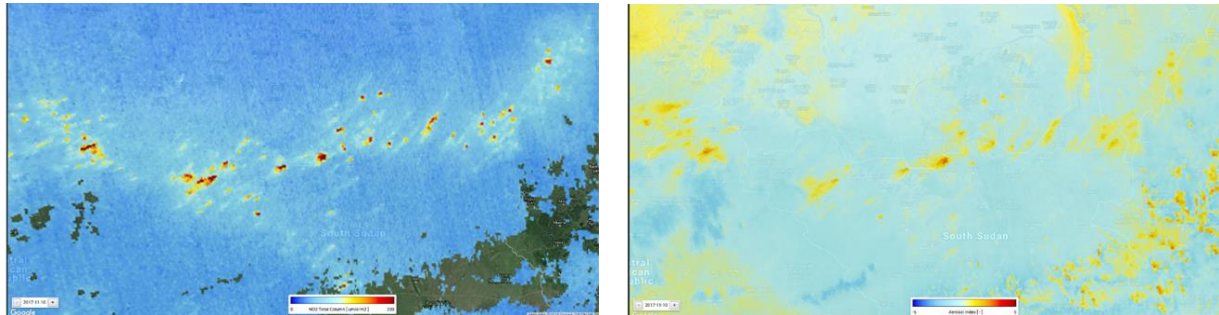
Figure 80: Comparison of NO_2 VCDs (left) and UVAI (right) obtained from S5P TROPOMI for sub-Saharan fires on 10 November 2017.

From the performed validation studies it is concluded that the L2_AER_AI UVAI from S5P TROPOMI is of very good quality and fulfilled the requirements until early 2019. The negative bias found in the S5P TROPOMI data, which continues to increase systematically is outside the bias requirements (+/- 1 UVAI unit) since the beginning of 2019. Here it should be noted that the bias is caused by the degradation of the level 1 irradiance data and will very probably be corrected after the new release of the level 1 data (foreseen at the end of 2019). Also the spread of the UVAI should be further investigated. Investigations are underway to possibly improve this spread by using a more realistic cloud model (Mie) and surface reflectance.

12.3.3   Bias

The systematic difference between S5P TROPOMI and other instruments measuring aerosol index (OMI and OMPS) was within the requirements earlier in the mission: bias < 1 UVAI unit. Comparisons based on the case studies listed in **Table 10** above conclude to a mean bias of -0.8990 AAI with OMPS (TROPOMI UVAI 354/388 – OMPS LER AI 340/378.5). Since the beginning of 2019 the UVAI is slightly outside (below 1 UVAI unit).

12.3.4   Dispersion

The S5P TROPOMI UVAI is very probably within the requirement for random errors of 0.1 UVAI unit. But this preliminary conclusion needs further investigation and confirmation.

12.3.5   Dependence on influence quantities

There is a slight cross-track dependence of -0.25 (West – East side of TROPOMI swath), which is related to the use of the LER model in the retrieval. It should be noted that this cross-track dependence decreases with increasing UVAI values. This finding needs further investigation too.

12.3.6   Short term variability

The global mean aerosol index is evaluated to give an overall indication of the stability of the data product. The global mean is calculated for all pixels on day with full global coverage and it is not expected to vary greatly from day-to-day. A time series of the global mean is given for the TROPOMI UVAI for both wavelength pairs and for the NRTI and OFFL data streams. The period of 20 July 2018 to mid-May 2019 is shown in **Figure 81** below, as the NRTI data coverage was only adequately complete starting 20 July 2018.

The global mean is more negative for the 340/380 wavelength pair as compared to the 354/388 pair. In general the values for both pairs are more negative than OMI and OMPS global mean averages. This may in part be related to a wavelength dependent degradation in the irradiance measurements where, shorter wavelengths are more affected. This is also most likely why the 340/380 pair is more negative than the 354/388 nm pair. The values of the global mean for all four plots show an overall decrease consistent with the overall degragation trend monitored by the L1b team. This degradation is known feature in the L1b data and will be addressed in the next Level 1 processor update at the end of 2019.

The values of the global mean and median are nearly identical between the NRTI and OFFL data. The differences are typically in the range of 0.01 - 0.1 and fall well within the expected errors of the UVAI. The structure of variability is slightly different but the overall shape is quite similar, where small structure differences are due to differences in global coverage and/or sampling between the two data streams. The structure and variability when comparing wavelength pairs for the same data stream (i.e. 340/380 NRTI vs. 354/388 NRTI) is also nearly identical. From this comparison it can be drawn that NRTI and OFFL data streams are comparable with only minor differences and that the wavelength pairs vary in a similar way with an absolute difference no larger than 0.3 UVAI units.
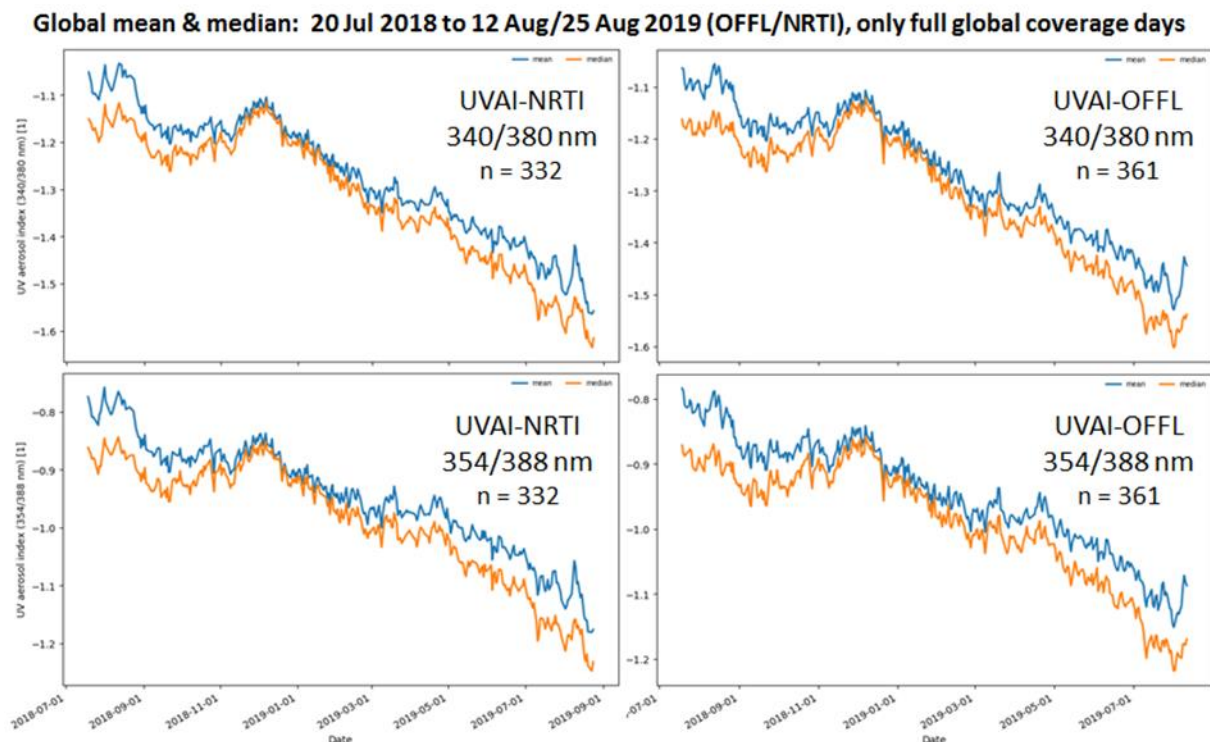
Figure 81: Comparison of the global daily mean and median for both L2_AER_AI UVAI wavelength pairs (340/380 and 354/388 nm) and for the NRTI and OFFL data streams, from 20 July 2018 through August 2019.
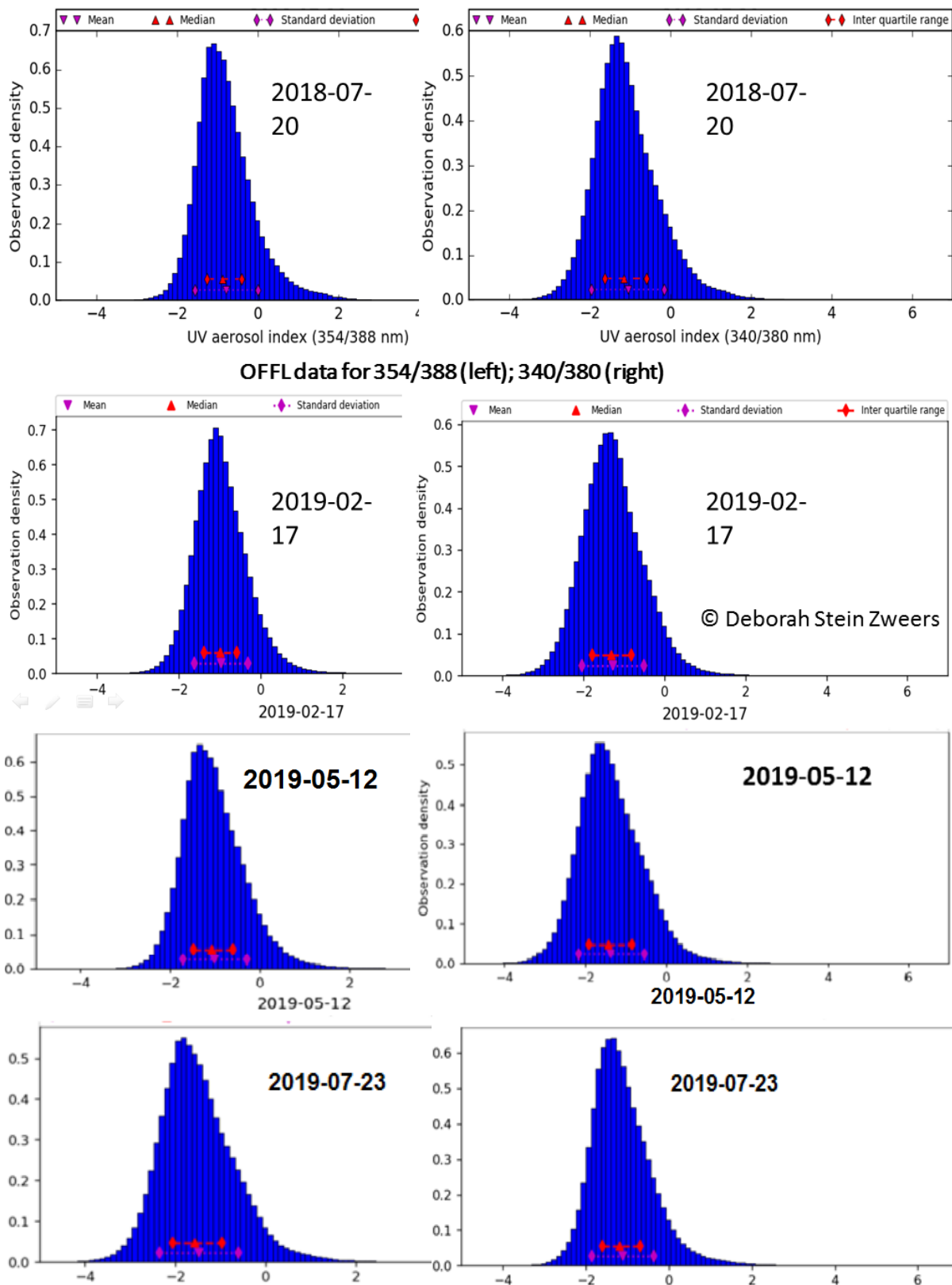
Figure 82: Comparison of the frequency distribution of the UVAI (left: 354/388m,, right: 340/380nm) for four selected days (20 July 2018, 17 February 2019, 19 May 2019, and 23 July 2019)

12.3.7　Geographical patterns

There are no obvious geographical features. For pixels (partially) covered by clouds with a small horizontal extent and a non-homogeneous vertical structure, these clouds are non-Lambertian and result in positive values similar to that of absorbing aerosol. It should also be noted that for many fully clouded scenes, aerosols might be located below the clouds and are therefore invisible for the satellite instrument.

12.3.8　Other features

As mentioned above, the (increasing) negative bias and spread of the S5P TROPOMI results should be reduced in further updates.

12.4   Equivalence of L2_AER_AI NRTI and OFFL products

Figure 83 below shows a comparison for a selected orbit on October 3, 2018. For this orbit the L2_AER_AI UV aerosol absorbing index for both wavelength pairs are very similar for the OFFL and NRTI products. Based on this comparison and also the comparison of the global means shown before, the close similarity in behaviour of both the NRTI and OFFL data streams indicates that the validation results for the NRTI data product are also valid for the OFFL data product.
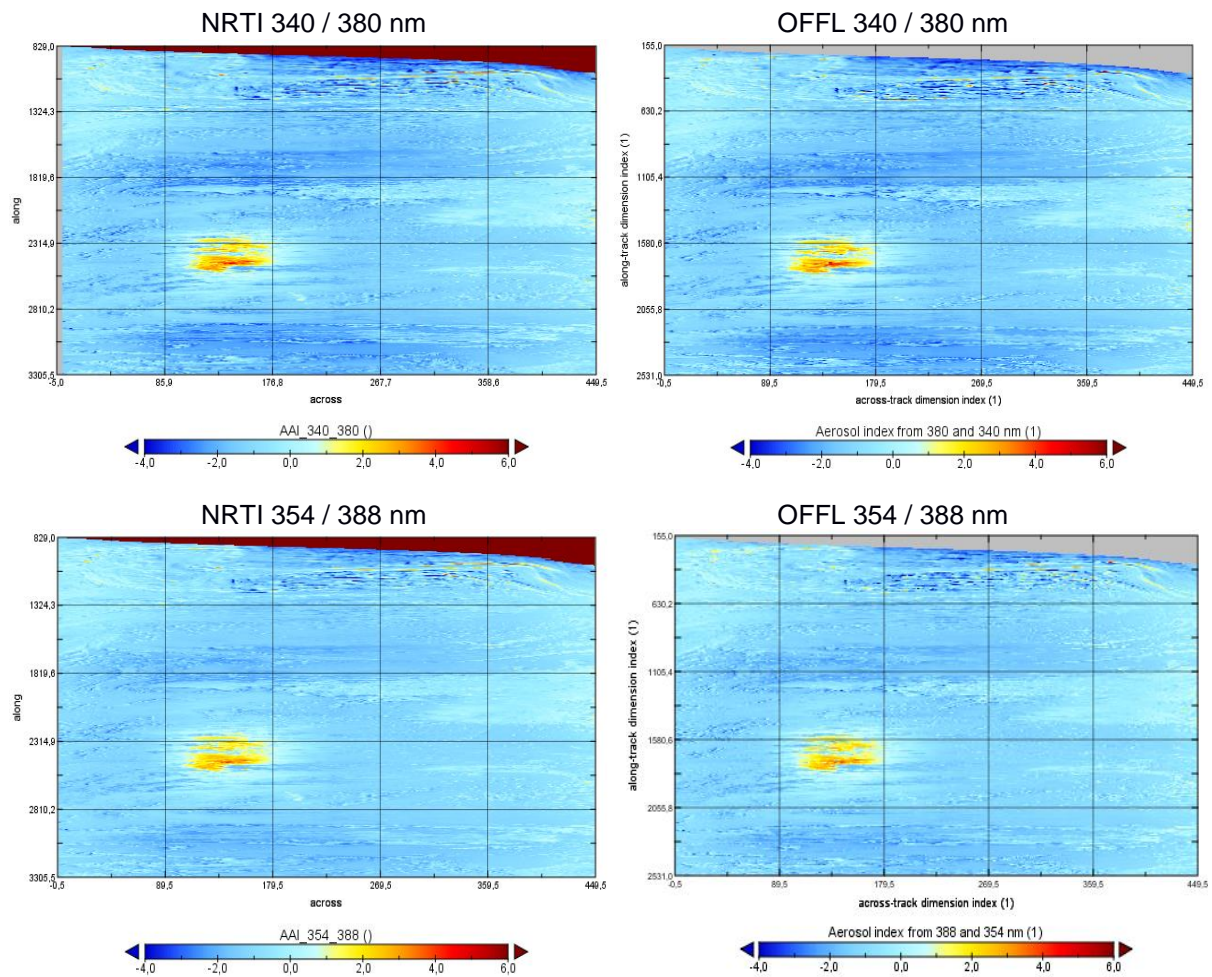
Figure 83: Comparison of the S5P TROPOMI UVAI for a selected orbit (#05033) on 3 October 2018 for the two wavelength pairs (top: 340 / 380 nm, bottom: 354 / 388 nm). While the geographical patterns are the same, the absolute values differ slightly with the NRT values (left) slightly higher than the offline values (right).

13   References

The validation activities and requirements applying to the operational phase of the S5P mission are described in the *S5P Cal/Val Plan for the Operational Phase* [S5P-CSCOP], the *S5P Geophysical Validation Requirements Document* [S5PVT-Req], the *Copernicus Sentinels 4 and 5 Mission Requirements Traceability Document* [S4/5-MRTD], and the recommendations formulated by ESL-L2 developers in their *Algorithm Theoretical Basis Documents* available on the ESA Copernicus Sentinel Online website [ER_CoperATBD].

13.1   Reference documents

[S5PVT-Req]   Requirements for the Geophysical Validation of Sentinel-5 Precursor Products
source: ESA; **ref:** S5P-RS-ESA-SY-164; **issue:**; **date:** 2014-05-21

[S5P-CSCOP]   ESA-EOPG-CSCOP-PL-0073, Sentinel-5 Precursor Calibration and Validation Plan for the Operational Phase
source: ESA; **ref:** ESA-EOPG-CSCOP-PL; **issue:** 1; **revision:** 1; **date:** 2017-11-06

[S4/5-MRTD]   Copernicus Sentinels 4 and 5 Mission Requirements Traceability Document
source: ESA; **ref:** EOP-SM/2413/BV-bv; **issue:** 1; **revision:** 0; **date:** 2012-09-20

[CEOS-Nom]   CEOS/ISO:19159 - Committee on Earth Observation Satellites (CEOS): general calibration and validation resources publicly available on http://calvalportal.ceos.org   / ISO TS 19159-1:2014(en), Geographic information - Calibration and validation of remote sensing imagery sensors and data — Part 1: Optical sensors

[JCGM-GUM]   GUM: Joint Committee for Guides in Metrology (JCGM/WG 1) 100:2008, Evaluation of measurement data – Guide to the expression of uncertainty in a measurement (GUM)

[JCGM-VIM]   VIM/ISO:99 Joint Committee for Guides in Metrology (JCGM/WG 2) 200:2012 & ISO/IEC Guide 99-12:2007, International Vocabulary of Metrology – Basic and General Concepts and Associated Terms (VIM)

[S5P-NomL1]   Terms, definitions and abbreviations for TROPOMI L01b data processor;
source: KNMI; **ref:** S5P-KNMI-L01B-0004-LI; **issue:** 3.0.0; **date:** 2013-11-08

[S5P-NomA]   Terms and symbols in the TROPOMI Algorithm Team;
source: KNMI; **ref:** SN-TROPOMI-KNMI-049; **issue:** 0.1.2; **date:** 2013-03-11

13.2   Reference articles

Basher, R. E., Review of the Dobson spectrophotometer and its accuracy, Rep. 13, WMO Global Ozone Res. and Monit. Proj., Geneva, Dec. [Available at http://www.esrl.noaa.gov/gmd/ozwv/dobson/papers/report13/report13.html], 1982.

Donlon, C., and G. Zibordi, 2014, In Situ Optical Radiometry, Chapter 3 of Optical Radiometry for Ocean Climate Measurements, Eds. G. Zibordi, C. Donlon and A. Parr; Experimental Methods in the Physical Sciences Series, Vol. 47, Elsevier Inc., ISBN: 978-0-12-417011-7, 17 November 2014.

Errera, Q. and Fonteyn, D.: Four-dimensional variational chemical assimilation of CRISTA stratospheric measurements, J. Geophys. Res., 106, 12253–12265, doi:10.1029/2001JD900010, 2001.

Garane, K., Lerot, C., Coldewey-Egbers, M., Verhoelst, T., Koukouli, M. E., Zyrichidou, I., Balis, D. S., Danckaert, T., Goutail, F., Granville, J., Hubert, D., Keppens, A., Lambert, J.-C., Loyola, D., Pommereau, J.-P., Van Roozendael, M., and Zehner, C.: Quality assessment of the Ozone_cci Climate Research Data Package (release 2017) – Part 1: Ground-based validation of total ozone column data products, Atmos. Meas. Tech., 11, 1385–1402, https://doi.org/10.5194/amt-11-1385-2018, 2018.

Garane, K., Koukouli, M.-E., Verhoelst, T., Fioletov, V., Lerot, C., Heue, K.-P., Bais, A., Balis, D., Bazureau, A., Dehn, A., Goutail, F., Granville, J., Griffin, D., Hubert, D., Keppens, A., Lambert, J.-C., Loyola, D., McLinden, C., Pazmino, A., Pommereau, J.-P., Redondas, A., Romahn, F., Valks, P., Van Roozendael, M., Xu, J., Zehner, C., Zerefos, C., and Zimmer, W.: TROPOMI/S5ptotal ozone column data: global ground-based validation & consistency with other satellite missions, Atmos. Meas. Tech. Discuss., https://doi.org/10.5194/amt-2019-147, in review, 2019.

Hendrick, F., Barret, B., Van Roozendael, M., Boesch, H., Butz, A., De Mazière, M., Goutail, F., Hermans, C., Lambert, J.-C., Pfeilsticker, K., and Pommereau, J.-P.: Retrieval of nitrogen dioxide stratospheric profiles from ground-based zenith-sky UV-visible observations: validation of the technique through correlative comparisons, Atmos. Chem. Phys., 4, 2091–2106, doi:10.5194/acp-4-2091-2004, 2004.

Hendrick, F., Pommereau, J.-P., Goutail, F., Evans, R. D., Ionov, D., Pazmino, A., Kyrö, E., Held, G., Eriksen, P., Dorokhov, V., Gil, M., and Van Roozendael, M.: NDACC/SAOZ UV-visible total ozone measurements: improved retrieval and comparison with correlative ground-based and satellite observations, Atmos. Chem. Phys., 11, 5975–5995, https://doi.org/10.5194/acp-11-5975-2011, 2011.

Herman, J., A. Cede, E. Spinei, G. Mount, M. Tzortziou, and N. Abuhassan, NO_2 column amounts from ground-based Pandora and MFDOAS spectrometers using the direct-sun DOAS technique: Intercomparisons and application to OMI validation, J. Geophys. Res., Vol. 114, D13307, doi:10.1029/2009JD011848, 2009.

Hubert, D., Lambert, J.-C., Verhoelst, T., Granville, J., Keppens, A., Baray, J.-L., Bourassa, A. E., Cortesi, U., Degenstein, D. A., Froidevaux, L., Godin-Beekmann, S., Hoppel, K. W., Johnson, B. J., Kyrölä, E., Leblanc, T., Lichtenberg, G., Marchand, M., McElroy, C. T., Murtagh, D., Nakane, H., Portafaix, T., Querel, R., Russell III, J. M., Salvador, J., Smit, H. G. J., Stebel, K., Steinbrecht, W., Strawbridge, K. B., Stübi, R., Swart, D. P. J., Taha, G., Tarasick, D. W., Thompson, A. M., Urban, J., van Gijsel, J. A. E., Van Malderen, R., von der Gathen, P., Walker, K. A., Wolfram, E., and Zawodny, J. M.: Ground-based assessment of the bias and long-term stability of 14 limb and occultation ozone profile data records, Atmos. Meas. Tech., 9, 2497-2534, https://doi.org/10.5194/amt-9-2497-2016, 2016.

Keppens, A., J.-C. Lambert, J. Granville, D. Hubert, T. Verhoelst, S. Compernolle, B. Latter, B. Kerridge, R. Siddans, A. Boynard, J. Hadji-Lazaro, C. Clerbaux, C. Wespes, D.R. Hurtmans, P.-F. Coheur, J. C. A. van Peet, R. J. van der A, K. Garane, M. E. Koukouli, D. S. Balis, A. Delcloo, R. Kivi, R. Stübi, S. Godin-Beekmann, M. Van Roozendael, and C. Zehner: Quality assessment of the Ozone_cci Climate Research Data Package (release 2017): 2. Ground-based validation of nadir ozone profile data products, Atmos. Meas. Tech., 11, 3769-3800, https://doi.org/10.5194/amt-11-3769-2018, 2018.

Keppens, A., Compernolle, S., Verhoelst, T., Hubert, D., and Lambert, J.-C.: Harmonization and comparison of vertically resolved atmospheric state observations: Methods, effects, and uncertainty budget, Atmos. Meas. Tech., 12, 4379–4391, https://doi.org/10.5194/amt-12-4379-2019, 2019.

Kerr, J. B., C. T. McElroy, and R. A. Olafson, Measurements of ozone with the Brewer ozone spectrophotometer, in Proceedings of the Quadrennial Ozone Symposium, Boulder, Colorado, edited by J. London, pp. 74–79, Natl. Cent. for Atmos. Res., Boulder, Colorado, 1981.

Kerr, J. B., I. A. Asbridge, and W. F. J. Evans, Intercomparison of total ozone measured by the Brewer and Dobson spectrophotometers at Toronto, J. Geophys. Res., 93, 11,129–11,140, doi:10.1029/JD093iD09p11129, 1988.

Lambert, J.-C., M. Van Roozendael, J. Granville, P. Gerard, P. Peeters, P.C. Simon, H. Claude and J. Staehelin, Comparison of the GOME ozone and NO_2 total amounts at mid-latitude with ground-based zenith-sky measurements, in Atmospheric Ozone - 18th Quad. Ozone Symp., L'Aquila, Italy, 1996, R. Bojkov and G. Visconti (Eds.), Vol. I, pp. 301-304, 1997.

Lambert, J.-C., M. Van Roozendael, M. De Mazière, P.C. Simon, J.-P. Pommereau, F. Goutail, A. Sarkissian, and J.F. Gleason, Investigation of pole-to-pole performances of spaceborne atmospheric chemistry sensors with the NDSC, Journal of the Atmospheric Sciences, Vol. 56, pp. 176-193, https://doi.org/10.1175/1520-0469(1999)056<0176:IOPTPP>2.0.CO;2 , 1999.

Loew, A., W. Bell, L. Brocca, C. E. Bulgin, J. Burdanowitz, X. Calbet, R. V. Donner, D. Ghent, A. Gruber, T. Kaminski,J. Kinzel, C. Klepp, J.-C. Lambert, G. Schaepman-Strub, M. Schröder, and T. Verhoelst, Validation practices for satellite based earth observation data across communities, Rev. Geophys., DOI: 10.1002/2017RG000562, 2017.

Nanda, S., Veefkind, J. P., de Graaf, M., Sneep, M., Stammes, P., de Haan, J. F., Sanders, A. F. J., Apituley, A., Tuinder, O., and Levelt, P. F.: A weighted least squares approach to retrieve aerosol layer height over bright surfaces applied to GOME-2 measurements of the oxygen A band for forest fire cases over Europe, Atmos. Meas. Tech., 11, 3263-3280, https://doi.org/10.5194/amt-11-3263-2018, 2018.

Pommereau, J. and Goutail, F.: O3 and NO2 ground-based measurements by visible spectrometry during Arctic winter and spring, Geophys. Res. Lett., 15, 891–894, https://doi.org/10.1029/GL015i008p00891, 1988.

Richter, A., M. Weber, J. P. Burrows, J.-C. Lambert, and A. van Gijsel, Validation Strategy for Satellite Observations of Tropospheric Reactive Gases, Annals of Geophysics, Vol. 56, 10.4401/AG-6335, 2013.

Schneider, M., Hase, F., and Blumenstock, T.: Ground-based remote sensing of HDO/H2O ratio profiles: introduction and validation of an innovative retrieval approach, Atmos. Chem. Phys., 6, 4705-4722, https://doi.org/10.5194/acp-6-4705-2006, 2006.

Verhoelst, T., Granville, J., Hendrick, F., Köhler, U., Lerot, C., Pommereau, J.-P., Redondas, A., Van Roozendael, M., and Lambert, J.-C.: Metrology of ground-based satellite validation: co-location mismatch and smoothing issues of total ozone comparisons, Atmos. Meas. Tech., 8, 5039-5062, https://doi.org/10.5194/amt-8-5039-2015, 2015.

13.3   Electronic references

[ER_TROPOMI]	TROPOMI website	http://www.tropomi.eu
[ER_VDAF]	TROPOMI Validation Website / Validation Data Analysis Facility	http://mpc-vdaf.tropomi.eu
[ER_VDAF-AVS]	Validation Data Analysis Facility Automated Validation Server	http://mpc-vdaf-server.tropomi.eu
[ER_CoperATBD]	Copernicus Sentinel-5p products and algorithms documents webpage	https://sentinels.copernicus.eu/web/sentinel/technical-guides/sentinel-5p/products-algorithms
[ER_MPS]	TROPOMI Portal for Instrument and Calibration	http://mps.tropomi.eu
[ER_L2QC]	TROPOMI Portal for Level-2 Data Quality Control	http://mpc-l2.tropomi.eu
[ER_S5PVT]	S5P Validation Team AO projects	https://earth.esa.int/web/guest/pi-community/apply-for-data/ao-s
[ER_2ndS5PVT]	Second S5PVT Meeting and First Results Workshop (including link to presentations)	https://atpi.eventsair.com/QuickEventWebsitePortal/2nd-sentinel-5-precursor-validation-team-and-early-results-meeting/website
[ER_CoperEC]	Copernicus Programme website	http://www.copernicus.eu
[ER_CoperESA]	ESA Copernicus website	http://www.esa.int/copernicus
[ER_CAMS]	Copernicus Atmosphere Monitoring Service (CAMS) website	http://atmosphere.copernicus.eu
[ER_C3S]	Copernicus Climate Change Service (C3S) website	http://climate.copernicus.eu
[ER_CEOS-Nom]	CEOS Cal/Val Terms and Definitions	http://calvalportal.ceos.org/documents/10136/551648/IASB-BIRA+Metrology+Terms+and+Definitions
[ER_GUM]	Guide to the expression of uncertainty in a measurement (GUM)	http://www.bipm.org/utils/common/documents/jcgm/JCGM_100_2008_E.pdf
[ER_VIM]	International Vocabulary of Metrology (VIM)	http://www.bipm.org/en/publications/guides/vim.html
[ER_BEAT]	Basic Envisat Atmospheric Toolbox	http://www.stcorp.nl/beat

ESA FRM Projects Websites

[ER_FRM4DOAS]	Fiducial Reference Measurements for Ground-Based DOAS Air-Quality Observations project website	http://frm4doas.aeronomie.be
[ER_FRM4GHG]	Fiducial Reference Measurements for Ground-Based Infrared Greenhouse Gas Observations project website	http://frm4ghg.aeronomie.be
[ER_Pandonia]	Fiducial Reference Measurements for Ground-Based Direct-Sun Air-Quality Observations project	http://pandonia.net

Monitoring Networks Websites and Data Centres

[ER_ACTRIS]	European Research Infrastructure for the observation of Aerosol, Clouds, and Trace gases website	http://www.actris.eu
[ER_Cloudnet]	Cloudnet remote sensing network website	http://www.cloud-net.org
[ER_EARLINET]	European Aerosol Research Lidar Network (EARLINET) website	http://www.earlinet.org
[ER_EUBREWNET]	COST Action for a coherent network of European Brewer Spectrophotometer monitoring stations (EUBREWNET) website	http://www.eubrewnet.org
[ER_EUMETNET]	European Meteorological Services Network (EUMETNET) website	http://eumetnet.eu
[ER_EVDC]	ESA Validation Data Centre (EVDC) website	http://evdc.esa.int
[ER_NDACC]	Network for the Detection of Atmospheric Composition Change (NDACC) website	http://ndacc.org
[ER_NOVAC]	Network for Observation of Volcanic and Atmospheric Change (NOVAC) website	http://novac-community.org/
[ER_SHADOZ]	Southern Hemisphere ADditional OZonesonde programme website	https://tropo.gsfc.nasa.gov/shadoz
[ER_TCCON]	Total Carbon Column Observing Network (TCCON) website	https://tccon-wiki.caltech.edu
[ER_TOLnet]	Tropospheric Ozone Lidar Network (TOLnet) website	http://www-air.larc.nasa.gov/missions/TOLNet
[ER_WOUDC]	World Ozone and Ultraviolet Data Centre (WOUDC) website	http://woudc.org

14   Acknowledgements

This Section acknowledges the authors of this report in charge of the MPC Routine Operations validation service (**Table 11**), the operators of S5P validation facilities, the providers of Fiducial Reference Measurements and other validation data, and the support provided by the Agencies.

14.1   S5P MPC Routine Operations Validation Service

Table 11 – Responsibilities for the S5P MPC routine operations validation service: Product Validation Coordinators responsible for validation and reporting per data product (third column), and Product Validation Contributors participating in the validation and reporting per data product (fourth column).

Product ID	S5P TROPOMI Data Product	Product Coordinator for Routine Operations Validation Activities	Product Contributors to Routine Operations Validation Activities
L1B	Radiance and irradiance	Q. Kleipool (KNMI)	
L2_O3	O_3 total column	T. Verhoelst (BIRA-IASB)	K. Garane (AUTH) K.-P. Heue (DLR)
L2_O3_PR	O_3 profile	A. Keppens (BIRA-IASB)	O. Tuinder (KNMI)
L2_O3_TCL	O_3 tropospheric column	D. Hubert (BIRA-IASB)	K.-P. Heue (DLR)
L2_NO2	NO_2 stratospheric column	K.-U. Eichmann (IUPB)	T. Verhoelst (BIRA-IASB)
	NO_2 tropospheric column		S. Compernolle (BIRA-IASB) H. Eskes (KNMI) P. Valks (DLR)
	NO_2 total column		
L2_SO2	SO_2 total column	T. Wagner (MPI-C)	P. Hedelt (DLR) N. Theys (BIRA-IASB)
L2_HCHO	HCHO total column	K.-U. Eichmann (IUPB)	K.L. Chan (DLR) S. Compernolle (BIRA-IASB) I. De Smedt (BIRA-IASB)
L2_CO	CO total column	B. Langerock (BIRA-IASB)	A. Keppens (BIRA-IASB) J. Landgraf (SRON)
L2_CH4	CH_4 total column	B. Langerock (BIRA-IASB)	J. Landgraf (SRON)
L2_CLOUD	Cloud Fraction	S. Compernolle (BIRA-IASB)	R. Lutz (DLR) P. Wang (KNMI)
	Cloud Height		A. Argyrouli (DLR) S. Compernolle (BIRA-IASB)
	Cloud Optical Thickness		P. Wang (KNMI)
L2_AER_AI	Aerosol Absorbing Index	T. Wagner (MPI-C)	D. Stein Zweers (KNMI)
	Aerosol Layer Height		M. de Graaf (KNMI) B. Langerock (BIRA-IASB)

14.2   S5P validation facilities

The ESA Atmospheric Validation Data Centre (EVDC) [ER_EVDC], hosted at the Norwegian Institute for Air Research (NILU) under the supervision of A.M. Fjæraa, is acknowledged for facilitating access to the validation data from ground-based monitoring networks and field campaigns.

The MPC Validation Data Analysis Facility (VDAF) [ER_VDAF] hosted at BIRA-IASB runs the TROPOMI Automated Validation Server developed and operated jointly by s[&]t and BIRA-IASB. This server is based on the HARP toolset developed and maintained by S. Niemeijer and B. Rino at s[&]t.

Part of the validation work for trace gases data relies on the Multi-TASTE versatile validation system, developed and operated at BIRA-IASB by S. Compernolle, J. Granville, D. Hubert, A. Keppens, J.-C. Lambert, and T. Verhoelst. Multi-TASTE has been supported by the Belgian Federal Science Policy Office (BELSPO), with additional support provided by the EC, ESA and EUMETSAT in the context of several satellite validation and metrology projects.

Part of the total ozone validation work makes use of the ozone validation facility operated at AUTH, and developed by D. Balis and ML. Koukouli with support from ESA and EUMETSAT.

14.3   Validation data

The ground-based data used in this study was obtained as part of the Brewer and Dobson ozone column monitoring networks ([ER_WOUDC], [ER_EUBREWNET]), the Network for the Detection of Atmospheric Composition Change (NDACC) [ER_NDACC], Southern Hemisphere Additional Ozonesonde programme (SHADOZ) [ER_SHADOZ], and the Total Carbon Column Observation Network (TCCON) [ER_TCCON], all contributors to WMO's Global Atmosphere Watch (GAW). Data archived in the associated data centres and lists of associated data originators are publicly available.

Instrument PIs, the scientific teams and the staff at the stations are thanked warmly for special processing efforts and faster data delivery dedicated to TROPOMI validation:

- Rapid delivery O_3 column data from the LATMOS_RT facility at IPSL/UVSQ, WMO's Ozone Mapping Centre in Thessaloniki and WOUDC in Toronto was gathered in the framework of the S5PVT AO project VALTOZ (ID #28568, PI D. Balis, AUTH, Co-Is ML. Koukouli, E. Zyrichidou, J.-C. Lambert, T. Verhoelst, J. Granville, A. Pazmino, F. Goutail, J.-P. Pommereau, A. Bazureau, and C. Zerefos).

- Rapid delivery O_3 profile data from the SHADOZ network was organised in the framework of the S5PVT AO project CHEOPS-5p (ID #28587, PIs A. Keppens and J.-C. Lambert, BIRA-IASB, Co-Is D. Balis, D. Hubert, W. Steinbrecht, T. Stavrakou, A. Delcloo, S. Godin-Beekmann, T. Leblanc, R. Stübi, A.M. Thompson, T. Verhoelst, G. Ancellet, and V. Duflot). Rapid delivery ozonesonde profile data were also provided by KNMI (A. Piters, M. Allaart) and NOAA (B.J. Johnson).

- Rapid delivery NO_2 data from NDACC MAX-DOAS and ZSL-DOAS stations was gathered in the framework of the S5PVT AO projects CESAR (ID #28596, PI A. Apituley, KNMI) and NIDFORVAL (ID #28607, PI G. Pinardi, BIRA-IASB).

- Rapid delivery HCHO data from NDACC MAX-DOAS and FTIR stations was gathered in the framework of the S5PVT AO projects CESAR (ID #28596, PI A. Apituley, KNMI) and NIDFORVAL (ID #28607, Co-PIs G. Pinardi and C. Vigouroux, BIRA-IASB).

14.4   Agency support

15   Terms, definitions and abbreviated terms

15.1   Terms and definitions

accuracy	closeness of agreement between a quantity value obtained by measurement and the true value of the measurand; note that it is not a quantity and it is not given a numerical quantity value [JCGM-VIM]
bias	(1) systematic error of indication of a measuring system [JCGM-VIM]
	(2) estimate of a systematic measurement error [JCGM-VIM]
error	(1) measured quantity value minus a reference quantity value [JCGM-VIM]
	(2) difference of quantity value obtained by measurement and true value of the measurand (CEOS/ISO)
influence quantity	quantity that, in a direct measurement, does not affect the quantity that is actually measured, but affects the relation between the indication and the measurement result [JCGM-VIM]
Level 1b data	calibrated, geo-located Earth reflectance and radiance spectra in all spectral bands; solar irradiance data, annotation data and references to used calibration data
Level 2 data	geophysical measurand at the same resolution and geolocation as the Level 1 source data from which it is derived
Level 3 data	data or retrieved geophysical parameters (i.e. derived from Level 1 or 2 data products) mapped on uniform space-time grid scales, usually with some completeness and consistency. Such re-sampling may include averaging, compositing, kriging, use of Kalman filters…
measurand	quantity intended to be measured [JCGM-VIM]
measurement bias	estimate of a systematic measurement error [JCGM-VIM]
measurement error	measured quantity value minus a reference quantity value [JCGM-VIM]
measurement uncertainty	non-negative parameter characterizing the dispersion of the quantity values being attributed to a measurand, based on the information used [JCGM-VIM]
precision	closeness of agreement between quantity values obtained by replicate measurements of a quantity on the same or similar object under specified conditions [JCGM-VIM]
random error	component of measurement error that in replicate measurements varies in an unpredictable manner; note that random measurement error equals measurement error minus systematic measurement error [JCGM-VIM]
relative standard uncertainty	standard measurement uncertainty divided by the absolute value of the measured quantity value [JCGM-VIM]
stability	ability of a measuring system to maintain its metrological characteristics constant with time [JCGM-VIM]
systematic error	component of measurement error that in replicate measurements remains constant or varies in a predictable manner [JCGM-VIM]
uncertainty	non-negative parameter that characterizes the dispersion of the quantity values that are being attributed to a measurand, based on the information used [JCGM-VIM]
validation	(1) the process of assessing, by independent means, the quality of the data products derived from the system outputs (CEOS/ISO)
	(2) verification where the specified requirements are adequate for an intended use [JCGM-VIM]
verification	the provision of objective evidence that a given data product fulfils specified requirements; note that, when applicable, measurement uncertainty should be taken into consideration [JCGM-VIM]

15.2   Acronyms and abbreviations

A(A)I	Aerosol (Absorbing) Index
AC-SAF	Atmospheric Composition Satellite Application Facility
ACTRIS	European Research Infrastructure for the observation of Aerosol, Clouds, and Trace gases
ALC	Automated Lidars and Ceilometers network
AMF	Air Mass Factor
AO	Announcement of Opportunity
ARM	Atmospheric Radiation Measurement program
ATBD	Algorithm Theoretical Basis Document
AVS	Automated Validation Server
AUTH	Aristotle University of Thessaloniki
BELSPO	Belgian Federal Science Policy Office
BIRA-IASB	Royal Belgian Institute for Space Aeronomy
C3S	Copernicus Climate Change Service
CAL	Clouds As Layers
CAMS	Copernicus Atmosphere Monitoring Service
CCD	Convective Cloud Differential method
CCI	Climate Change Initiative
CESAR	Cabauw Experimental Research Site for Atmospheric Research
CF	Cloud Fraction (fractional cloud cover)
CHEOPS-5p	Validation of Copernicus HEight-resolved Ozone data Products from Sentinel-5p
CLOUDNET	Cloud properties monitoring Network
COT	Cloud Optical thickness
CRB	Clouds as Reflecting Boundaries
C(T)H	Cloud (Top) Height
DLR	German Aerospace Center / Deutsches Zentrum für Luft- und Raumfahrt
DOAS	Differential Optical Absorption Spectroscopy
DU	Dobson Unit
EARLINET	European Aerosol Research Lidar Network
EC	European Commission
ECMWF	European Centre for Medium-Range Weather Forecasts
EOS	Earth Observing System
EPS	EUMETSAT Polar System
ESA	European Space Agency
ESL	Expert Support Laboratory
EU	European Union
EUMETNET	European Meteorological Services Network
EUMETSAT	European Organisation for the Exploitation of Meteorological Satellites
EVDC	ESA Atmospheric Validation Data Centre

FRM	Fiducial Reference Measurement
FTIR	Fourier Transform Infra-Red
GAW	Global Atmosphere Watch
GOME(-2)	Global Ozone Monitoring Experiment(-2)
GOSAT(-2)	Greenhouse gases Observing SATellite(-2)
GSFC	Goddard Space Flight Center
GUM	Guide to the Expression of Uncertainty in Measurement
IPSL/UVSQ	Institut Pierre-Simon Laplace / Université de Versailles Saint-Quentin-en-Yvelines
IUP-UB	Institute of Environmental Physics - University of Bremen
JCGM	Joint Committee for Guides in Metrology
KNMI	Koninklijk Netherlands Meteorologisch Instituut / Royal Dutch Meteorological Institute
LATMOS	Laboratoire Atmosphères, Milieux, Observations Spatiales
LER	Lambert-equivalent reflectivity
Lidar	LIght Detection And Ranging
MAX-DOAS	Multi Axis Differential Optical Absorption Spectroscopy
MetOp	polar orbiting Meteorological Operational satellite
MPC	Mission Performance Centre
MPI-C	Max Planck Institute for Chemistry
NASA	National Aeronautics and Space Administration
NDACC	Network for the Detection of Atmospheric Composition Change
NIDFORVAL	S5P NItrogen Dioxide and FORmaldehyde VALidation using NDACC and complementary FTIR and UV-Vis DOAS ground-based remote sensing data
NOVAC	Network for Observation of Volcanic and Atmospheric Change
NILU	Norsk Institutt for Luftforskning / Norwegian Institute for Air Research
NOAA	National Oceanic and Atmospheric Administration
NRT	Near Real Time
NSO	Netherlands Space Office
PANDORA	not an acronym; direct Sun UV-visible spectrometer
OFFL	Off-line
OMI	Ozone Monitoring Instrument
OMPS	Ozone Mapper and Profiling Suite
PDGS	Payload Data Ground Segment
PI	Principal Investigator
PRF	Product Readme File
PUM	Product User Manual
QA4EO	Quality Assurance framework for Earth Observation
QC	Quality Control
QWG	Quality Working Group
RAL	Rutherford Appleton Laboratory
S5P	Sentinel-5 Precursor

S5PVT	Sentinel-5 Precursor Validation Team
SAOZ	Système d'Analyse par Observation Zénithale
SCIAMACHY	SCanning Imaging Absorption spectroMeter for Atmospheric CartograpHY
SHADOZ	Southern Hemisphere ADditional OZonesonde programme
SRON	Netherlands Institute for Space Research
Suomi-NPP	Suomi National Polar-orbiting Partnership
TCCON	Total Carbon Column Observing Network
TCCON4S5P	Validation of S5P Methane and Carbon Monoxide with TCCON Data
TOLNet	Tropospheric Ozone Lidar Network
TROPOMI	Tropospheric Monitoring Instrument
UVAI	Ultraviolet aerosol absorbing index
VDAF	Validation Data Analysis Facility
VIIRS	Visible Infrared Imaging Radiometer Suite
VIM	International Vocabulary of Metrology
WMO	World Meteorological Organization
WOUDC	World Ozone and Ultraviolet Data Centre
ZSL-DOAS	Zenith-Scattered-Light Differential Optical Absorption Spectroscopy

END OF DOCUMENT